THESIS FOR THE DEGREE OF DOCTOR OF PHILOSOPHY

# Homogeneous Lean Combustion in Downsized Spark-Ignited Engines

KRISTOFFER CLASÉN

Division of Combustion and Propulsion Systems
*Department of Mechanics and Maritime Sciences*
CHALMERS UNIVERSITY OF TECHNOLOGY
Göteborg, Sweden, 2022

Homogeneous Lean Combustion in Downsized Spark-Ignited Engines

KRISTOFFER CLASÉN

ISBN 978-91-7905-614-8



Doktorsavhandlingar vid Chalmers tekniska högskola
Ny serie nr. 5080
ISSN 0346-718X

Division of Combustion and Propulsion Systems
*Department of Mechanics and Maritime Sciences*
Chalmers University of Technology
SE-412 96 Gothenburg
Sweden
Telephone +46(0)31 772 1000

*First page image illustrates a flash-over inside of an engine cylinder which is caused by excessive voltage applied to an igniter to initiate combustion of a fuel-lean cylinder charge*

Chalmers Reproservice
Göteborg, Sweden, 2022

# Homogeneous Lean Combustion in Downsized Spark-Ignited Engines

KRISTOFFER CLASÉN

Division of Combustion and Propulsion Systems
*Department of Mechanics and Maritime Sciences*
CHALMERS UNIVERSITY OF TECHNOLOGY

# Abstract

Emissions of greenhouse-gasses and noxious compounds from internal combustion engines propelling personal transportation vehicles is an imminent issue in the society. Therefore, it is vital to find means of reducing these emissions to decrease the impacts of transportation. Despite the current rapid electrification of the light duty vehicle fleet, it is expected that there will still be a substantial share of vehicles, produced and sold, that are propelled either solely or partly by combustion engines in the next decades to come. An advantage of combustion engines is that they consume hydrocarbon fuels, which are energy dense and can be produced from renewable sources enabling elimination of net carbon emissions. These fuels can be distributed using the current infrastructure, allowing for a fast transition into a low-carbon transportation system. The sources of renewables are however limited, and production of renewable fuels requires energy, which is why the fuel efficiency of combustion engines is key.

This thesis addresses the need for reduced emissions from personal transportation vehicles by investigating homogeneous lean combustion in downsized spark-ignited engines as a means of improving combustion engine fuel efficiency. Lean combustion offers substantial efficiency improvements to the current already well-developed combustion systems. However, historically, it has been proven difficult to achieve robust lean combustion that achieves both efficiency improvements and sufficiently low emissions of nitrogen oxides. In this thesis, the focus has been to investigate the potentially synergetic combination of high engine loads above 10 bar brake mean effective pressure, a common attribute of downsized engines, and lean combustion. The idea is that lean combustion reduces knocking combustion, a harmful event that limits engine efficiency due to cylinder pressure limitations. Simultaneously, it is hypothesized that higher engine loads will lead to faster and more stable combustion, allowing important reductions in nitrogen oxides.

Using engine experiments and simulations, homogeneous lean combustion has been investigated. From the experiments it could be concluded that lean combustion can be sustained at high loads. One of the world's first two-stage turbochargers designed solely for lean combustion was utilized for this purpose and found to be successful. However, it was discovered that lean combustion does not eliminate knocking combustion completely, nor did high load operation eliminate cyclic dispersion of combustion, which imposes limitations. Using improved in-cylinder charge motion and alternative fuels, these limitations can be mitigated, allowing for stable, efficient, low nitrogen oxide high load lean combustion.

**Keywords**: engine, efficiency, emissions, lean, combustion

# List of publications

This thesis is based upon the work contained in the following publications:

**I** Clasén, K., Koopmans, L., and Dahl, D., “Homogeneous Lean Combustion in a 2lt Gasoline Direct Injected Engine with an Enhanced Turbo Charging System,” SAE Technical Paper 2018-01-1670, 2018, doi:10.4271/2018-01-1670.

**II** Clasén, K. and Koopmans, L., "Investigation of Homogeneous Lean SI Combustion in High Load Operating Conditions", *SAE Int. J. Advances & Current Practices in Mobility* 2(4):2051-2066, 2020, doi:10.4271/2020-01-0959.

**III** Clasén, K., Melaika, M., Koopmans, L., and Dahlander, P., "High Load Lean SI-combustion Analysis of DI Methane and Gasoline using Optical Diagnostics with Endoscope", SAE Technical Paper 2021-24-0046, 2021, doi:10.4271/2021-24-0046.

**IV** Clasén, K. and Koopmans, L., “Influence of Trapped Residual Gasses in Air-Diluted Spark Ignited Combustion”, manuscript accepted by *SAE Int. J. Engines*, 2022.

Other contributions and publications not included in this thesis:

**V** Lock, J., Clasén, K., Sjöblom, J., and McKelvey, T., "A Control-Oriented Spatially Resolved Thermal Model of the Three-Way-Catalyst", SAE Technical Paper 2021-01-0597, 2021, doi:10.4271/2021-01-0597.

**VI** Lock, J., Clasén, K., Sjöblom, J., and McKelvey, T., "Cold-Start Modeling and On-Line Optimal Control of the Three-Way Catalyst", *Emission Control Science and Technology*: 1-27, 2021, doi:10.1007/s40825-021-00199-x.

# Acknowledgements

I have been supported by a lot of people in my pursuit for a PhD degree. I would like to thank Dr. Anders Johansson for opening the door for me to the Division of Combustion and Propulsion Systems at Chalmers. Today I would be elsewhere without your invitation to the division. I would also like to thank Professor Ingemar Denbratt for kindly offering me this PhD position which involved me in the European Upgrade-project. Ingemar's tireless support, patience, and skills to navigate and negotiate throughout the Upgrade-project was crucial to end the project successfully. I would also like to thank Dr. Gerben Doornbos who both acted as my sponsor in the beginning of my PhD studies, but also paved the way for homogeneous lean combustion research at our division.

The engineers and PhDs that worked at Volvo Cars, most of them working at Aurobay today, who have been supporting me in this project have been invaluable. Dr. Daniel Dahl, Dr. Stefan Bohatsch, Anton Ajne, Mark O'Malley, Fredrik Wemmert, Lars Davidson, Magnus Örngrip, Joel Ohlsson, Peter Kroon, Martin Johansson, Robert Mattans, Peter Svensson, Peter Sandberg are only the ones I have been bothering the most, but I wish to thank all employees at Volvo that kindly have been providing their support.

My colleagues at the division naturally deserves to be acknowledged for always being kind friends who creates the outstanding working environment with high spirits and laughter all week long. A particular bunch of astonishing co-workers that deserve a special thank is the "laboratory engineers" of the engine lab at the division, who keeps the difficult and challenging experimental activities running in the lab. Dr. Timothy Benham, Anders Bragée, Robert Buadu, Dr. Alf-Hugo Magnusson, Anders Mattsson, Patrik Wåhlin. For an experimentalist such as myself, their support has been invaluable. I would also like to thank Joop Somhorst for his support in various technical details such as signal filtering and for his encouragement. Dr. Mindaugas Melaika, for a great collaboration when we investigated the use of methane on high load lean combustion together.

Professor Dr. Lucien Koopmans, my supervisor, has had the difficult task of guiding both me, and the whole division, through challenging times due to a rapidly evolving automotive industry. However, Lucien is hard as a rock made of tungsten carbide and any challenges that are thrown at him washes off like some grains of sand on top of glass. He is an excellent supervisor and I appreciate his efforts to push me all this way. For his patience, guidance, and belief in my capabilities he deserves my outmost gratitude.

I am forever grateful to my fiancée, Josefin. She has been endlessly supportive ever since we met, and she has always shown great understanding and patience to me at times when this work has completely consumed me. It is safe to say that I would not have come to this point without her. To my parents, and family, who has always believed in me.

Part of the work included in this thesis was performed within a project called Upgrade, "High efficient Particulate free gasoline Engines", which was funded by the European Union Horizon 2020 Research and Innovation program's call for Green Vehicles, grant agreement no. 724036.

# Contents

## I – Introductory Chapters



## II – Appended Papers

# Part I.

# Introductory Chapters

# 1 Introduction

Ever since the beginning of the industrial revolution, the ability of artificial transportation of goods and people have had a central role in the human society and industrial revolution. Today, we are heavily dependent on the functioning of those high-technology supply chains that enables transportation over vast distances in short frames of time. Transportation enables us to live where we wish and to buy what we need and want, without the need for us to live and work at the origins of our supplies. Transportation bridges the gap between supplier and customer, which enables us to focus various kinds of production, from food to industrial manufacturing, to places where the processes are suitable and can be conducted in larges scales, making the processes more efficient. Modern transportation enables people to travel, for example from short distances between home and work, to long distances across the globe, for business or pleasure.

However, the ability to conduct transportation in large scales comes at a cost in terms of energy. Only a minority of transport can be realized, on land and in water, by natural resources such as wind and animal propulsion. Hence, artificial propulsion has gradually taken its place ever since the introduction of the high-pressure steam engine in the early 1800's. Today, the vast majority of vehicles are reliant upon the use of the internal combustion engine as a source of propulsion power, such as approximately 1.4 billion cars and 200 million trucks. The internal combustion engine is small relative to its power output, comparatively easy and cheap to manufacture in large scales and relatively efficient. With few exceptions, internal combustion engines rely upon the consumption of hydrocarbon fuels, liquid or gaseous, to produce power. Hydrocarbons contain stable chemical energy at high energy densities, which enables large energy storages at low costs in terms of mass and volume, which in turn enables long range capabilities for vehicles. Most hydrocarbon fuels originate from fossil crude oil or natural gas which are parts of gigantic underground repositories of hydrocarbons that have formed during millions of years from decomposed biomasses. When hydrocarbons are oxidized through combustion to release chemical energy, like in an internal combustion engine, water and carbon dioxide are created as a result and emitted to the atmosphere through the exhaust. Carbon dioxide is a harmless compound in regular concentrations, is very stable and accumulates in the atmosphere. It is even crucial for plants who rely upon the photosynthesis to grow. Carbon dioxides do however absorb radiation from sunlight and heats up, why it is called a greenhouse gas. Thus, by burning hydrocarbon fuels originating from fossils, the hydrocarbon repository is moved from below ground, up to the atmosphere, where they contribute to the heating of the earth. The consequences of the increasing carbon dioxide concentrations in the atmosphere are highly disputed, but it is a fact that our burning of fossils alters a global balance that has been undisturbed for a very long time.

Not only does the burning of hydrocarbons result in carbon dioxide emissions, but combustion also contributes to local pollutions by emitting noxious compounds such as nitrogen oxides, unburned hydrocarbons such as methane (another greenhouse gas), carbon monoxide, and particulates, which cause harm to the local environment and cause premature deaths. There are some indications that such pollutions even cause harm to unborn children and infants [1].

In 2016, it was estimated that transportation alone accounted for 27% of all carbon dioxide ($CO_2$) emissions emitted within Europe. Cars are responsible for 41% of these emissions and making cars contribute to a total of 11% of the European total carbon

dioxide emissions [2]. The car provides unprecedented mobility of an individual. It provides freedom, comfort, and convenient mobility from door to door. Perhaps this explains why the car has been widely embraced by society. Infrastructure and city planning are nowadays shaped by the existence of cars, therefore rendering a car a necessity for some people to accommodate to their daily life. However, the car is not merely a purely useful tool of transportation, but it is also subject to prestige, luxury, and desire. Competition amongst manufacturers of market shares drives developments that sometimes can be considered as abundant. Cars have been growing bigger, performance has become higher and the numbers of cars have increased historically [3]. Despite remarkable efforts to reduce emissions and fuel consumption from car engines during 100 years, the car sector remains the only one that has not managed to decrease its total $CO_2$ emissions in Europe in later years [2].

The evolution of personal transportation in the 21$^{st}$ century is facing substantial challenges to ensure that the urgent demand for decreased emissions of $CO_2$ and reduced air pollutions are met. Three main tracks are under consideration in the automotive industry as potential answers to these challenges: Electrification, hydrogen, and renewable fuels. A battery electric vehicle has several advantages such as zero tailpipe emissions, reduced noise, and reduced maintenance. Hydrogen can be used both to fuel a fuel cell which converts hydrogen to electricity, or as a fuel in an internal combustion engine. By using hydrogen, no $CO_2$ is emitted from the tailpipe since there is no carbon in the fuel. Renewable fuels are sourced from biological products, biomass, such as waste, crops, forest or even algae, and are created from absorbed $CO_2$ from the atmosphere. Hydrocarbon fuels can also be synthesized using atmospheric $CO_2$, commonly known as E-fuels. Renewable- and E-fuels result in a theoretical zero net $CO_2$ emission when they are burned since the $CO_2$-molecules emitted are reused again though absorption from the atmosphere. However, all these alternatives to conventional fossil fuels and internal combustion have drawbacks.

To charge a battery, produce hydrogen or convert biomass to fuel, energy is required. Energy, in the form of electricity, is in many times scarce and expensive. Approximately 63% of the global electricity is sourced from fossil sources such as coal, oil and gas [4, 5]. Another issue is the storage of energy. A modern lithium-ion battery has an energy density of approximately 0.26 kWh/kg [6]. Research prospects may increase this number by a factor of 10 in the future. As comparison, gasoline and diesel contains approximately 13 kWh/kg. Renewable hydrogen contains approximately 32.8 kWh/kg of energy, but has a very low volumetric energy density due to its low density [7]. When compressed to 700 bar, which requires substantial energy, hydrogen contains 1.3 kWh/L. In contrast, the renewable fuel ethanol contains approximately 6.4 kWh/L, or 8 kWh/kg on a mass basis, in liquid form [8]. Therefore, liquid hydrocarbons such as ethanol provides the most efficient storage of energy, both in terms of mass and space, of the three alternatives. The weight of the propulsion system, including the energy storage, is a very important factor in vehicles since it affects the vehicle weight and range. Additionally, manufacturing of batteries for battery electric vehicles requires substantial amounts of rare earth materials, which results in a higher environmental impact before the vehicle has left the factory. The process of synthesizing and compressing hydrogen is energy demanding. On the other hand, burning a hydrocarbon fuel in an internal combustion engine is rather inefficient. Market leading gasoline engines can reach 40% thermal efficiency, which means that 60% of the fuel energy is wasted as heat [9]. However, in reality, the thermal efficiency is significantly lower for most car engines during their daily use since the combustion engine rarely is utilized at its peak efficiency operating point.

Evidently, there is no clear answer to which propulsion system that is the most suitable. In recent years, a rapid electrification has been taking place, driven by factors such as beneficial legislation, zero tailpipe emissions, and increasing popularity. Despite this, it is still expected that internal combustion engines will provide a significant share of propulsion, either solely, or in combination with electrification, in the next coming decades [10]. Therefore, the continuation of developing the internal combustion engine will be important to provide clean, efficient, and affordable propulsion for future vehicles. The realization of zero net carbon internal combustion engines will be significant to meet the global need of environmentally friendly transportation.

One of the most common types of engines fitted to light duty vehicles, such as cars, is the spark-ignited engine. More commonly, the spark-ignited engine is known as the gasoline engine. In 2020, approximately 47.5% of all newly sold cars in Europe were fitted with a spark-ignited engine. An additional 11.9% were hybrid-electric cars, which are almost exclusively fitted with a spark-ignited engine [11]. During the third quarter of 2021, these numbers had changed to 39.5% gasoline cars and 20.7% hybrid-electric, respectively, indicating an overall increase of the market share of gasoline engines (58% versus 60.2%) [12]. These numbers do not include plug-in hybrid electric vehicles, which is an additional growing sector of cars that are commonly provided with gasoline engines. Globally, gasoline engines are even more frequent. In 2019, an estimated 78% share of cars sold globally were fitted with a gasoline engine, and the trend of sales is expected to follow a similar trend as the European with a decreasing share of solely gasoline engine propelled cars but with an increasing share of hybrid-electric powertrains [13].

The main reason for the popularity of the gasoline, spark-ignited, engine ought to be that they are less complex, and therefore cheaper, to build, compared to other types of engines such as diesel engines. Due to the spark-ignited engine being very common, it is therefore strategically motivated to direct efforts in improving this type of engines to maximize the total reduction of environmental impact from combustion engines. However, modern conventional spark-ignited engines have already been refined to a high level of matureness through decades of developments and are providing efficiencies that are ever closer to the theoretical limits, making it increasingly difficult to achieve further improvements of spark-ignited engine thermal efficiency.

Ambitious targets to reduce vehicle fleet average $CO_2$ emissions are enforced through legislation to push developments further. In the European Union, a 15% reduction in $CO_2$ emissions from new cars was enforced in 2021, and further reductions of 37.5%, compared to levels prior 2021, will be enforced in 2030 [14]. These challenges force consideration of non-conventional technological alternatives. Air-diluted spark-ignited combustion, known as lean combustion or lean burn, is one of such non-conventional alternatives, that can accomplish a significant efficiency increase in spark-ignited internal combustion engines. Despite being well-known, lean combustion has not yet seen a main breakthrough. There are two main types of lean spark-ignited combustion: stratified charge and homogeneous charge. Stratified charge denotes a stratification of the air and fuel mixture inside the combustion chamber. Stratified lean combustion has previously been introduced to the market but with limited success due to difficulties in managing $NO_x$- and soot-emissions. Additionally, the applicable operating range was limited to low engine loads [15, 16]. A homogeneous charge on the other hand, when sufficiently diluted with air, can produce very low $NO_x$-emissions, is less prone to form particulates during combustion, and is not limited in the operating range. Due to its advantages, the homogeneous mode has received increased attention by the research community in recent years. Additionally, developments in lean exhaust aftertreatment systems create new

opportunities of realizing lean combustion with clean tailpipe emissions, which has previously been difficult to achieve. The main drawback with a highly diluted homogeneous charge is that it is more difficult to ignite and combust, limiting the maximum applicable quantity of air-dilution. Combustion difficulties are commonly obtained at low load engine operation. At low loads, the charge motion inside the cylinder is less intense, and density and temperatures are lower which negatively impact combustion. These drawbacks present obstacles to industrial implementation and challenges to the research community.

Another more common strategy to reduce fuel consumption that has been widely adopted amongst car manufacturers during the last decade is engine downsizing. During regular driving, most of the engine operation time is spent producing only low torque at low speeds, seldomly exceeding 10% of the rated power capacity of the engine. This leaves most of the engine capability unutilized but also makes it more inefficient since combustion engines are generally more efficient at higher engine loads. Downsizing mitigates this issue by decreasing the engine displacement which forces the engine to work harder, relative to its size, to produce the same power output as a larger engine. By downsizing, the engine operating point of maximum engine efficiency therefore comes closer to the point of maximum time-density of regular driving. To compensate for the lower displacement and corresponding loss of maximum power, downsized engines are commonly equipped with turbochargers to preserve the peak torque and power output compared to their larger counterparts. Another advantage of a small, turbocharged engine is that it will become a more frequent utilizer of the turbocharger which, if properly designed, can positively contribute to the overall engine efficiency. It is common that the specific engine load of the downsized engine is doubled compared to a naturally aspirated engine. However, such high specific loads result in problems with heat, pressure, and auto-ignition. Therefore, downsized engines are usually forced to adapt non-ideal mitigation techniques such as ignition retardation or fuel-enrichment to decrease thermal loading and auto-ignition during high load operation. This penalizes the fuel efficiency and emission footprint, especially if the engine is utilized in high load conditions such as uphill or aggressive driving. Additionally, since 2021, all new cars sold in Europe must comply with the Euro 6d legislation which includes the real driving emissions (RDE) test procedure [17]. The RDE test makes it challenging for a heavily downsized engine to reach its rated power when conventional over-fueling cannot be used.

## *1.1 Objectives*

The research described in this thesis aims at investigating the potential synergetic combination of downsized spark-ignited engines and homogeneous lean combustion to improve internal combustion engine thermal efficiency, addressing the need to reduce the environmental impact of transportation. Previous research has indicated that the stability of homogeneous lean combustion benefits from engine operation at higher loads. Increased engine loads increase charge temperature and turbulence, which promotes combustion of a lean charge. Homogeneous lean combustion has also been shown to decrease combustion temperatures which can be utilized for mitigation of auto-ignition. This capability to mitigate auto-ignition is beneficial especially for downsized engines operating on elevated loads and it may reduce or eliminate the need for over-fueling.

To realize applicable homogeneous lean combustion in a downsized engine, the following investigation with main objectives were defined:

- Achieve an engine load of 16 bar brake mean effective pressure (BMEP) with highly diluted homogeneous lean combustion by turbocharging.
- Determine any potential boundaries which limits maximum applicable engine load with lean combustion.
- Achieve low engine out $NO_x$-emissions, sub 1 g/kWh.

# 2 Theory, Literature Review and Gap of Knowledge

This chapter serves to introduce the reader to the combustion engine and homogeneous lean combustion.

## *2.1 Internal Combustion Engines*

Car engines are almost exclusively part of the category of reciprocating, four-stroke, internal combustion engines. These engines utilize internal combustion to convert chemical energy of a fuel to mechanical work that provides propulsion. This process is conducted in four strokes. Reciprocating engines consist of a crankshaft, an engine block with cylinders containing pistons connected to the crankshaft by connecting rods, and a cylinder head which manages the exchange of gasses through the engine. Each stroke is half a turn of the crank shaft and the strokes consist of intake, compression, combustion-expansion, and exhaust. A complete cycle consisting of the four strokes is commonly known as an engine combustion cycle and corresponds to two turns of the crank shaft, or 720° crank angles.

Combustion is a chemical process where combustible molecules are oxidized by oxygen to a lower state of potential energy which results in the release of chemical energy as heat. The release of heat results in expansion of the combustion gasses which creates an increase in pressure. This pressure is harvested as work by the piston inside the engine cylinder. The piston transfers the work to a crankshaft which results in torque that can be used for propulsion. Combustion in a spark-ignited (gasoline) engine is regularly stoichiometric. This means that there is a balance between fuel and oxygen molecules so that all hydrogen atoms of the fuel can be oxidized to form water, and all carbon atoms of the fuel oxidized to carbon dioxide. As an example, consider the oxidation of the simplest hydrocarbon molecule, methane ($CH_4$):

$$CH_4 + 2(O_2 + 3.77N_2) \rightarrow CO_2 + 2H_2O + 7.55N_2 + Q \quad (1)$$

$Q$ denotes the energy released through oxidation. Apart from oxygen, atmospheric air also consists of approximately 79% nitrogen ($N_2$). Nitrogen is however a stable and non-reactive molecule at most cases and is ideally not involved in the combustion process. Depending on the amount of carbon and hydrogen for various fuels, the stoichiometric air-fuel ratio (AFR) change. Fuels such as alcohols also contain fuel-bond oxygen. The stoichiometric air-fuel ratio is commonly defined on a mass basis as:

$$AFR_{stoichiometric} = \left(\frac{m_{air}}{m_{fuel}}\right)_{stoichiometric} \quad (2)$$

The reaction described in Equation 1 is a gross simplification of the actual reaction scheme of fuel oxidation and only shows ideal start- and finish products. In reality, there are hundreds of various intermediate reactions taking place when the fuel molecules are decomposed and partially oxidized to various non-equilibrium states depending on the varying combustion temperatures [18].

### 2.1.1 Spark Ignition versus Compression Ignition

Two main types of reciprocating internal combustion engines exist: spark-ignition (gasoline) and compression-ignition (diesel) engines. Spark-ignited engines are also referred to as Otto-engines since they work by the principle of the idealized

thermodynamic Otto-cycle, named after its inventor Nicolaus Otto. Compression ignition engines work by the ideal Diesel-cycle, named after Rudolf Diesel. In a spark-ignition engine, the air and fuel are pre-mixed prior to combustion and the combustion is initiated by a spark. A compression-ignition engine on the other hand injects the fuel directly into the cylinder to initiate combustion.

The two types of combustion modes are referred to as pre-mixed combustion and diffusion combustion respectively, and there exist some fundamental differences between them. In pre-mixed homogeneous combustion, the fuel and air are mixed inside the cylinder and compressed during the compression stroke. This means that the fuel, during compression and combustion, must persist autoignition prior to being intentionally consumed by the progressing flame. A measure of the persistence to autoignition of the fuel is the octane rating number. Due to the imminent chance of auto-ignition, the compression ratio must be limited in a spark-ignited engine utilizing pre-mixed combustion.

In diffusion combustion, the fuel is injected into the cylinder and mixed with the air during the combustion which means that the fuel cannot auto-ignite prior to the intended combustion. A compression-ignition engine with diffusion combustion can therefore operate on a significantly higher compression ratio. High compression ratio is also necessary to heat the charge air during compression sufficiently for the fuel to ignite during injection. Fuels used in compression-ignition engines should have a low octane rating, and a high cetane rating instead.

A spark-ignited engine is controlled by a throttle which governs the amount of air that is admitted into the cylinders. Depending on the amount of air, a certain amount of fuel is added to the air so that a certain air-fuel ratio is maintained, stoichiometric in most cases. The amount of fuel is proportional to the resulting torque output of the engine. Throttling does however result in pumping losses which reduces the overall fuel efficiency. A compression-ignition engine is solely controlled by the amount of fuel that is injected into the cylinders. The fuel injection is independent of the amount of air inside the cylinder, as long as there is sufficient oxygen to oxidize all of the injected fuel. This means that a compression-ignition engine can operate without a throttle and hence without any additional pumping losses.

The main drawback of a compression-ignition engine is that the diffusion combustion results in more particulate emissions. Also, a compression-ignition engine normally operates with lean combustion which means that a standard three-way catalyst cannot be used to clean $NO_x$-emissions, as can be done on a stoichiometric spark-ignited engine. The direct injection of fuel at ultra-high pressures, often in the range of 2500 bar, also requires a more sophisticated and expensive fuel system. The spark-ignited engine on the other hand is less complex, allows a “simpler” means of achieving clean emissions and is therefore cheaper to make. However, the fuel efficiency of a spark-ignited engine is lower compared to a corresponding compression-ignition engine, due to the need for throttling, limited compression ratio, and higher heat losses.

### 2.1.2 Ignition and Flame Development

In pre-mixed spark-ignited combustion, the ignition and consecutive flame development is essential. The spark initiates an exothermic reaction that is the progressing self-sustaining flame front that consumes the unburned mixture. The unburned mixture is also called the cylinder charge.

The ignition is commonly accomplished by an ignition system constituted by a transistor coil and a spark plug. Alternative systems will be presented later in this thesis. The working principals of spark-ignition have been rigorously entailed by Heywood, Keck et al., Baritaud [19-21], and others and will be briefly described here. The spark plug has commonly two electrodes: cathode and anode (ground). At the event of ignition, the coil releases its energy which results in a large voltage over the spark plug electrodes, around 10 kV. The gas between the electrodes ionizes and dissociates in a phase that is called the breakdown phase. This phase is very rapid and efficient. When the voltage is sufficiently high, and the impedance in the space reduced due to the ionization, electrons start to flow in the electrode gap creating an arc which is denoted the arc phase. During the arc phase, the voltage drops, and current flow maximizes. The arc is sometimes referred to as a thermal plasma and much energy is dissipated from the arc as heat to the electrodes and surrounding gasses. The dissociation of molecules and the heat due to the breakdown, and arc, initiates exothermic reactions which grow into a kernel. If sufficient energy is supplied, the kernel grows into a progressing laminar flame. The kernel and flame have a very thin reaction zone which is the flame front which separates the unburned and burned gasses, and within the reaction zone, the oxidation occurs. For the flame to progress, it must have sufficient temperature and size to sustain the reactions in the reaction zone, which should exceed the energy that is dissipated to the surrounding. If the kernel size and temperatures are insufficient, the kernel quenches and reactions stop. If the flame progresses and reaches sizes in the same length scale as the smallest turbulent length scale, the flame front is wrinkled and transitions into a turbulent flame. The flame progresses and is partly displaced by the expanding hot burned gasses. The corresponding buildup in temperature due to the closed volume of the combustion chamber which consist of the cylinder and piston increases the flame speed. Eventually, the flame transitions into a fully developed flame that quickly consumes the remaining charge. Additional pressure buildup inside the combustion chamber due to the position of the piston, with corresponding additional increase in end-gas temperatures as a result, aids this process.

## 2.2 Lean Combustion

Lean combustion offers the opportunities to mitigate some of the characteristic drawbacks of the spark-ignited engine. Lean combustion is realized by the addition of excess air to the stoichiometric mixture, which results in a so-called over-stoichiometric mixture. For example, if an additional 50% air is added to the combustion of methane, the theoretical reaction corresponds to:

$$CH_4 + 3(O_2 + 3.77N_2) \rightarrow CO_2 + 2H_2O + 11.31N_2 + O_2 + Q \quad (3)$$

As can be seen in Equation 3, lean combustion results in additional nitrogen and unburned oxygen among the combustion products on the right-hand side of the equation. The fundamental combustion process does however remain the very same as with stoichiometric combustion. The addition of excess air to the combustion process is called air-dilution. To quantify the amount of air-dilution, the relative air-fuel ratio, lambda (λ), is commonly used, which is defined as:

$$\lambda = \frac{\left(m_{air}/m_{fuel}\right)_{actual}}{\left(m_{air}/m_{fuel}\right)_{stoichiometric}} \quad (4)$$

Another common measure of the amount of air-dilution is the equivalence ratio, phi (φ), which is the inverse of the relative air-fuel ratio. Lambda = 1 denotes stoichiometric combustion, while lambda > 1 denotes fuel-lean combustion and lambda < 1 denotes fuel-

rich combustion. The example of lean combustion provided in Equation 3 corresponds to a relative air-fuel ratio, lambda, of 1.5.

### 2.2.1 Historical Perspective of Lean Combustion

The research field of lean combustion in spark-ignited engines has a surprisingly long history, dating back as far as the beginning of the 20$^{th}$ century. In 1908, professor Bertrand Hopkins realized the importance of leaning out the air and fuel mixture, creating what was then called a weak mixture, in spark-ignited internal combustion engines to increase thermal efficiency [22]. The work published by Hopkins ought to be one of the earliest publications available in the topic. Hopkins pointed out two main causes of the lean combustion superiority; Firstly, the ideal thermal efficiency was improved by weaker mixtures since weaker mixtures increased the specific heat capacity of the working gasses. In other words, it meant that by an increased share of air in the mixture, the combustion cycle came closer to resemble the ideal air cycle. The ideal air cycle is the corresponding thermodynamic cycle of which highest theoretical thermal efficiency can be obtained of an internal combustion engine consuming air. Secondly, Hopkins highlighted that combustion of weaker mixtures also resulted in less heat losses to the cylinder walls. Hopkins proved his suggestion by experimental investigations in a 40 Bhp Crossley-engine running on coal-gas, equipped with a then state-of-the-art optical indicator to obtain cylinder pressure diagrams.

Another example of early pioneering work is the investigations made by Sir Harry Ricardo. In 1920, Ricardo conducted research on how to reduce thermal loading on the combustion chamber components by utilizing lean combustion and supercharging [23]. During his research, Ricardo identified problems with ignition of the lean charge, and therefore implemented the use of a so-called stratified charge to allow reductions in the global mixture strength with maintained ignitability. Stratification works by locally increasing the ignitability and flame speed by introducing a richer portion of air-fuel mixture near the spark plug inside the combustion chamber which improves the initial combustion. By doing so, very lean global air-fuel mixtures can theoretically be combusted with maintained stability and robustness.

Despite some promising studies and the evident theoretical advantages, lean combustion did not seem to attract engine manufacturers, perhaps due to the practical issues. The hydrocarbon fuels used in spark-ignited engines proved difficult to ignite using lean mixtures, partly due to undeveloped carburetor techniques and weak ignition systems. Efforts made to reduce engine auto-ignition resulted in progressively less volatile fuel which in turn proved even more disadvantageous for ignitability [24]. It also became clear that lean combustion was sensitive to variations in operating conditions. Additionally, other issues such as maldistribution in multi-cylinder engine inlet-manifolds further implicated the use of lean combustion. Instead, most engines operated on rich mixtures to account for the manifold maldistributions, the poor ignitability, and the poor evaporative capability of the current carburetors. Apart from worse fuel economy, operating stoichiometric, and particularly fuel-rich, would inevitably result in significant carbon monoxide and hydrocarbon emissions. These were some issues noted by Bolt and Holkeboer who were amongst the researchers that showed further interest in lean combustion in the sixties. In 1962, they conducted a study on the influence of compression ratio upon lean combustion and lean combustion limitations. They commented in their discussion that “future engines will undoubtedly run lean on part load” [25]. In 1967, Bolt and Harrington further investigated the influence of mixture motion on combustion stability and characteristics of lean charges, in a constant volume

combustion bomb [26]. Their research effort was driven by indications from contemporary research that variations in the in-cylinder flow were the principal cause of combustion instability.

Additionally, during the sixties the effects of vehicle emissions started to become a major concern. This led to legislative actions such as the introduction of the Clean Air Act in the USA by 1970 [27]. In 1968, Lee and Wimmer emphasized the need for reduced noxious emissions such as hydrocarbons (HC), carbon monoxide (CO) and nitrogen oxides ($NO_x$), and therefore studied the combination of various fuels and lean combustion to reduce those emissions, with promising results [28]. Similarly, in 1971 Tanuma et al. turned to lean combustion to reduce pollutant emissions and studied means of improving lean combustion such as turbulence, spark energy and combustion chamber geometry [29]. Consequently, due to the oil crisis of 1973 which caused a drastic increase in global market oil prices, there was an increased demand for more fuel-efficient vehicles. During the seventies, several automakers introduced lean combustion in production engines to meet these demands. The need for fuel efficiency sparked development efforts in the field of lean combustion which led to the emerge of a technology called pre-chamber stratification. The pre-chamber provided a means of mechanical stratification through rich fuel injection in the pre-chamber. With a spark plug located inside the pre-chamber, ignitibility issues (common to regular combustion chambers and lean mixtures) were improved. Pre-chambers were incorporated by Honda in their so called CVCC (compound vortex-controlled combustion) engine. Toyota introduced their corresponding TGP system (turbulent generating pot) [30, 31]. Other manufacturers such as Chrysler developed an electronically controlled homogeneous lean combustion system called ELB (electronic lean burn), and Ford developed a direct injected stratified engine called PROCO [32]. Despite significant progress in technology development, and introduction of the lean combustion engine to the market, lean combustion engines did not reach any breakthrough and remained mostly marginalized. In reality, harsh engine running, poor acceleration capabilities, remaining problems with fuel distribution in the engines and occasional misfires were strongly discouraging arguments, as pointed out by Germane et al. in their review of lean combustion in -83 [33]. They also concluded that the pre-chamber technology failed due to cost, auto-ignition tendencies and sensitivity to residual gasses in the combustion chamber. Yet, Germane et al. also praised the concept of lean combustion as a promising technology for the future.

In parallel to the work in lean combustion technology, progress was being made in developing catalytic converters as an alternative mean of reducing noxious emissions. From 1975, most new vehicles in USA were equipped with so-called two-way catalysts, that could oxidize carbon monoxide and hydrocarbon emissions, to comply with the regulations posed by EPA [27, 34]. Later, the three-way catalyst was developed which provided the additional capability of reducing nitrogen oxides. In 1976, Volvo Cars introduced the exhaust gas oxygen sensor (Lambda sensor) to control the catalytic converter system and by 1988 approximately 70% of newly produced cars by Volvo were equipped with this system [35, 36]. The three-way catalytic converter provided the possibility to operate an engine with stoichiometric combustion and simultaneously achieve clean emissions, free from unburned hydrocarbons, carbon monoxide and nitrogen oxides. Stoichiometric combustion is more stable and robust as opposed to lean combustion and therefore preferrable from a manufacturer's perspective. With a catalytic converter that enabled compliance with emissions legislation, little incentives remained to keep investing in inconvenient alternative combustion processes. Since it emerged, the

three-way catalyst became standard equipment on most spark-ignited engines and that still holds true today.

In the nineties, lean combustion received renewed attention through a reawaken interest in stratified combustion. Stratified combustion became the latest technology in-line believed to answer the need for further improvements in fuel efficiency of spark-ignited engines. New more modern combustion systems with four valve cylinder heads and electronic fuel-injection enabled better control of the combustion process, which improved the prospects of utilizing the sensitive lean combustion mode. One of the concepts which was investigated in the field of stratification was the barrel stratification. Barrel stratification was introduced by intake port fuel-injection in one of the two intake ports, together with an in-cylinder tumble-flow. This created a vertical separation in the cylinder creating two halves consisting of a rich and a lean portion. The barrel stratification resulted in a stratified charge that was easier to ignite and combust which meant that higher air-fuel ratios could be achieved, compared to a regular homogeneous lean charge [37, 38]. With the emerge of the technology of direct-injected fuel into the cylinder, further opportunities arose to implement in-cylinder stratified lean combustion. One such system was developed by Mitsubishi, where they used a reverse tumble flow and a wall guided fuel injection system [39]. A similar system was developed by Toyota that incorporated swirl flow [40]. Additionally, AVL imposed a tumble-based wall guided direct injection system. AVL did however conclude that the stratified lean operation was limited to low loads due to issues with smoke and $NO_x$ emissions [41]. The wall-guided systems were also troublesome due to the inevitable wall-wetting by fuel of the piston surface, creating high levels of soot, and most manufacturers focus on spray- or air-guided systems today [42].

Again, difficulties in managing emissions and increasingly stringent emission legislation proved troublesome for lean combustion to be utilized on the market. Around 2008, a lean $NO_x$ aftertreatment technology was commercialized to cope with Tier 2 and Euro 5 regulations that could solve the problems with lean combustion emissions [43]. The system was called the lean $NO_x$ storage catalyst, or lean $NO_x$ trap (LNT). Combustion deficiencies from lean combustion, resulting in $NO_x$, could now be managed by exhaust after-treatment, in the same manner as the three-way catalyst saved stoichiometric combustion. The system was implemented in the BMW 120i from 2007, which utilized a combination of stratified lean combustion at low loads and homogeneous lean combustion at intermediate loads [44]. Similarly, Mercedes developed and launched direct injected spray-guided stratified engines from 2006. Later, Mercedes introduced their so called BlueDIRECT. This system was based upon precision direct injection which enabled spray guided stratification. Engines with stratified lean combustion were utilized together with a lean $NO_x$ storage catalyst in several of Mercedes powertrains from 2012, but have later been discontinued [45, 46]. Another example of lean combustion technology that has been introduced to the market is the Volkswagen FSI engines, that were originally stratified lean. FSI stands for fuel stratified injection and the brand has persisted for many years, despite that the engines have been produced with homogeneous combustion technology in later years. Some Japanese carmakers also persisted in producing lean combustion engines, which were available on the market between the early nineties until approximately 2005. Honda used the VTEC engine which in different versions was adapted to lean combustion. One of them; the VTEC-E. The VTEC-E engine was operated on port injected stratified lean combustion with in-cylinder swirl [38].

In reality, the bulk flow and turbulence makes it difficult to position the richer (ignitable) portion at the desired location inside of the cylinder in a stratified combustion system.

Another issue is that higher combustion temperatures are generated when burning a local richer mixture, which increases the formation of $NO_x$ [47]. Additionally, if the stratified local air-fuel mixing is poor and wall wetting occurs, then the consecutive combustion is likely to cause significant soot formation and therefore particulate emissions [48, 49]. Also, a major drawback of lean $NO_x$ adsorbers is that they frequently need to be regenerated to reduce and purge the stored $NO_x$ molecules. The regeneration causes a fuel penalty that diminish the gains from lean combustion. Additionally, the emission legislation is consistently being revised to become more restrictive, making it harder to achieve lean combustion combined with tailpipe emissions complying with these regulations. Between 2015 and 2021, there has been little activity reported from industry regarding the production of lean combustion spark-ignited engines for market purposes. Despite a long history of evolution and with consistent progress in understanding the phenomena behind the challenges of lean combustion, improved technology, and emerging after-treatment for $NO_x$ reduction; lean combustion has not yet seen a major, permanent breakthrough on the market. It appears that the interest for lean combustion is periodically awoken when demands for further improvements in fuel efficiency (or $CO_2$ reduction) are imposed, but the interest is repeatedly diminished when other, less complex or more robust solutions are discovered that fulfill the current needs. Despite development in engine technologies, the challenge remains to achieve desired fuel efficiency gains from lean combustion, in combination with low tailpipe emissions. Perhaps will the decade of 2020, that precedes the introduction of the toughest demands on combustion engines ever seen, be the time when market introduction of lean combustion finally will succeed.

### 2.2.2 Advantages of Lean Combustion

With the historical perspective of the lean combustion research field in mind, it is safe to state that the working principles and the benefits that can be derived from air-diluted combustion are very well known. As discovered over 100 years ago, when the share of air is increased in the fuel air mixture, the share of two-atom molecules in the air-fuel mixture increases which increases the ratio of specific heats $\gamma$. The ratio of specific heats is the ratio of the heat capacity of a fluid, at constant pressure, $c_p$, and constant volume, $c_v$:

$$\gamma = \frac{c_p}{c_v} \tag{5}$$

This has a direct effect on efficiency, given by the classical equation of ideal thermal efficiency, $\eta_t$, of the Otto-cycle:

$$\eta_t = 1 - \frac{1}{{r_c}^{\gamma-1}} \tag{6}$$

$r_c$ denotes ratio of compression, commonly known as compression ratio. Thus, as can be concluded from equation 6: the higher the share of air, the higher the theoretical thermal efficiency, until the ideal air-cycle is reached and there is no fuel left in the combustion. The ratio of specific heats can be considered as a measure of how much work that can be extracted from a fluid when a certain amount of heat is added. The influence of increased air dilution, and the corresponding increase of the ratio of specific heats, is illustrated in Figure 1.

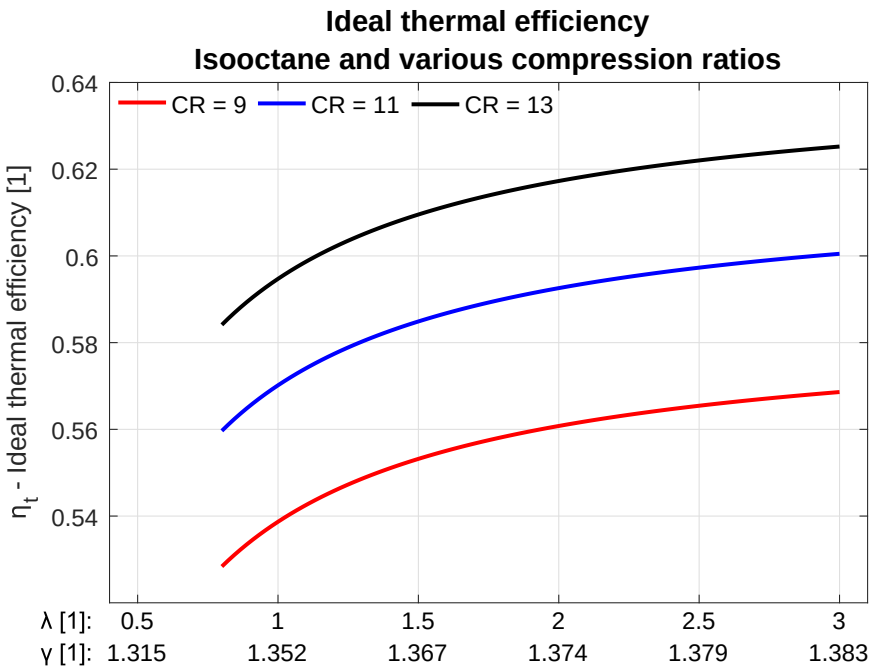


*Figure 1. Ideal thermal efficiency computed for various mixtures of isooctane and air defined by the relative air-fuel ratio lambda (λ). With increased lambda, the ratio of specific heats (γ) increases proportionally, as indicated on the x-axis. Three compression ratios have been included as example. Atmospheric conditions. It should be noted that the presented ideal efficiencies are ideal, thus not considering any losses. In reality, the numbers are significantly lower.*

When the cylinder charge is diluted, the flame temperature and therefore the combustion temperature, decreases. This results in a lower thermal gradient between the combustion chamber walls and the combustion gasses. The reduced thermal gradient means that less heat is conducted through the combustion chamber walls and therefore less energy is lost as heat losses to the engine coolant and surroundings. The heat losses are a particularly important factor in spark ignited engines since stoichiometric combustion burns with high flame temperatures. Most of the heat from the fuel is released through combustion close to the top dead center position of the piston, at the beginning of the expansion stroke. This means that the combustion chamber is exposed to hot gasses for a comparatively long time while the piston expands the gasses during the expansion stroke. At many operating conditions, the heat losses are the single largest source of energy loss and may be larger than the actual output of useful work. An example of the influence of increased air dilution on the in-cylinder maximum gas temperatures and the effect on the corresponding heat losses are shown in Figure 2.

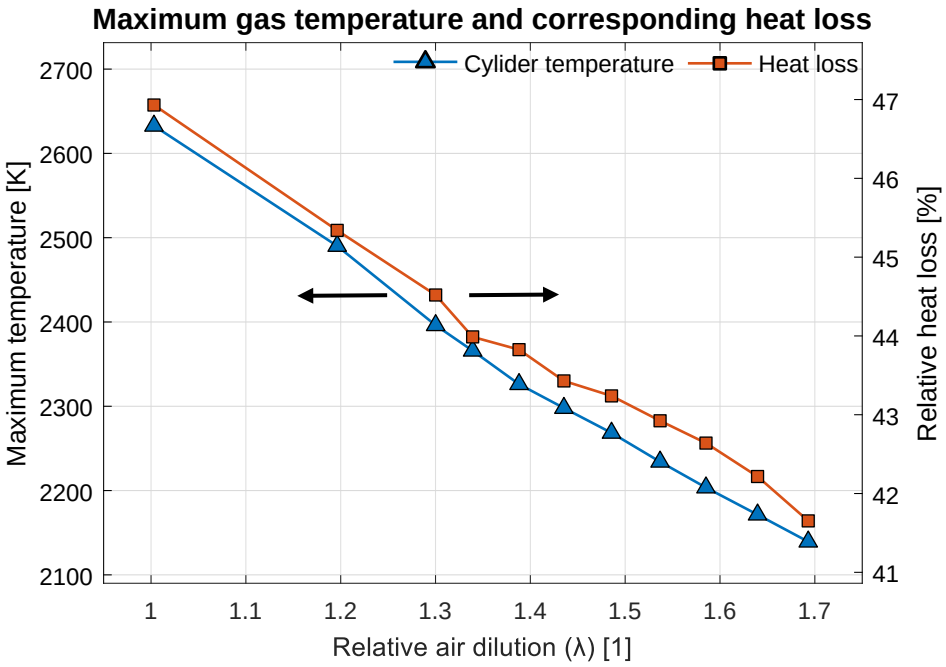


*Figure 2. Maximum in-cylinder temperature of gasses and the corresponding relative heat losses as share of supplied fuel energy, at an engine speed of 2000 rpm and load of 2.62 bar BMEP, at various relative air-fuel ratios lambda. Cylinder temperature extracted from GT-Power simulations calibrated by experimental data from campaign 4. Heat loss computed according to Clasén et al. [50].*

As can be observed from the results presented in Figure 2, the maximum in-cylinder gas temperature exceeds 2600 K. When the fuel molecules are oxidized through combustion, various intermediate species are formed which constitute the burnt gasses. These intermediate species are equilibrated to various states depending on the temperature of these gasses. When the piston expands the gasses, the temperature drops quickly and freezes further reactions. This causes some of the intermediate species to remain in a non-equilibrium state, such as carbon monoxide. This phenomenon is called dissociation losses and is very much dependent on the combustion temperature. The dissociation losses prevent a homogeneous, stoichiometric mixture to be fully oxidized into the desired products that were shown in Equation 1. It also results in some undesired noxious biproducts to remain post combustion, such as nitrogen oxides (NO and $NO_2$) [51, 52]. Another issue with stoichiometric combustion is that, even if the overall mixture is stoichiometric, there may be spatial variation of the air-fuel ratio (inhomogeneities) which causes some parts of the mixture in the combustion chamber to burn rich, and other to burn lean, which also impedes the ability to fully oxidize the fuel. Dissociation- and inhomogeneity losses are commonly noted as combustion inefficiency and can be measured by the concentration of leftover unburned and partially oxidized fuel in the exhaust stream. These unoxidized or partially oxidized constituents contains chemical energy that is unutilized. Lean combustion lowers the combustion temperatures significantly, which results in the intermediate species to equilibrate to a lower state post combustion in the burned gasses. Also, the additional air and therefore additional oxygen molecules, result in a higher average air-fuel ratio in the combustion chamber, which reduces the probability of forming fuel-rich portions in the combustion chamber. This in turn reduces the probability of local rich combustion. Homogeneous lean combustion has been shown to reduce the number of particulates by approximately two orders of

magnitude at certain conditions, compared to stoichiometric combustion [49]. An example of the effect of air-dilution on combustion inefficiency, or combustion losses, is illustrated in Figure 3. As can be observed in the illustration of Figure 3, the decrease of combustion losses is not monotonous throughout the range of air-dilution, an observation that will be discussed later in the section of disadvantages.

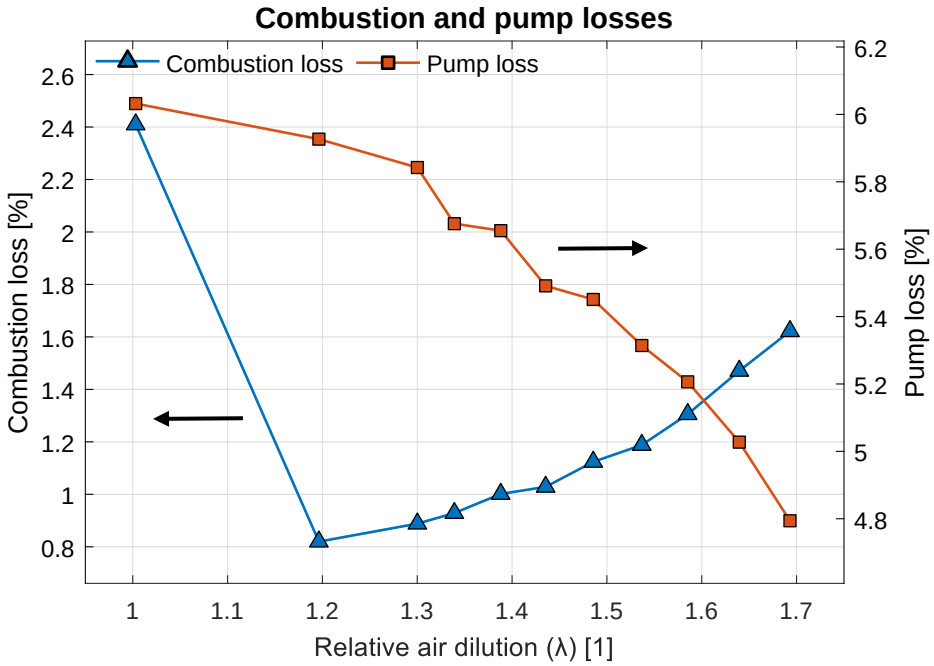


*Figure 3. Relative combustion- and pumping losses as share of supplied fuel energy versus relative air dilution lambda, at an engine speed of 2000 rpm and load of 2.62 bar BMEP. Experimental data from campaign 4.*

Another positive impact of lean combustion, air-dilution, is that the additional mass flow of air may reduce pumping losses. The corresponding effect of air-dilution on pumping losses were illustrated in Figure 3, in combination with the previously discussed combustion losses. Since higher air mass flows are required to obtain lean combustion, less throttling of the inlet air flow is necessary and pumping losses are therefore reduced. This is an important aspect of part load engine operation since pumping losses can be substantial at low engine loads. Pumping losses are not the single greatest contributor to inefficiency but the majority of operation of combustion engines is spent at low loads, where the pumping losses are the greatest. Therefore, even small improvements in terms of pumping losses provide high yields in total real life fuel efficiency. Ideally, a lean burn engine should accept such amounts of air-dilution that the engine could operate with the throttle fully open at idling, hence eliminating the throttle and corresponding pumping losses completely, like a diesel engine. Pumping losses have been partly mitigated by the utilization of the downsizing concept, but still remains as a significant source of losses.

In Figure 4, an example is visualized including two pie charts that illustrate the major shares of various energy outputs of the corresponding converted chemical energy of the injected fuel, from within the combustion chamber of a spark-ignited engine. An example with stoichiometric combustion is illustrated to the left, and a lean to the right. Common of them both is that the work output in watts is approximately the same. Due to an increase in net thermal efficiency, the required amount of fuel energy to produce the same power decreases, when introducing lean combustion. Net thermal efficiency corresponds to the

share of net work, that is the useful work output from the piston that is transferred to the crankshaft. In addition to heat-, pump-, and combustion losses, Figure 4 presents an additional fourth source of losses that are exhaust losses. Exhaust losses are the enthalpy of the hot burned gasses that are expelled into the exhaust system during the exhaust stroke. Since lean combustion decreases the combustion temperatures, it also lowers exhaust temperatures which reduces the amount of wasted exhaust enthalpy.

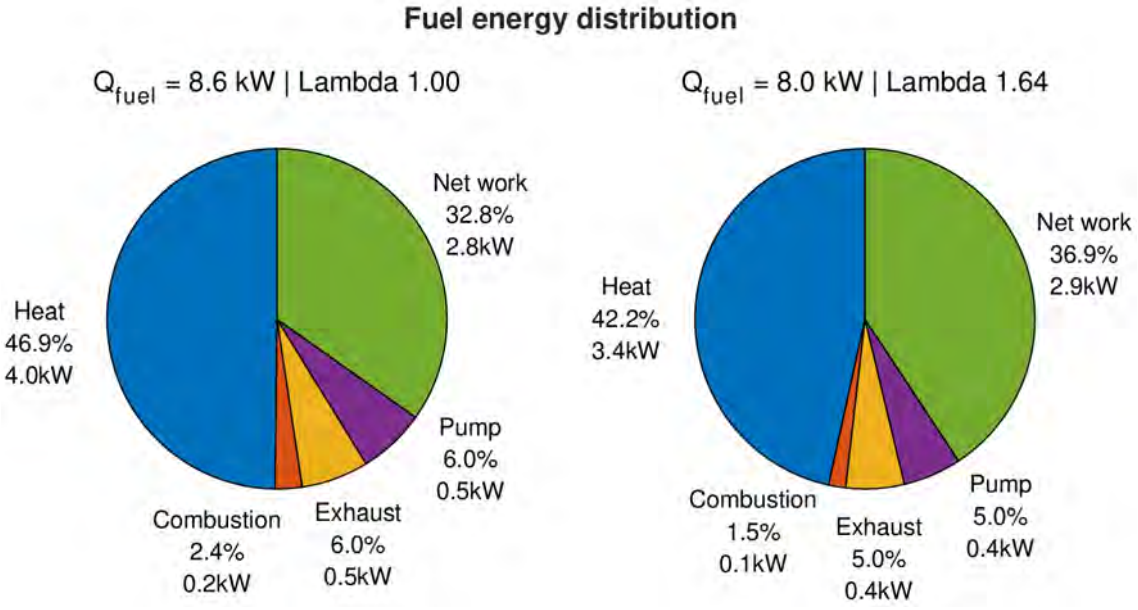


*Figure 4. Indicated distribution of provided fuel energy at an engine speed of 2000 rpm and ~2.62 bar BMEP. Left: Stoichiometric combustion. Right: Lean combustion. Experimental data obtained from measurement campaign 4. Energy balance computed according to Clasén et al. [50].*

### 2.2.3 Disadvantages of Lean Combustion

Due to the excess oxygen in the exhaust gasses from lean combustion, it is not possible to reduce nitrogen oxides with a regular three-way catalyst [53]. Therefore, emissions of $NO_x$ have become the main challenge of lean combustion concepts. Due to this aspect, the success of lean combustion relies upon the ability to achieve sufficiently low $NO_x$ emissions, low enough so that the emissions become negligible or manageable by a so-called lean $NO_x$ exhaust aftertreatment system. Common to all existing lean $NO_x$ aftertreatment systems is that they impose a penalty proportional to the $NO_x$ emissions. The penalty consists either of additional fuel that must be used to regenerate (or purge) the lean $NO_x$ aftertreatment system, or by a $NO_x$ reducing agent. Another issue is that lean combustion generally results in deceased exhaust temperatures which may reduce the rate of exothermic reactions in the aftertreatment system catalysts. The reduced exhaust temperatures also make it more difficult to reach light-off- or activation temperatures of the catalysts during cold engine start-ups.

Nitrogen oxides are formed during combustion and are prevalent to most engine types and combustion processes. The largest source of is the so called thermally formed nitrogen oxides, which originates from oxidation of atmospheric molecular nitrogen. The most prevalent type of nitrogen oxides is NO, but significant shares of $NO_2$ can also be obtained particularly with large excess of oxygen. The arbitrary mix of NO and $NO_2$ is known as $NO_x$. The mechanism of the formation of nitrogen oxides is commonly referred to as the (extended) Zeldovich mechanism [54]. The formation of thermal $NO_x$ is highly

nonlinearly dependent on temperature, and significant formation through various reactions starts to occur at temperatures at or above approximately 1600 K [19]. The reactions that form $NO_x$ are fast and may achieve temporal equilibrium in the hot burned gasses during the combustion event. The mechanisms of the reverse reactions are however much slower, and a majority of the formed $NO_x$ molecules fail to re-equilibrate during the expansion stroke which is why they freeze in a non-equilibrium state and remains as $NO_x$-molecules. This is because the fast expansion results in a rate of reduction of the temperature of the burned gasses which is faster than the rate of reverse reactions that may decompose the $NO_x$-molecules [51].

Since the combustion temperatures decrease with increased amount of air-dilution, as was demonstrated in Figure 2, it is desirable to maximize air-dilution to achieve maximum suppression of $NO_x$ formation. An example of $NO_x$-emissions in relation to air-dilution is shown in Figure 5.

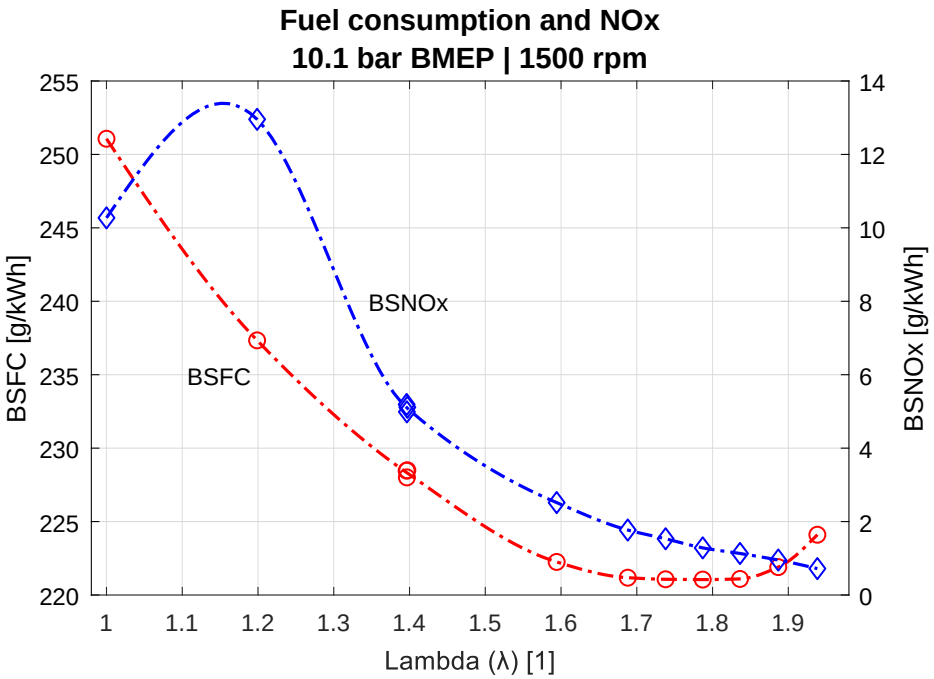


*Figure 5. Engine out Brake specific $NO_x$ emissions (BSNOx) and brake-specific fuel consumption (BSFC), versus lambda. The graph of $NO_x$ illustrates how the $NO_x$-emissions increase when lambda is increased from stoichiometry to slightly lean, lambda = 1.2, and then steadily decrease when exceeding lambda = 1.4. Additionally, the graph of BSFC illustrates an increase in fuel consumption at very lean operation (lambda > 1.85) due to increased combustion instability.*

As can be observed in Figure 5, the reduction of $NO_x$-emissions due to increase amount of air-dilution is not monotonous. Adding small amounts of air-dilution results in a significant increase of the $NO_x$-emissions to levels exceeding the stoichiometric conditions. This is due to the excess oxygen present during combustion that aids the oxidation of nitrogen. However, the encouraging effect is not proportional to the amount of air-dilution but diminishes after lambda = 1.2. Instead, the effect of dilution that lowers the flame and gas temperatures takes over at dilution rates beyond lambda = 1.4 which suppresses formation of $NO_x$ and leads to a steady decrease of the $NO_x$-emissions. Due to the "$NO_x$-bump", it is particularly undesirable to operate an engine with small amounts of air-dilution since the corresponding $NO_x$-emissions would become substantial and unmanageable. The "$NO_x$-bump" is also problematic when an engine performs a mode

switch, i.e., changes from stoichiometric operation to lean, or vice versa, because the engine will pass over the "bump" during the switch which causes a temporal spike of $NO_x$-emissions.

With increased amount of air-dilution, the adiabatic flame temperature decreases, and so does the flame speed. When the unburned mixture of fuel and air is diluted, the amount of heat released from the flame is absorbed by a larger mass which reduces the temperature of the flame. In other words, this means that there is less available chemical and corresponding thermal energy per unit mass of cylinder charge in the reaction and preheat zone of the propagating flame, which in turn results in a slower reaction. The flame speed of a pre-mixed, quiescent mixture is called the laminar flame speed. A correlation of laminar flame speed, $S_L$, of isooctane versus equivalence ratio (inverse of lambda), temperature and pressure has been proposed by Heywood [19] as:

$$\begin{gathered} S_L = S_{L,0}\left(\frac{T_u}{T_0}\right)^{\alpha}\left(\frac{P_u}{P_0}\right)^{\beta} \\ \alpha = 2.18 - 0.8(\phi - 1) \\ \beta = -0.16 + 0.22(\phi - 1) \end{gathered} \tag{7}$$

A more elaborated model of laminar flame speed has been proposed by Amirante et al. [55], which is illustrated in Figure 6. Figure 6 shows that the laminar flame speed decreases substantially with increased air-dilution. Increased temperature of the mixture, prior to combustion, increases the laminar flame speed, while increased pressure decreases the flame speed. The decrease in flame speed from increased pressure is due to that the thickness of the reaction zone of the flame decreases, which in turn decreases the flame's consumption rate of unburned mixture.

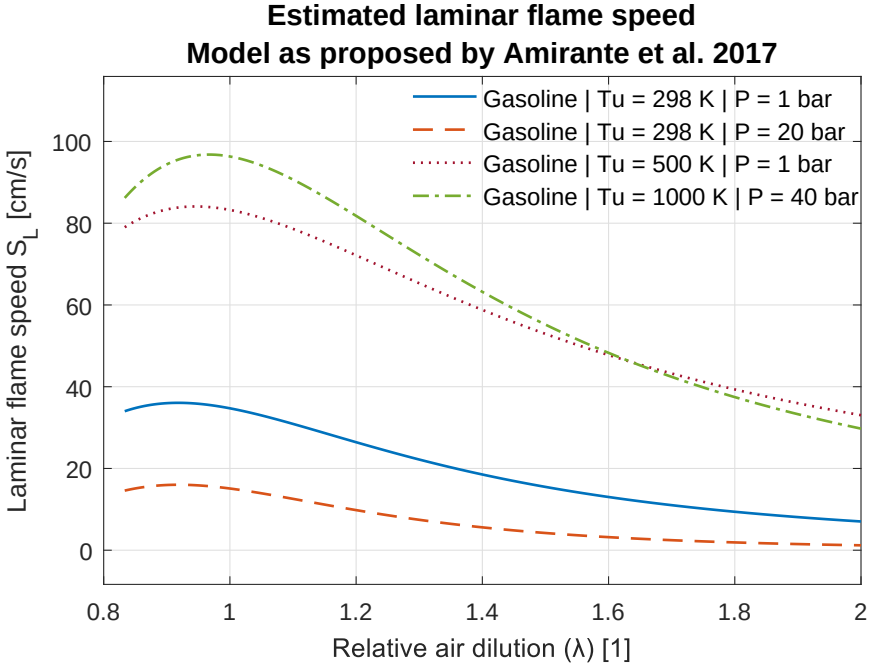


*Figure 6. Laminar flame speed of gasoline at various temperatures and pressures of the unburned mixture, versus relative air dilution lambda. Reproduced by the model proposed by Amirante et al. [55].*

Ideally, the flame speed and corresponding release of heat should be rapid to achieve stable and efficient combustion. When the release of heat is instant, constant volume

combustion can be achieved which corresponds to the ideal thermodynamic Otto-cycle and would result in maximized thermal efficiency. This is not true in reality, due to heat losses [56]. When the combustion duration is extended, less chemical energy can be converted into useful mechanical work. Slow combustion results in increased amount of heat being released during the compression stroke which increases negative work to the piston, and more energy being released late in the expansion stroke, where little energy can be extracted. Excessively slow combustion may not even complete before the end of the expansion stroke due to quenching of the flame when the temperatures decrease. Not only does slower laminar flame speed impede combustion, but it also means that the charge becomes increasingly difficult to ignite. The energy required to initiate combustion is called the minimum ignition energy (MIE) and the required energy increases substantially with increased dilution [57].

An engine with a certain volume has a limited volumetric capacity, i.e., the amount of air that can be consumed. This means that an engine has a limited maximum torque since the amount of fuel that can be consumed by the engine is proportional to the amount of air. If air-dilution is introduced, either the volumetric capacity must be increased to maintain the same torque output, or the maximum torque must be reduced. In a naturally aspirated engine, this can be solved by operating the engine stoichiometric when peak torque is requested. Alternatively, a boosting system can be used to increase the volumetric capacity of an engine beyond its limitations of natural atmospheric aspiration if the engine is to be operated with lean combustion with remained, or increased, torque output. Rather than providing decreased pumping losses, operating a lean combustion engine above the naturally aspirated limit can instead increase the pumping losses due to increased friction and inefficiency of the boosting system.

### 2.2.4 The Lean Limit

The amount of air-dilution that can be utilized in pre-mixed combustion is limited by the so called lean-limit. Theoretically, an air-fuel mixture will sustain a propagating flame until the flammability limit is exceeded – either too rich (the rich flammability limit) or too lean (the lean flammability limit). The lean flammability limit, $LFL$, is temperature dependent and this relation can be described by the modified Burgess-Wheeler equation:

$$\frac{LFL(T)}{LFL(T_0)} = 1 - \frac{\overline{C}_{p,fuel-air}}{LFL(T_0)(-\Delta H_c)}(T - T_0) \tag{8}$$

Where $\overline{C}_{p,fuel-air}$ is the total ideal gas heat capacity and $\Delta H_c$ is the increase in enthalpy from combustion [58]. A reference value $LFL(T_0)$ is needed for the equation to produce meaningful results. However, in practice, the lean flammability limit is never reached at engine operating conditions. Instead, it is the lean stability limit that governs maximum dilution. The lean stability limit is usually referred to as the lean limit, air-dilution limit, or air-dilution tolerance. A more generic terminology is the dilution stability limit, since the very same phenomena applies when any diluent is added to reciprocating internal combustion, and not just air. However, in research considering lean combustion, air is the common quantifier of dilution and therefore often attributed to the corresponding characteristics of stability. The lean limit, or dilution limit, is commonly defined as the threshold of which, when exceeded, the combustion instability becomes unacceptably high. Combustion instability is also known as cyclic dispersion or cycle-to-cycle variation, which denotes the variation of combustion between engine combustion cycles. The dispersion of combustion originates from that the combustion process itself, the development and propagation of the flame, is highly unstable and susceptible to any

influence from the conditions inside the combustion chamber. These very same conditions are not constant between cycles but change due to underlying fluctuations with various degree of randomness. Some research indicates that these fluctuations are partly deterministic in nature [59]. Combustion instability is present to some degree in all reciprocating internal combustion engines. In regular engine designs, during regular operating conditions, these variations are hardly noticeable. When dilution is added, the combustion becomes more susceptible to variations of the conditions since the overall characteristic of the combustion is weaker.

The dispersion of combustion has several implications. Due to variations of the flame propagation, the rate of heat release and the corresponding pressure rise in the cylinder of the engine vary between combustion cycles. This causes some combustion cycles to produce less work than others, resulting in oscillations of the engine output torque which influence the drivability and comfort of the vehicle. If the variations are large, some cycles may even fail to burn completely. An example of disperse combustion is visualized in Figure 7.

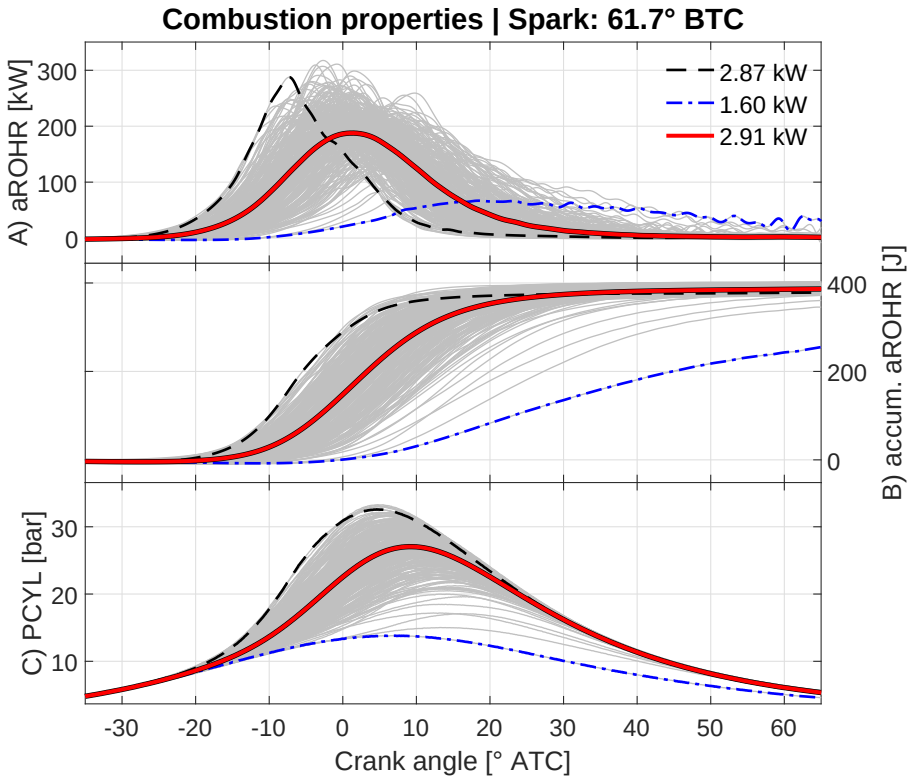


*Figure 7. Example of 300 combustion cycles of one engine cylinder, showing A) apparent rate of heat release, B) accumulated apparent rate of heat release, and C) cylinder pressure. Lambda = 1.66, 2.62 bar BMEP, 2000 rpm. Experimental data acquired from campaign 4.*

Figure 7 illustrates the dispersion of the crank angle resolved in-cylinder pressure of 300 individual combustion cycles at highly diluted conditions. The average combustion cycle has been highlighted with a solid line. The average cycle produces 2.91 kW of net work. Ideally, all combustion cycles should resemble the average combustion cycle, but this is not the case as can be seen from all the presented individual cycles in Figure 7. The combustion cycles with the earliest, and latest, occurring heat releases have been indicated in Figure 7 with dashed and dot-dashed lines. The combustion cycle that burns

the slowest/ latest fails to release all heat prior to 60° crank angles (CA) and is a so-called partial burn combustion cycle.

If a combustion cycle fails to burn completely, it results in poor combustion efficiency and corresponding losses of unburnt fuel to the exhaust. This is both a loss in terms of fuel efficiency, but also detrimental in terms of pollutions since unburned fuel produces noxious emissions. Full oxidation, complete combustion, of the fuel becomes increasingly difficult at very lean conditions, both because of temporal partial burns, but also due to the overall lower temperature of the flame which struggles to consume the charge bulk prior to the late expansion stroke. This is why the combustion losses could be seen to increase beyond lambda = 1.2 in Figure 3, and also part of why the fuel consumption can be seen to increase in the last increments of lambda beyond lambda = 1.8 in Figure 5.

At highly diluted conditions, the phasing, or timing, of combustion relative to the top dead center (TDC) position becomes increasingly important due to the lower flame speeds. The spark initiates a flame kernel growth which transitions into a progressing flame. This flame kernel growth is very slow at highly diluted conditions, averaging approximately 40° CA in the example provided in Figure 7. If the flame kernel growth is sufficient, it will result in a rapid heat release near TDC due to the corresponding heat and pressure build up from both compression by the piston and combustion. If the flame kernel growth is insufficient, as with the indicated late combustion example in Figure 7, the pressure and corresponding temperature build up prior to TDC will be insufficient to achieve a transition into rapid combustion, and the flame will instead progress slowly. This creates a second order effect which makes diluted combustion very sensitive to variations in the duration of the initial flame development.

There are different ways to quantify the combustion instability, and there are likewise various threshold values applied in the scientific community and industry. The instability is often defined statistically, and the most commonly applied measure is the coefficient of variation (CoV) of the cycle-resolved indicated net mean effective pressure (NMEP). The CoV is simply a normalized standard deviation of the work output, NMEP of a sample of arbitrary size:

$$CoV_{NMEP} = \frac{\sigma_{NMEP}}{\mu_{NMEP}} \cdot 100 \text{ [\%]} \tag{9}$$

At high loads, when the mean ($\mu$) of NMEP is high, the influence of the standard deviation ($\sigma$) diminishes, why it might be suitable to adopt the standard deviation directly as a measurement of dispersion at high loads. Consequently, at low loads, when the average of NMEP approaches zero, the CoV approaches infinity. Instead, it may be preferable to use a suitable value of standard deviation as the threshold for the low load stability as well. Values of CoV of NMEP thresholds vary between applications and manufacturers but are usually found to be within the interval of 2-5% and sometimes up to 10% for special applications [60]. Another important statistical quantity that can be used to assess instability is the lowest normalized value (LNV) of NMEP:

$$LNV_{NMEP} = \frac{\min(NMEP)}{\mu_{NMEP}} \cdot 100 \text{ [\%]} \tag{10}$$

LNV of NMEP is a number that identifies misfires or partial burns by accounting for statistical outliers, or extreme values. CoV and LNV are usually correlated to some extent, but an engine can produce high numbers of CoV if the combustion is consistently fluctuating with moderate amplitude, creating a high standard deviation, but with no

outliers. It is also possible that the engine combustion is stable, comparatively consistent, with low standard deviation resulting in a low number of CoV, but with one occasional misfire or partial burn that has little influence on standard deviation but detrimental effect on the minimum value. As an example, the combustion presented in Figure 7 produced a CoV of NMEP at 3.65%, which is not severe and can be accepted at the corresponding engine load. However, the same combustion sequence also produced a value of LNV of NMEP at 55.0%, indicating a severe partial burn, which is unacceptable.

A partial burn or misfire is particularly undesirable, not only because it results in drastically increased emissions of unburned fuel and reduced efficiency, but also since it can be sensed by the driver as a sudden vibration from the powertrain. A general guideline is that the number of LNV should not fall below 85% to be noticeable nor detrimental, but this number varies amongst practitioners and situations. To stretch the lean limit, it may be acceptable to allow lower numbers, presuming the emissions and efficiency do not suffer. At low loads, it is also accustomed to adopting lower LNV threshold values due to that combustion tends to be more disperse at low loads. In this thesis, a general threshold of maximum 3% in CoV of NMEP and minimum 85% LNV of NMEP has been used. At low loads, below 5 bar NMEP, 5% CoV of NMEP was tolerated and 75% LNV. At high loads, above 12 bar NMEP, 2% CoV of NMEP was used.

An example of how the combustion characteristics change in relation to increased air-dilution, lambda, is presented in Figure 8. The top subfigure of Figure 8 shows the spark timing and selected combustion angles. The combustion angles denote the corresponding crank angle of the various degrees of mass fractions burned (MFB) of the fuel, also called the release of heat. The error bars denote the standard deviation of the dispersion of the various parameters of their corresponding sample. As the figure shows, the duration between the timing of the spark to 90% mass fractions burned (CA90), increases substantially with increased air-dilution, and so does the dispersion. The corresponding CoV and LNV of NMEP is presented in the bottom subfigure of Figure 8. These graphs show typical trends with a steady increase in combustion duration and dispersion, until a certain point where the stability rapidly deteriorates. In the example illustrated, the deterioration occurs after lambda = 1.6.

The lean limit is a major obstacle in achieving $NO_x$-suppression. The $NO_x$-emissions are often reduced to low levels at the lean limit since the combustion becomes very weak at that stage. In practice however, the engine cannot be operated at the lean limit since it is difficult to balance the engine near the edge, but also since the fuel efficiency tends to suffer near the limit. Dilution rates beyond lambda = 1.6, occasionally referred to as ultra-lean, is often required to obtain reasonable suppression of $NO_x$-emissions, at or below 2 g/kWh.

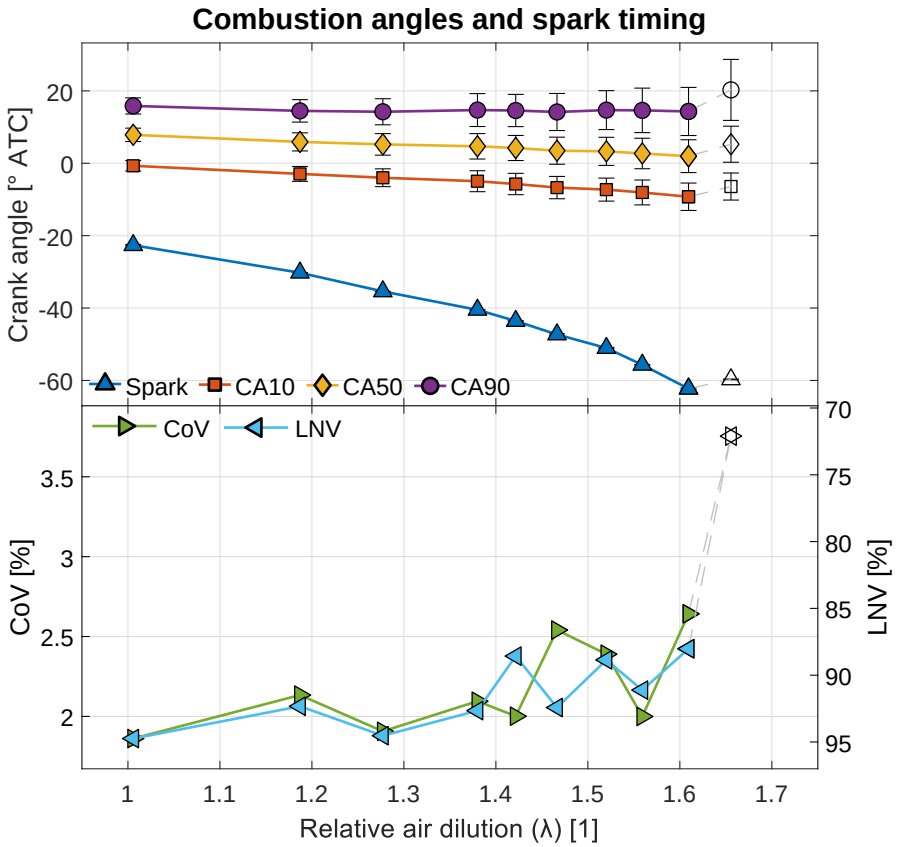


*Figure 8. Example of top) combustion angles denoting heat release (mass fractions burned) and corresponding spark timing, bottom) CoV and LNV of NMEP versus lambda. A stability limit of 3% CoV of NMEP and 85% LNV of NMEP was imposed as stability limits. Noncompliant data is illustrated as open markers and grey lines. Engine load was 2.62 bar BMEP, 2000 rpm. Experimental data acquired from campaign 4.*

### 2.2.5 Sources of Dispersion

The sources of combustion dispersion are, and have been for some time, quite well known to the research community and industry. Several important causes were discussed and determined already during the sixties [25, 26]. Extensive reviews of then previous research was written in the eighties by researchers such as Young [61], and Germane et al. [33]. However, the phenomenon continues to pose challenges to the implementation of lean combustion since countermeasures to dispersion of combustion has proved to be complicated to achieve.

Both Young and Germane et al. defined the initial flame development as a critical event to the success of a combustion cycle. So did Keck et al. in 1987 [20]. Another example is Aleiferis et al., whom conducted extensive research in an optical engine to characterize the nature of the early flame development in 2003 [62]. These are few examples of several similar works that exist in the literature of the topic, and it highlights the general agreement regarding the importance of the early flame development in cyclic dispersion of combustion.

The conditions that influence the flame development and ignition process are partly determined by the gas exchange process. Between combustion cycles, the combustion products are exhaled through the exhaust valve during the exhaust stroke and fresh charge inhaled during the intake stroke during the intake valve. Between these two strokes, some

amounts of combustion products, so called residual gasses, are trapped inside the combustion chamber due to the clearance volume of the combustion chamber. These gasses remain inside the chamber and are therefore incorporated in the consecutive combustion cycle. Depending on the pressure ratio between inlet and exhaust manifold, and velocities of the gasses, different amounts of residual gasses are trapped inside the combustion chamber. The residual gasses consist mostly of inert gasses such as nitrogen, carbon dioxide, water vapor, but may also contain excess oxygen, if the previous combustion cycle was fuel lean, and other various pollutants and unburned fuel such as nitrogen oxide, carbon monoxide and hydrocarbons. The residual gasses are a diluent like excess air and mixes with the fresh air during the intake stroke. During the gas exchange process, fuel is also added to the cylinder charge. This is either done externally, for example injected into the inlet port (port fuel injection, PFI), or directly injected into the cylinder (direct injection, DI). Ideally, air, residual gasses and fuel should be mixed homogeneously.

***In-homogeneities***

In reality, most engines fail to produce a completely homogeneous charge. In-homogeneities are a potential source of dispersion that influence the ignition, flame development and combustion. In-homogeneities may also be known as stratification or spatial maldistribution. A non-heterogeneous, in-homogeneous, charge results in spatial variation of the flame speed. If an unfavorable portion of the mixture is located at, or around, the spark plug during the onset of ignition, it can severely impede the flame development. In the next combustion cycle, a completely different mixture may be present near the spark plug, causing a successful ignition and flame development. The local laminar flame speed is affected by the local temperature, air-fuel ratio, and the amounts of additional diluents such as residual gasses. The residual gasses are commonly of high temperatures, the same order as the exhaust temperatures which may range between 300 to 1000° C. The residual gasses may therefore cause large spatial distribution of the in-cylinder temperature if these gasses are not homogeneously blended with the fresh cylinder charge. Despite their high temperatures, the residual gasses are mostly inert and are known to decrease the flame speed in engines, which is why their presence near the spark-plug at ignition would be disadvantageous for initial flame development [63]. However, in-homogeneities, heterogeneities, are not necessarily negative, as pointed out by Johansson [64]. If a mixture with high flame speed, like a fuel-enriched pocket, would be placed near the spark plug at the ignition event intentionally, it could improve the ignitability substantially and reduce cyclic dispersion of combustion. This can be accomplished by port fuel injection in only one of two ports, or by a late direct injection of fuel inside the cylinder. However, these concepts are challenging because it is difficult to control the stratification, due to poor mixing, and due to little mixing time inside the cylinder which may result in both high soot and $NO_x$ emissions. These issues are evident considering the modest progress that has been made historically of the stratified combustion concepts.

Hansel conducted engine experiments in 1971 and attributed 2/3 of experienced cyclic dispersion of combustion to in-homogeneities in the charge [65]. Hansel utilized skip-firing operation of the engine to purge one cylinder of the multi-cylinder test engine from residual gasses. The first fired cycle after purging was sampled, and the process repeated. In this way, Hansel could assess combustion without influence of residual gasses. Additionally, Hansel compared well-mixed propane with regular gasoline as fuels to assess air-fuel homogeneity. However, as pointed out by Young, the method used by

Hansel cannot provide neither quantitative nor qualitative characterization of the influence of homogeneity [61].

During the nineties, significant improvements were made in the field of optical diagnostics which made it possible to measure in-cylinder quantities non-intrusively. In 1995, Johansson et al. utilized planar laser-induced fluorescence (LIF) with a fuel tracer in an optically accessible engine to correlate local air-fuel ratios near the spark plug with combustion characteristics [64]. The experiments could clearly show that local air-fuel ratios affected the heat release rate on a cycle-to-cycle basis. In 1997, Berckmüller et al. conducted an experimental investigation using an optical engine based upon a port injected Honda VTEC-E engine, using swirl and a stratified charge [66]. For visualization, planar fuel-tracer LIF was utilized to track fuel distribution and LIF of NO as tracer for the residual gasses. They observed both significant fluctuations in the air-fuel ratio and residual gasses near the spark plug which they linked to consecutive fluctuations in the flame development. Since the engine they investigated was port fuel injected and therefore partly pre-mixed with the charge air prior to entering the cylinder, they hypothesized that the reason for in-homogeneities in fuel distribution was caused by the residual gasses. They also concluded that for convection of the flame to be successful, favorable mixtures were required downstream of the initial flame, but once the flame front was developed it was less sensitive to local variations in the bulk. Since the engine in question operated with intentional charge air-fuel stratification, larger in-homogeneities could be expected compared to a combustion system that is designed for maximum homogenization. The use of NO as a tracer, representative of the residual gasses, are convenient, but the concentrations of NO in the residual gasses is highly dependent on the quality of the previous combustion cycle, why it may be inappropriate to use NO for quantitative estimations.

In a consecutive study in 1996, Johansson investigated the influence of several parameters such as spatial distribution of residual gasses, distribution of air-fuel ratio, temperature and more, using various measurement techniques probing the volume in the vicinity of the spark plug [67]. Amongst several correlations, both residual gasses and local air-fuel ratio were observed to fluctuate and correlate to the dispersion of combustion. The correlation was however lower for the residual gasses which was unexpected. This was hypothesized to be a consequence of the measurement technique utilized that resulted in comparatively weak signals, which could result in an underestimation of the variation of the residual gasses. It should be noted that the engine used by Johansson was a two-valve engine with pancake combustion chamber. An engine that is less representative of more modern four valve pent-roof cylinder heads.

In 1998, Miles and Hinze utilized another diagnostical method called spontaneous Raman scattering inside a side-valve optical engine with pancake combustion chamber, to measure multiple species simultaneously [68]. Using this technique, the spatial distribution of both fuel and residual gasses could be assessed simultaneously. They did not investigate the distribution of fuel, nor did they correlate the optical measurements with combustion (heat release) but they found both temporal and spatial variations in the concentrations of the residual gasses. Interestingly, they could conclude that there were large variations in the temporal spatial distribution of residual gasses concentrations, but these stabilized during the compression stroke. Additionally, they investigated the influence of in-cylinder swirl motion of the charge, which resulted in a persistent spatial variation in the residual gas concentration, an axial stratification along the cylinder axis. Hinze and Miles later conducted a similar investigation in 1999, utilizing a modern 4-valve cylinder head fitted to an optical engine [69]. Similar to the previous investigation,

they noted large spatial variation in residual gas concentrations during the inlet stroke, but the heterogeneity decreased during the compression stroke and was less than 1% root-mean-square (rms) at the time of ignition at 15° before TC. These observations are interesting in the sense that they clearly show that there are substantial variations, in-homogeneities, in the charge, but during compression when the piston compresses the charge and the flow structure inside the cylinder decays into smaller eddies, the charge becomes increasingly homogeneous.

In 2017, Hanabusa et al. conducted an investigation in a research engine were they utilized an endoscopic infrared light absorption probe mounted through the spark-plug [70]. In this way, they could measure local air-fuel ratio near the spark plug electrodes during realistic engine operating conditions since the small endoscopic probe did not pose any pressure nor thermal constraints to engine operation. They utilized three fuel systems, regular gasoline direct injection, port fuel injection and an upstream pre-heated mixing tank. They could clearly observe that the temporal- and cyclic variation in air-fuel ratio was heavily dependent on the type of fuel system used. Both on a temporal and cycle-resolved basis, direct injection caused the most signal noise, port injection less and the upstream preheated mixing tank the least. Despite that the pre-mixing tank achieved a high degree of homogeneity, there was still dispersion of combustion on a cycle-to-cycle basis recorded. Another interesting aspect was that regardless of fuel system; the local variation in air-fuel ratio drastically decreased at the end of the compression stroke.

### *External influences*

Another hypothesis regarding the origin of cyclic dispersion of combustion is that it is caused by external influences. In 1994, Grünefeld et al. utilized spontaneous Raman scattering in an optically accessible engine to assess the influence on combustion from cycle-to-cycle variations both in terms of residual gasses and air-fuel ratio [71, 72]. Their measurements showed that there were considerable fluctuations in both air-fuel ratio and residual gasses between cycles. The variations in air-fuel ratio were attributed to variations in the port fuel injection system, and therefore, they suggested that improvements should be made to the stability of the injection system to suppress cyclic dispersion of combustion. Additionally, Grünefeld et al. commented that the cyclic dispersion of the flame during combustion was predominantly caused by prior effects in the charge originating from external influences and fluid mechanical effects during the gas exchange, rather than that the progressing flame would be inherently random in itself.

Another example of influences from external sources is the ignition system. In 2000, Aleiferis et al. studied the correlation between cyclic fluctuations in spark energy and the corresponding flame development [73]. From the measurements, they could conclude that there were fluctuations in ignition energy on a cycle basis. However, it could not be determined whether these fluctuations in ignition energy was due to the ignition system itself or not. An alternative explanation was that the in-cylinder conditions influenced the impedance of the gasses near the electrodes and therefore affected the spark and corresponding spark energy. They could however conclude that the delivered spark energy had high degree of correlation to the quality of flame initiation.

Other examples of research on the influence of external factors are scarce in the literature. There are hypothetically several potential sources that may induce cyclic dispersion. Apart from ignition and fuel injection, modern engines contain several mechanically and/ or electronically controlled actuators such as the throttle, turbocharger system, camshaft phasers and more, which may oscillate as a consequence of the various PID-controllers

that governs them. Some modern engines utilize hydraulic valve adjusters, which may cause inconsistent valve events. However, evident as they might seem, these various factors may be difficult to assess and may be less relevant, particularly in regular non-diluted engine operation. This could explain why little efforts have been made in researching this field. Despite that external influence may not be the main source of cyclic dispersion, the noise introduced by external factors may be superimposed on other sources of dispersion which may increase the overall cyclic dispersion of combustion.

***Flow***

Another important factor that may contribute to cyclic dispersion of combustion is the in-cylinder flow of the charge. Inside the combustion chamber, a complicated, dynamic flow structure occurs during the gas exchange, compression and combustion which have large impact on the characteristics of combustion in general. It is therefore reasonable to expect that the flow, if it is not consistent, may have an impact on cyclic variability of combustion.

The flow inside the cylinder is highly turbulent and the corresponding structure of the flow can with simplified terms be described as a sum of large and small structures. The large flow pattern, also known as the bulk flow, has an integral length scale similar to the dimensions of the combustion chamber itself, while the smaller scales are turbulent fluctuations and substructures with various length scales. There are two main types of bulk flows utilized in spark-ignited engines; swirl, which revolves around the center axis of the cylinder, and tumble, which revolves around an axis parallel to the crankshaft. Modern 4-valve SI-engines almost exclusively utilize tumble.

Turbulent flow is random by nature, which means that locally, the flow is unpredictable despite that the bulk flow appears as consistent. If the local flow field at the location of the ignition event varies from cycle to cycle, it can consequently have implications on the ignition and flame development. The flow is sensitive and there are multiple factors that, additional to the randomness of the turbulence itself, affect the flow pattern on different scales. Pulses in inlet manifold and exhaust manifold, vortices created by various hardware components disturbing the flow, and characteristics of the remaining residuals from the previous cycle are examples of such features that could affect the characteristics of the flow. The flow structure is also heavily dependent on the position of the piston and the corresponding stroke due to the correspondingly evolving geometry of the combustion chamber.

Already in 1967, Patterson presented the hypothesis that fluctuations in the flow field during the ignition event was the major cause of cyclic dispersion of combustion [74]. He compared regular carbureted indolene with well premixed propane and found that propane indeed reduced the cyclic dispersion of combustion, but not completely. Additionally, Patterson assessed the influence of using a shrouded inlet valve, which increased the in-cylinder swirl flow, versus a non-shrouded inlet valve on the corresponding combustion characteristics. He observed that increased swirl increased the rate of combustion, why it was concluded that variations in the swirl and mixture motion were the major causes of cycle-to-cycle variation of combustion, and therefore engine torque output. Indeed, using a well pre-mixed charge could theoretically eliminate the influence of air-fuel inhomogeneities, and manipulating the swirl allowed assessment of the influence of the flow, but other sources of dispersion could not be excluded nor could any cyclic dispersion of in-cylinder flow be investigated. The same year, Bolt and Harrington presented results from an investigation conducted in a constant volume

combustion bomb [26]. They investigated the influence of charge velocity on the ignitability and rate of combustion and found that ignitability was reduced with increased flow. On the other hand, the rate of combustion was aided by increased mixture velocities when the mixture of propane and air was made leaner, indicating the importance of increased bulk flow to compensate for reduced laminar flame speed of diluted mixtures. The work of Bolt and Harrington did not consider cyclic dispersion, but their work presented examples of the influence of bulk flow properties on ignition and flame propagation.

In 1983, Matekunas performed experiments in a research engine with optical access through the piston crown [75]. Using three different intake geometries generating various degree of swirl, the influence of bulk flow inside the combustion chamber could be assessed. Matekunas stated two major conclusions: Regular cyclic variability with undiluted charges appeared to be caused by inconsistency in the bulk flow which deflected the flame, and not by the local conditions near the spark plug. When the lean limit was approached, the initial flame tended to partly quench and therefore not develop sufficiently to progress at piston top dead center. The spark timing could not be further advanced to mitigate the slow initial flame growth, but instead caused increased instability. Quader had previously investigated the very same phenomenon [76, 77]. Quader determined that there existed a maximum spark advance for a given air-dilution, of which when exceeded caused misfires, and a minimum spark advance, when exceeded caused partial burns. The reason for the misfire limited spark advance was attributed to that the conditions at the early compression stroke was equivalent to low temperatures and high bulk flow velocities that simply quenched the initial flame. Both Quader and Matekunas suggested that the misfires could be suppressed by facilitating faster combustion, allowing for later spark advances, together with increased charge temperature and reduced dilution by residuals to aid flame development during ignition.

In 1996, Johansson investigated both bulk flow, turbulence, time- and length scales inside the cylinder, and their corresponding influence on initial combustion, using laser-doppler velocimetry (LDV) in an optical engine [67]. The dispersion of flow in terms of bulk velocity and turbulence intensity was found to be the most significant factor explaining dispersion of heat release, together with charge in-homogeneity. Uncertainties in the origins of dispersion did however remain, and Johansson pointed out that the one-dimensional LDV measurement did not fully characterize the three-dimensional flow and was therefore not expected to achieve a higher degree of correlation.

Another interesting investigation is the one conducted by Krüger et al. in 2016 [78]. They utilized dual-plane particle image velocimetry (PIV), combined with computational fluid dynamics (CFD) simulations, in an optical engine with a four-valve pent-roof cylinder head and stratified charge operation. The PIV-images of the two vertical planes, one in the center of the cylinder and one intersecting one of the inlet valves, showed that there was occasional flow directed upwards during the late compression stroke that obscured the ignition process in some cycles. The upward draught was linked to variations in the bulk flow and the corresponding variation of the tumble vortex axis. When they investigated the flow structures further by CFD, they could determine that there were two major flow structures evolving during the intake stroke, in different directions, which later collided and caused unsteady bulk flow as a result. Therefore, they proposed methodologies to prevent competing flow structures to occur, such as tumble-promoting inlet ports. This work is one of few that has presented clear explanations to the origins of the unsteady flow inside the combustion chamber of spark-ignited engines.

Another interesting work was conducted by Wang et al. in 2017 [79]. When investigating the influence of spark plug ground electrode indexing angles on the corresponding flame development in an optical engine, they found that the flame was deflected in different directions between cycles. The engine was fitted with a four-valve cylinder head generating tumble, utilized direct injection of gasoline, and was operated at a speed of 1000 rpm and 2.5 bar NMEP. Despite that the engine was designed to produce a counterclockwise tumble motion inside the combustion chamber, seen from the front of the engine, some flames of individual combustion cycles were deflected, burned, in the opposite direction of the intended bulk flow. This discovery evidently sparked interest, since Wang et al. conducted further research into the characteristics of the flow near the spark-plug in a consecutive investigation in 2018 [80]. The same optical engine was utilized, but with an added tumble-plate in the inlet port to manipulate, increase, the in-cylinder tumble intensity. Experiments were conducted at both 1000 rpm and 1500 rpm, at 2.5 bar NMEP. By high-speed imaging, they could track both spark stretching and flame kernel development. Increased tumble and increased engine speed resulted in an increased share of combustion cycles with flame deflection in co-direction with the nominal bulk flow. By using PIV-images, Wang et al. observed that the flow near the spark plug clearly changed in magnitude and direction between cycles in a similar manner as the flame was inconsistently deflected. The consistency of the flow was however improved by increased tumble, in the same manner as was suggested by Krüger et al. In 2017, Teh et al. utilized PIV in an optical engine to investigate cyclic dispersion of the tumble flow [81]. They utilized a technique called moment normalization to identify and assess flow structures. Teh et al. could observe that the research engine in question, with a pent-roof four-valve cylinder head, produced two counter-rotating tumble vortices, one larger and stronger than the other. These vortices changed on a cycle-to-cycle basis in terms of location and rotational magnitude. The results presented by Teh et al. is yet another example of the very unpredictable nature of the in-cylinder flow pattern.

### *Determinism*

Another interesting research field linked to cyclic dispersion of combustion is determinism. Some researchers have investigated the statistical behavior of dispersion of combustion and found evidence that the dispersion is not completely random, but rather, exhibit some degree of stochastic and periodic distribution [59, 82, 83]. This means that the dispersion of combustion may be partly deterministic, and therefore may be predicted to some extent. If the deterministic pattern can be identified, the dispersion may be mitigated by control mechanisms, as some researchers have suggested. By revealing the pattern, it might even be possible to locate the physical source and thus re-engineer the combustion system to eliminate the origin of dispersion. The insight that dispersion of combustion may be partly deterministic gives hope in the quest for a solution to combustion instabilities because it would mean that there are sources to the dispersion which can be found and resolved, rather than being caused by completely random noise of which there is no physical source that can be eliminated.

### *Concluding remarks*

Substantial research into the origins of cyclic dispersion has been conducted for more than 60 years. It is evident that the initial flame development is the factor that determines the quality of combustion. In turn, the literature points to that in-homogeneities and dispersion of the in-cylinder flow jointly influence the quality of the initial flame development. The dispersion of the initial flame appears to increase when the spark

timing is advanced. The advancement of the spark timing is forced to maintain the phasing of the release of heat of the main combustion.

## *2.3 Homogeneous Lean Combustion*

The homogeneous mode of lean combustion is currently the alternative that receives the most attention in the field of spark-ignited air-diluted combustion. The main reason ought to be that the homogeneous mode is the most likely to achieve sufficient $NO_x$-suppression in combination with increased fuel efficiency. The advantage in terms of $NO_x$-emissions is well known [84, 85]. In addition to the research conducted to investigate the origins of cyclic dispersion of combustion, extensive research has been conducted to mitigate the instability and to increase the lean dilution limit to suppress $NO_x$-emissions. The following sections are devoted to a review of some of these research efforts.

### 2.3.1 Improvement Strategies, State of the Art

***Ignition***

The development of the initial flame can be supported by increased ignition energy and prolonged spark duration. Generally, when the charge is made weaker, fuel-lean, the minimum ignition energy (MIE) demand increases which is why increased spark energy is required. It has also been shown that increased velocity of the flow, in relation to the spark, increases the MIE demand due to cooling and flame stretch [26].

If higher amounts of energy can be supplied to the flame kernel, the flame is more likely to progress rapidly and becomes less prone of quenching. Yu et al. investigated the influence of ignition energy on the ignition in a cross flow with a regular spark plug and found that the arc could stretch much more with increased energy [86]. Spark stretch was highlighted as particularly important, since an increased volume of the arc by flow-stretching increased the discharge volume and thereby contact between arc and gas, which resulted in a larger initial flame kernel. Shiraishi et al. investigated this particular phenomena and also assessed the possibility of restrike after spark blowouts during ignition events in high speed flows, to extend the dilution limit [87]. Another influential factor is the geometry and position of the spark plug. Aleiferis et. al demonstrated that a perpendicular position of the spark plug ground electrode in its relation to the direction of the local bulk flow was the most beneficial to support flame development since that position of the ground was least likely to interact with the arc and kernel during deflection [73]. Similar observations were made by Lee and Boehler in 2005 [88]. Lee and Boehler compared different spark plug geometries and concluded that a single ground electrode and sharp electrode tips were the most beneficial, determined from constant volume combustion vessel experiments. By perpendicular positioning of the ground, and sharp electrodes, the interaction between the gas flow and spark increased which facilitated flame kernel growth. Additionally, sharper electrodes and deflection of the arc may decrease heat losses from the spark and flame kernel to the electrodes [89]. An example of a spark with deflection, arc stretch, is presented in Figure 9.

Another method to increase the available spark energy is to utilize high energy ignition coils. One technology that can provide this is multi-coil ignition systems. A common alternative is the dual coil ignition (DCI) system, that utilizes twin parallel coils that release their energy and recharge sequentially which creates a continuous spark that can be sustained for an extended period of time. The extended, pulsating, spark current increases interaction and energy transfer to the gasses. Additionally, the extended

duration of the spark increases the probability that an ignitable mixture, in an in-homogeneous, moving charge, passes by the spark gap during ignition. A dual coil ignition system was demonstrated and assed by Alger et al. in 2011 [90]. Other examples of research into the usage of DCI were the experiments conducted by Doornbos et al. in 2015 [91]. The system could sustain sparks of a duration up to 5 ms. Doornbos et al. observed that improvements in combustion stability was obtained mostly from increased spark duration rather than increased energy. This indicated that there was a maximum transferable energy to the charge per unit time and this was saturated by the high energy ignition system. By extending the duration of the spark, the timeframe of the energy transfer could be extended. A negative consequence of high ignition currents and sharp electrodes is the increased electrode erosion, which must be considered in terms of durability in real life applications.

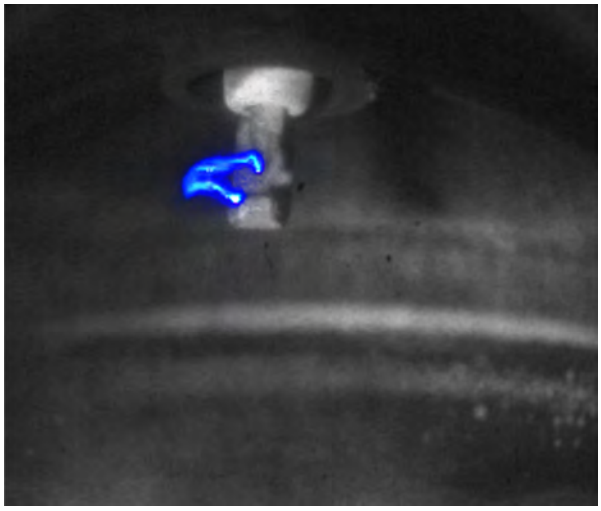

*Figure 9. Example of spark (arc) from a regular spark-plug ignition system between the ground (lower) electrode and the central electrode (upper). The arc stretches (deflects) away from the electrodes due to the flow. Image acquired from campaign 3.*

An alternative to regular spark plug based ignition systems is the high-frequency ignition system (HFI). An HFI system works without creating any arc. Instead, HFI utilizes the initial breakdown stage that is experienced with a regular spark plug prior to the arc phase. A regular ignition system utilizes direct current. The high-frequency system on the other hand utilizes pulsating or alternating current, applied to one or several electrodes in parallel. The combustion chamber is used as ground and the unit comprising the electrodes is called the igniter. When charged, the electrodes of the igniter produce ion streamers, filaments, often referred to as corona discharges. An example of a corona discharge is presented in Figure 10. Electrons are pushed from the electrodes which can both create electron-impact ionization of the surrounding molecules, but also cause dissociation of diatomic molecules, which initiates exothermal reactions that leads to combustion [92]. The corona discharge occurs without the formation of an arc, and therefore, no current flow occurs. The transfer of energy is therefore very efficient since no thermal plasma is created. As much as >1J of energy may be transferred into the gasses of the combustion chamber [93]. The absence of current flow also eliminates electrode erosion. The maximum applicable voltage of the igniter electrodes is determined by the impedance of the combustion chamber. The impedance depends upon the conductivity of the gasses, which are inversely proportional to the pressure, and the physical distance to surrounding combustion chamber walls. If the impedance is exceeded, an arc can be

formed, which leads to a current flow. The formation of an arc is referred to as a flash-over, which causes erosion of the electrode and consumes the electrical energy from the corona discharge. An example of a flash-over is presented in Figure 11. The HFI-system has been investigated by several researchers, such as Yun et al., Doornbos et al, Suess et al., to minimize cyclic dispersion [94-96]. One evident benefit is that an HFI igniter, with ion streamers penetrating the volume of the combustion chamber, can create large flame kernels. With multiple electrodes, this can be realized at several positions simultaneously, which can suppress the influence of charge in-homogeneities. An example of the impact of HFI on combustion stability is illustrated in Figure 12.

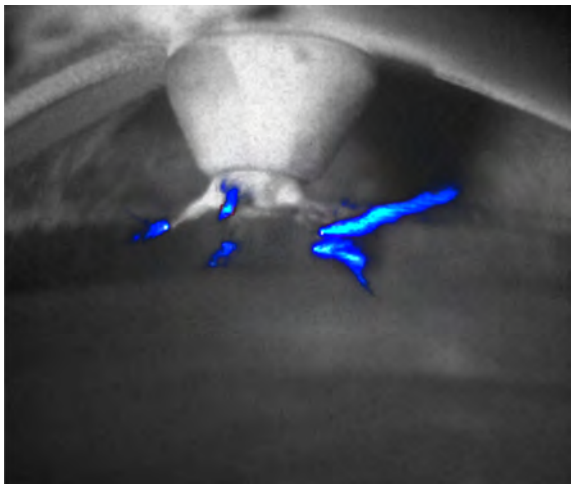

*Figure 10. Example of corona discharge (plasma streamers) from a 5-electrode high-frequency igniter. Image acquired from campaign 3.*

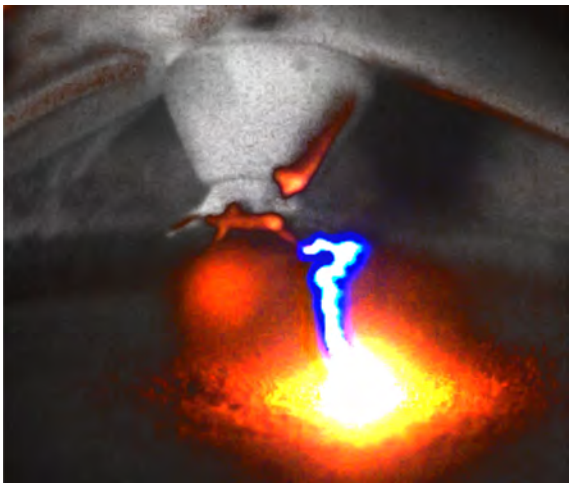

*Figure 11. Example of a flash over (arcing) of the high-frequency ignition system, between the 5-electrode igniter and the piston. Image acquired from campaign 3.*

Jet-ignition is yet another type of ignition system that has received increased attention in recent years. Jet-ignition is fundamentally similar to pre-chamber ignition that was common amongst lean burn engines during the seventies. Modern jet-ignition systems utilize very small pre-chambers, around 5% of the main combustion chamber volume or smaller and are fueled by dedicated small direct-injectors. A spark plug ignites the mixture inside the chamber, and the mixture is ejected into the main chamber [97]. By careful design of the pre-chamber, jet-streams of radicals may be created rather than rich burning flames. This means that heat losses and locally produced $NO_x$ can be minimized, which were main drawbacks of the older systems. Jet-ignition is indeed a promising technology which has been demonstrated to outperform regular ignition systems in terms of stability and dilution limits. Researchers such as Bunce et al. and others have investigated these systems extensively [97-101]. The jet-ignition system has however not been considered in the work conducted to establish this thesis and will not be reviewed in more detail.

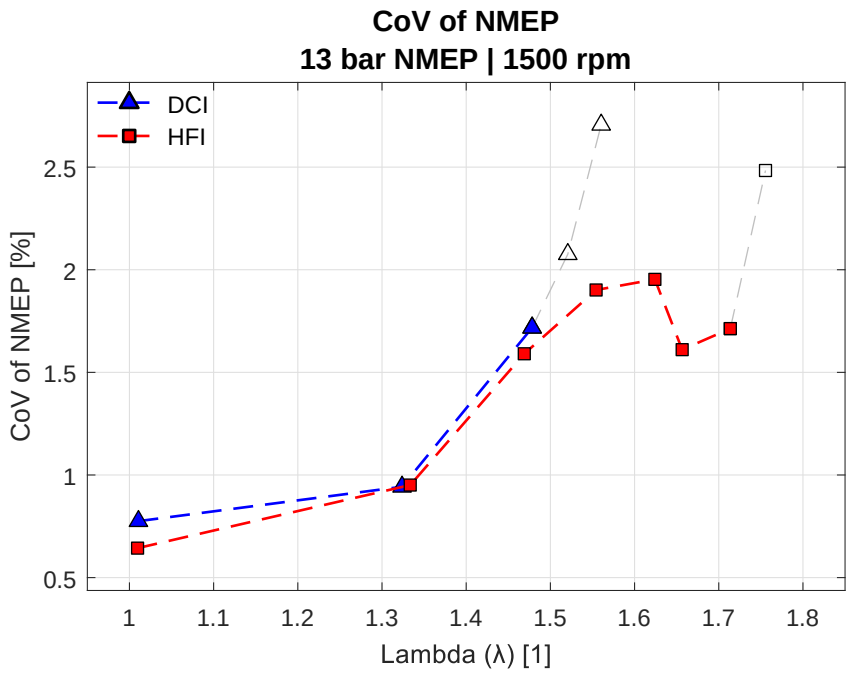


*Figure 12. Example of the difference in the lean limit (air dilution tolerance) between a dual coil ignition system (DCI) and a high frequency ignition (HFI) system. As can be seen, it was possible to extend the lean limit 0.25 lambda units using the HFI system. The stability limit was set to 2% CoV of NMEP in this case. Gray lines and open markers denote operating points exceeding the stability criterion. Data acquired from campaign 2.*

### *Turbulence*

Increasing turbulence is a common approach to increase combustion speed. The laminar flame speed is adversely affected by increased air-dilution which results in slow combustion. Most of the flame propagation is however turbulent, and the turbulent flame speed can be increased by increased turbulence intensity to counteract for lower laminar flame speed. The local velocity, $u$, of a turbulent flow is commonly described using Reynolds' decomposition:

$$u = \bar{u} + u' \tag{11}$$

Where $\bar{u}$ is the mean velocity, and $u'$ is the fluctuation (signal noise), denoted turbulence intensity. A simple relation between laminar flame speed, turbulence intensity and turbulent flame speed was proposed a long time ago by Damköhler [102]:

$$S_T = S_L + u' \tag{12}$$

This model has since been extended by many researchers and in practice the turbulent flame speed is subject to very complex mechanisms not captured by this proposed relation. The main weakness of the model in Equation 12 is that the model predicts flame propagation even when the laminar flame speed is zero. However, the equation illustrates the importance of increased turbulence intensity in relation to the total flame speed. Turbulence promotes the flame speed by wrinkling the flame front which in turns increases the total area of the flame front, the reaction zone. The wrinkling of the reaction zone is believed to be influenced by its thickness. Increased pressure of the gasses is known to decrease the reaction zone thickness, and thereby lowering the laminar flame speed. A decrease in flame thickness may however allow more wrinkling, why increased combustion chamber pressure might be beneficial to the turbulent flame speed.

The flow field inside the cylinder, the combustion chamber, is complex and evolves as the piston moves in the cylinder liner. In a combustion chamber, which is designed to generate tumble, as most four-valve pent-roof combustion chambers are, a vertical main vortex of the bulk flow is created during the intake stroke. The characteristic length scale of the flow is approximately proportional to the minimum distance between piston and cylinder head or the cylinder diameter, and therefore changes during the strokes. During the compression stroke, the main tumble vortex is crushed and decays into smaller eddies. Extensive research has been conducted in the topic by Baum et al., and Baumann et al. [103, 104]. Historically, in two-valve combustion chambers, there has been abundant cylinder head deck surface available to generate squish-induced turbulence. However, modern four-valve combustion chambers have limited deck-surface available for squish, and therefore, these combustion chambers become reliant upon turbulence generated from conversion of the bulk flow [105, 106]. As stated by Kiyota et al., turbulence is subject to dissipation and it is therefore desirable to preserve the bulk flow motion and convert the bulk vortex into turbulence in the late compression stroke before combustion, rather than inducing turbulence during the inlet stroke [15]. To maximize the turbulence, it is important to maximize the induction of kinetic energy into the bulk flow during the intake stroke. This can be accomplished by manipulation of the inlet port and valve events of the intake valves. Designing of inlet ports is a difficult task since the port design is a trade-off between friction, choking, and the flow-targeting to induce a certain pattern of the flow [107].

As previously stated, tumble is the most common mode of bulk flow amongst modern four-valve pent-roof cylinder head SI-engines. Swirl is another option, more common amongst diesel engines, older stratified charge spark ignited engines, and two-valve pancake combustion chamber engines. Swirl does not decay in the same manner as tumble during compression since the characteristic length scale of the swirl vortex is determined in the horizontal plane which equals to the diameter of the cylinder, which therefore remains roughly constant. These two main flow-patterns may be mixed to generate so-called slant-swirl which may achieve both preservation of turbulent kinetic energy into the late compression stroke combined with a reasonable amount of turbulence intensity. This has been demonstrated by researchers such as He et al. who termed the flow pattern as “swumble” [108]. A similar approach was investigated by Johansson and Söderberg. They utilized laser doppler velocimetry in a four-valve optical engine with various valve timings to investigate the corresponding in-cylinder slant-swirl flow [109]. The name “twirl” has also appeared in the literature to denote the mixed flow that is the combination of swirl and tumble.

A tumble port is commonly straightened to direct the flow towards the exhaust side of the combustion chamber, and sometimes the port cross sectional area is made smaller to increase the gas velocity. Current trends in combustion chamber design requires decreased included valve-angles to make the pent-roof flatter to allow for higher compression ratios and lower surface to volume ratios. Decreased included valve angles create additional challenges to promote tumble flow since there is a maximum applicable angle between the valve seat and the axis of the inlet port. Additionally, it may be challenging to design a port which sufficiently promotes bulk flow kinetic energy at lower mass flows, which simultaneously allows for high flows at peak power. Variable tumble systems have been proposed as a solution to this problem. Such systems are denoted as tumble-plates or tumble-flaps. These devices work by partially blocking the inlet ports, which in turn increases the gas velocity and targets the flow towards the top side of the intake valve, which results in promoted tumble motion [110-112]. An example of such a

system is shown in Figure 13, which is the system utilized in some of the experimental activities included in this thesis.

Not only is increased kinetic energy of the bulk flow accompanied with increased port friction, but a strong bulk-flow vortex may deflect direct injected fuel sprays and/ or stratify the charge due to centrifugation of the fuel droplets, which may result in wall wetting [113]. Increased bulk-flow may also increase heat losses to the cylinder walls due to increased convection during the combustion. As was highlighted by Krüger et al., it is also crucial to suppress competing flow structures to avoid instability of the flow that cause cyclic dispersion [78]. It is not necessarily true that solely increased bulk-flow kinetic energy by induced tumble or swirl minimizes these effects.

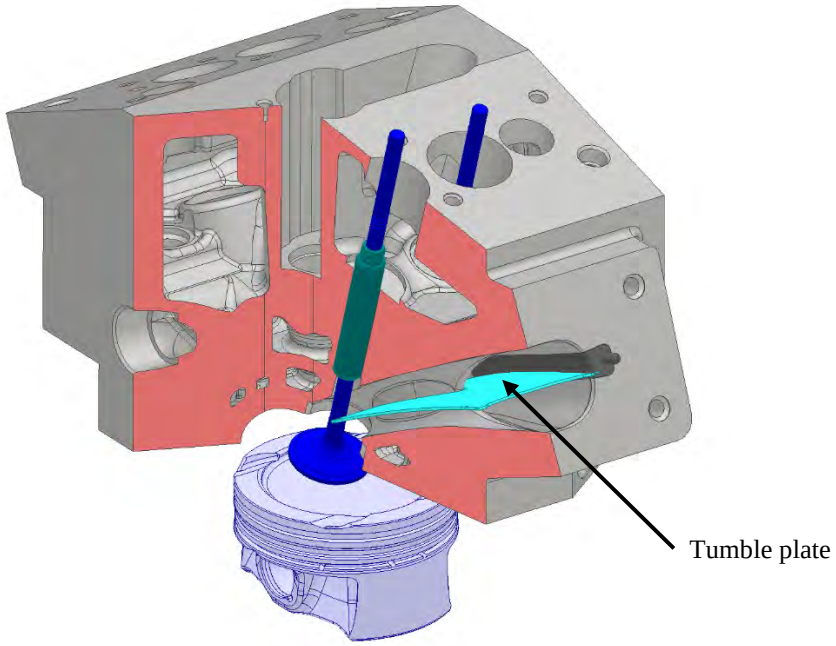


*Figure 13. Section-view of a CAD-model of a cylinder head with fitted tumble plate (colored cyan). By blocking the lower side of the plate, the inlet port cross-sectional area is reduced by 50% which increases the gas velocity during intake and improves targeting towards the top side of the inlet valve plate. This technique was used in the single-cylinder engine of campaign 2 to 4.*

Another implication of high turbulence intensity is that the flame may be excessively wrinkled and stretched, which may cause quenching of the flame, rather than promoting it [114]. This effect has been attributed to the Karlovitz number, $Ka$:

$$Ka = \frac{\delta u'}{S_L L} \tag{13}$$

Where $\delta$ is the flame thickness, $u'$ and $S_L$ the familiar turbulent intensity and laminar flame speed respectively, and $L$ the turbulent length scale. As can be seen from Equation 13, the Karlovitz number increases with increased turbulence and reduced laminar flame speed. The Karlovitz number decreases with increased length scale and decreased thickness of the flame front. A high Karlovitz number is associated with high stretch rates of the flame, which increases the chances of quenching and ultimately extinction [115].

Another influential factor in turbulent pre-mixed combustion is the Lewis number, $Le$:

$$Le = \frac{k}{\rho C_p D} \tag{14}$$

Where $k$ is the thermal conductivity, $\rho$ the density, $C_p$ the heat capacity and $D$ the diffusion coefficient. The Lewis number is the ratio of thermal- to mass diffusivity and an increased Lewis number indicates that the flame is more prone of quenching [116]. The Lewis number increases as air-dilution is added to hydrocarbon fuels. Particularly vulnerable to quenching is the initial flame kernel before transitioning into a fully developed flame. This makes the ignition process sensitive to high levels of turbulence and may result in misfires if the levels are too high.

***Compression ratio and piston design***

Since the flame speed is dependent on temperature, it has been proven beneficial to increase the charge temperature to reduce cyclic dispersion and increase combustion speed. This can be accomplished by increasing the temperature of the inlet air, at the expense of decreased volumetric efficiency [117]. Increased charge temperature prior to ignition may also be accomplished by increased compression ratio. This was investigated already in the sixties by Bolt and Holkeboer [25]. Apart from increased efficiency, increasing compression ratio also has the advantage that the top dead clearance volume decreases which in turn decreases the amounts of trapped residual gasses during the gas exchange. However, by improper design, the piston may impair the flow and result in excessive decay of the turbulence prior to piston TDC and combustion. The influence of various piston bowl designs were investigated by Changming and Sichuan were they concluded that a spherical piston bowl (piston crown) and tumble intake ports were the most efficient in establishing a tumble vortex that remained into the late compression stroke [111]. Other investigated alternatives showed tendency of creating reversed tumble flow during the compression stroke. The influence of various piston shapes of high-compression pistons was extensively investigated by a research group from Mazda in 2011 [118, 119]. They found that high compression pistons that resulted in flat, thin, combustion chambers at TDC were accompanied by large surface to volume ratios. Larger surface to volume ratio resulted in larger heat losses and increased flame-wall interaction obstructing and cooling the flame. By providing the pistons with a central spherical cavity, bowl, the local surface/ volume ratio could be reduced and heat losses during early combustion reduced. A similar conclusion was made by Serrano et al. in 2019, whom were developing and investigating a prototype lean combustion concept including jet-ignition, high compression ratio, optimized piston- and combustion chamber geometry with minimized surface/ volume ratio, late inlet valve closing resulting in a miller cycle, which all resulted in a measured indicated thermal efficiency of up to 46% [120]. Due to the nature of pre-mixed combustion, increased compression ratios must be applied with care. Increases of compression ratio is commonly accompanied by increased tendency of knocking combustion, which limits the effective benefits from theoretical efficiency improvements.

***Charge preparation***

Homogeneity has repeatedly been highlighted as important to achieve stable lean combustion, a factor that is highly dependent on the fuel injection system and corresponding injection strategy. As previously discussed, Hanabusa et al. conducted a study where port injection and direct injection was compared [70]. Their investigation clearly showed that direct injection resulted in increased heterogeneity of the charge, as opposed to port fuel injection. It is therefore tempting to consider port injection prior to

direct injection in a lean combustion system. Direct injection has the benefit that it reduces in-cylinder temperatures due to that the vaporization of fuel sources its energy from inside the cylinder. This increases volumetric efficiency and reduces tendency of knocking combustion. These are advantages that are traded away if port fuel injection is chosen for the sake of increasing charge homogeneity. Serrano et al. compared direct injection and port fuel injection in their research engine operating on high compression ratio and jet-ignition [120]. They found that most factors such as efficiency and emissions were benefitted from the use of PFI, rather than DI. DI was beneficial near stoichiometric operation since DI allowed for slight advancement of the combustion phasing due to corresponding mitigation of knocking combustion, but this advantage diminished at very lean conditions. The load point investigated was 3000 rpm and 13 bar NMEP. These results indicate that a PFI system may be equally, or ever better, performing in a lean burn system compared to DI.

***Homogeneous lean combustion demonstrators***

An example of the progression in the field of lean combustion is the work presented by Osborne et al. [121]. In 2021, they introduced a Jaguar XE demonstrator car with a two-liter ingenium engine operating on homogeneous lean combustion. The engine was fitted with a variable nozzle turbine (VNT) turbocharger together with an E-booster to provide the necessary air mass flows required for high load lean operation. The engine was also fitted with an exhaust aftertreatment system consisting of a lean $NO_x$ trap (LNT), a gasoline particulate filter (GPF) and a selective catalytic reduction (SCR) catalyst. Both the LNT and GPF were coated to facilitate three-way catalytic capabilities. The engine operated lean at loads ranging from 1 to 14 bar BMEP, and engine speeds between 1000 and 3500 rpm. Applied relative air-fuel ratios, lambda, during lean operation varied between 1.55 and 1.4 with corresponding engine out $NO_x$-emissions between 200 and 600 ppm. These amounts of $NO_x$-emissions are far from tailpipe-compliant but were reduced primarily by the use of the active SCR system utilizing urea-injection. The demonstrator proved compliant with Euro 6d legislation, including the real driving emission test. The work presented by Osborne et al. shows two important things: With modern technology, it is indeed possible to produce an engine that can operate with, and benefit from, homogeneous lean combustion. It also shows that modern aftertreatment can realize clean tailpipe emissions, despite that engine out emissions such as $NO_x$ cannot be suppressed completely.

### 2.3.2 SCR

The selective catalytic reduction (SCR) technology is without doubt an important technology for realizing tailpipe emissions free from $NO_x$, from diesel and lean-burn engines. The advantages have been proven by several researchers and urea-SCR systems are currently in production and are standard on several brands of newly produced diesel-cars. Therefore, the novelty of SCR systems is limited, and exhaust aftertreatment is outside of the scope of this thesis. Therefore, the SCR technology will not be further discussed in terms of benefits. However, it is important to consider the backsides of the SCR technology. Impressive as it might seem, relying upon an SCR to clean excessive $NO_x$-emissions results in increased urea consumption of the SCR. Urea has the chemical formula:

$$CO(NH_2)_2 \tag{15}$$

Which, when decomposed in the SCR, partly forms $NH_3$ (ammonia) and $CO_2$. Therefore, consumption of ammonia actually produces $CO_2$-emissions. Ammonia is the substance that is used to consume the oxygen that is bonded to the nitrogen of $NO_x$-molecules.

Commercially available urea for the use in SCR systems is sold as a solvent, commonly known as adBlue. adBlue contains water and approximately 32.5% urea. For each gram per kilowatt-hour of $NO_x$-emissions that are emitted from the engine, the SCR requires approximately 3.4 g/kWh ammonia (assuming an $NO/NO_2$ ratio of 3 of the emissions) to eliminate the $NO_x$ molecules. This in turn results in n corresponding consumption of adBlue at 10 g/kWh. A factor of approximately 1.29 of $CO_2$ is produced per mass unit ammonia that is consumed:

$$m_{CO2} = \frac{M_{CO2}}{M_{urea}} \cdot \frac{M_{urea}}{2(M_{NH3})} \cdot m_{NH3} \approx \frac{44}{34} \cdot m_{NH3} \tag{16}$$

Where $m$ is mass and $M$ is molar mass. This results in almost 4.4 g/kWh in $CO_2$ emissions, or 4.4 g/kWh of $CO_2$ per 1 g/kWh $NO_x$. In this example, it is assumed that there are no conversion losses of ammonia and $NO_x$ in the process, which is not true in reality.

As another example, we can consider a modern two-liter SI-engine with a minimum stoichiometric fuel consumption of 240 g/kWh. Osborne et al. presented a peak of 12% fuel efficiency improvement from utilizing lean combustion, which corresponds to a decrease of 29 g/kWh in fuel consumption. If the engine emits 1 g/kWh of $NO_x$, at least 10 g/kWh adBlue is needed, which is a third of the reduction of fuel consumption.

For a regular gasoline containing 10% ethanol, during average stoichiometric combustion conditions, each gram of fuel results in approximately three times the amount in grams of $CO_2$ emissions when combusted. Therefore, 29 g/kWh of fuel consumption reduction results in an approximate reduction of 87 g/kWh in $CO_2$. The penalty of 4.4 g/kWh of $CO_2$ per gram of $NO_x$-emission therefore seems diminishingly small, compared to what is saved from increased efficiency. If the $NO_x$-emissions would be three times as high, and the ammonia-to-$NO_x$ efficiency of the SCR system 50%, the $CO_2$ cost would instead be 26 g/kWh. This would also mean that the consumption of adBlue could exceed the benefit in terms of fuel consumption.

The SCR technology is, once again, a promising technology that can compensate for the deficiencies of lean combustion. It is particularly useful at dynamic conditions such as transients and mode-switching when there may be temporal bursts of $NO_x$-emissions which are difficult to mitigate and otherwise would cause $NO_x$-slip into the environment. However, the usability of an SCR system as a mean of removal of excessive $NO_x$-emissions in long term is limited since the cost could outweigh the benefits. This clearly shows that despite the emerge of SCR systems, it is still vital to find means of suppressing the formation of $NO_x$ during combustion inside the engine.

### 2.3.3 Knock and High Load Lean Combustion

Knocking combustion is considered as one of the main obstacles against improving spark-ignited engine efficiency. Knock is considered as an abnormal combustion event that threatens the integrity of the engine. The phenomenon is also sometimes referred to as ringing, a name that originates from the distinct ringing sound that is emitted from an engine when significant knock occurs. Knock is known to occur due to auto-ignition of the unburnt end-gas during combustion. The rapid pressure and temperature build up combined with radiation of heat, due to the progressing flame front, trigger ignition of so-

called exothermic centers. These centers consist of small volumes of gasses with higher reactivity compared to the mean end-gas properties. The exothermic centers may be created by fuel rich pockets, locally concentrated hot residual gasses or hot spots on the combustion chamber walls [122]. The auto-ignition triggers a very rapid release of heat with a corresponding high-pressure gradient equated with shockwaves oscillating in the natural frequencies of the combustion chamber, usually in the frequency band of 5-50 kHz. The pressure waves are normally attributed by moderate pressure amplitudes, not itself challenging to the combustion chamber integrity. Instead, the rapid heat release and consequent compression of the end-gas due to sequential ignition of exothermic centers result in high heat-flux between the combustion products and the combustion chamber walls, which thermally stresses the material [123]. Additionally, focusing of the shockwaves in crevices, such as the top ring-land of the piston, may occur which may lead to cracks in the material and consecutive seizing of the piston inside the liner.

The occurrence of knock is strongly dependent on the reactivity, pressure and temperature of the end-gas and can be described by the characteristic time delay, $\tau$, of auto-ignition, as proposed by Heywood [19]:

$$\tau = C_1 P^{-n} e^{\left(\frac{C_2}{T}\right)} \tag{17}$$

Where $C_x$, $n$ are empirical constants and $P$, $T$ are pressure and temperature, respectively. If the time-delay $\tau$ of auto-ignition is longer than the time that is required for the flame to consume the end-gas, auto-ignition do not occur. Therefore, it is desirable to increase the auto-ignition delay time and decrease the duration of combustion. However, enhanced combustion is commonly accompanied by increases in temperature and pressure.

The end-gas reactivity can be decreased by dilution by air or exhaust gas recirculation (EGR). Addition of excess air and cooled EGR was investigated by Grandin and Ångström, as a mean of reducing the need for high load fuel-enrichment in a turbocharged engine [124]. The attempt at utilizing excess air as a diluent, replacing enrichment at high load, proved un-fruitful since the addition of air could not recover sufficient spark advance to compensate for slower combustion and increased cyclic dispersion. However, the amount of air-dilution that was implemented was modest, not exceeding a relative air-fuel ratio of lambda = 1.2. This was mainly a consequence of a limitation of the gas exchange-system which was utilizing a regular turbocharger that could not produce higher rates of excess air flow. In a consecutive study, Grandin et al. studied the effect of the different diluents on end-gas heat release prior to auto-ignition to assess the influence of different chemistries [125]. Notably, when diluting with air, the highest knock intensities were encountered, explained by that the increase of ratio of specific heats led to increased compression temperatures. Similarly, Grandin et al. applied rather low amounts of excess air in this study as well, which peaked at a relative air-fuel ratio of lambda = 1.3. Topinka et al. reported similar conclusions in that leaning out the air-fuel mixture required slightly increased octane rating requirement of the fuel [126].

If the relative air-fuel ratio lambda is increased beyond lambda = 1.3, a substantial cooling effect is obtained which influences the knocking properties. Doornbos et al. conducted a study in 2018 to investigate the effects of high amounts of air-dilution on knocking combustion [95]. They operated their test engine at 1500 rpm and a load of 11 bar NMEP. The study revealed non-linear effects on the tendency of knock in relation to air-fuel ratio. An increase of lambda, moving from stoichiometric to slightly lean of lambda = 1.2, was shown to increase the tendency of knocking. This confirmed the observations made by Grandin et al. However, when lambda was increased further, beyond lambda = 1.4, a

significant drop in tendency of knock was achieved. Another study, conducted by Stokes et al. in 2000 aimed at realizing knock mitigation by lean boosting in a downsized engine [127]. They conducted an experimental study in a single-cylinder research engine with artificial boosting and could demonstrate lean combustion within the combustion stability limits up to a load of 14 bar NMEP. However, it was not stated at which air-dilution rates the highest loads were achieved, nor were the corresponding $NO_x$-emissions presented. Ratnak et al. also conducted a study of boosted lean combustion on higher loads [128]. They operated their test engine at a speed of 4000 rpm and up to loads of 11 bar NMEP, with limited dilution rates of lambda = 1.3. In 2016, Bunce and Blaxill reported loads up to 14 bar BMEP in a single-cylinder research engine [97]. Bunce and Blaxill achieved air dilution rates of lambda = 1.6 at the highest loads and a peak air-dilution of lambda = 2.1, which is one of the most promising results found in the literature regarding high load lean operation. Consequently, the $NO_x$-emissions were reduced to 100 ppm levels, despite operating on loads above 10 bar BMEP. Bunce and Blaxill did however utilize turbulent jet ignition rather than regular spark ignition, explaining the extended lean combustion capabilities compared to conventional spark plug ignited lean combustion.

From the studies reviewed that have considered high load lean combustion, it has repeatedly been reported that it is possible to apply lean charges to high load engine operation, but the results are mixed. Opinions about knock-suppression from air-dilution are divided. Studies that have presented high loads, >14 bar NMEP, with very lean combustion, using regular spark-ignition, are difficult to find in the literature. The reasons to this are unknown, but it is clear that the lack of high load lean research is a gap of knowledge that is inconvenient considering the current trends in adopting to high load operation in heavily downsized engines, where efficiency improvements are needed more than ever.

### 2.3.4 Concluding Remarks

The ongoing research suggests that in-homogeneities and unsteady, non-repeatable flow structures are the main sources of cyclic dispersion of combustion. Therefore, maximized homogeneity and promotion of a dominant, stable flow structure inside the combustion chamber is preferred. Compression ratio is favorably increased to promote flame speed by increased temperatures and pressures, but care should be applied to piston design to minimize surface to volume ratio and allow for flame development without wall-interaction. Theory of turbulent combustion and experimental investigations suggest that high kinetic energy should be induced in the bulk flow. The ignition process is benefitted from high gas velocity, but with only moderate turbulence intensity, to increase spark deflection and its corresponding interaction volume without quenching of the initial flame kernel. Combustion of the bulk necessitates high turbulence intensity at top dead center, but excessive turbulence may quench the flame and prohibit consumption of the end-gas. The design of the combustion chamber and ports therefore require a balance between strong bulk flow with minimal turbulence intensity for ignitability, and strong turbulence to rapidly combust the bulk. Increasing turbulence requires promoted bulk flow in the combustion chamber to increase the kinetic energy. Redesigning the ports towards tumble-promotion may be done at the expense of increased port friction and decreased volumetric efficiency, which increases the pumping losses. Slow initial flame development often necessitates very early spark timing, which in turn reduces ignitability and increases dispersion of combustion. The research indicates that high rates of air-dilution can be utilized to mitigate knock. It is therefore sensible that lean combustion would be ideal in high load conditions, since increased temperatures would promote the

initial flame kernel, allowing later spark timings and more stable ignition, and the air-dilution would suppress knock, allowing more beneficial combustion phasing angles. Higher turbulent kinetic energy due to increased mass flow at higher loads may reduce the dispersion of the in-cylinder flow, which may reduce cyclic dispersion of combustion and increase the consumption rate of the flame, thus allowing for higher rates of air-dilution that ultimately leads to lowered $NO_x$-emissions.

## 2.4 Research Questions

From the reviewed literature, the following questions arose regarding homogeneous lean combustion in a downsized spark-ignited engine:

- Can the dilution limit of homogeneous lean combustion be extended by increasing the engine load?
- Is there a limit in applicable engine loads when an engine operates with homogeneous lean combustion, and if so, what are the mechanisms that cause the limit?
- Can high amounts of air-dilution suppress end-gas auto-ignition at high engine loads?
- Is it possible to achieve reasonable $NO_x$-suppression by air-dilution at high engine loads?
- What is the effect of residual gasses upon homogeneous lean combustion, and can residual gasses be used to achieve additional $NO_x$-suppression?
- Is it possible to sustain high load homogeneous lean combustion by utilizing a turbocharger optimized for lean combustion, without artificial supercharging?

It was hypothesized that increased engine loads will provide conditions that aid diluted combustion, which will result in increased combustion tolerance to charge dilution which will benefit robustness and $NO_x$-emission suppression. Additionally, it was hypothesized that very lean conditions will sufficiently suppress auto ignition which in turn will allow for unlimited high load lean combustion operation within the mechanical limitations of the engine and air supply. It was hypothesized that engines trap high amounts of residual gasses at low loads which inhibit air-dilution, but that residual gasses can be used to decrease the formation of $NO_x$ by reducing the oxygen concentration of the charge.

# 3 Experimental Equipment and Methods

To answer the research questions and to achieve the stated goals, experimental research has been conducted utilizing various hardware and different approaches. The experimental work has been divided into four major experimental campaigns, corresponding to the four publications that are included in this thesis. Two test-engines have been utilized for the various experimental activities: a modified multi-cylinder engine, and a single-cylinder research engine. The experimental approach, utilizing test-engines, was chosen since disperse internal combustion in a reciprocating engine is difficult to study using other techniques. A test engine, adequately instrumented, provides an environment that can produce the physical phenomena in question and allows the acquiring of corresponding strategic measurement data that can be used to quantify and analyze the characteristics of combustion.

## *3.1 Overview of Experimental Activities*

Campaign 1 utilized the multi-cylinder engine. The aim of this campaign was to verify the hypothesis that lean combustion could be sustained in, and benefitted from, a downsized boosted lean combustion system. To do this, a multi-cylinder engine was fitted with a prototype two-stage turbocharger and was mapped at various operating points to assess the corresponding characteristics of lean combustion.

Campaign 2 utilized the single-cylinder research engine. From the results obtained from the first research campaign, it was concluded that more research into high load lean combustion was needed using an engine that could offer extended decoupled degrees of freedom and calibration access. The single-cylinder engine was chosen since it enabled decoupling of inlet and exhaust pressures, which are otherwise dictated by the turbocharger characteristics (when used). To enable high load lean combustion, a mechanical boosting system was fitted to the engine, allowing 2 bar gauge inlet pressures.

Campaign 3 again utilized the single-cylinder research engine. Results obtained from the second research campaign necessitated further experiments to investigate unanswered questions regarding limitations of high load lean combustion. The engine was fitted with a new cylinder head with optical, endoscopic access to the combustion chamber allowing in-cylinder high speed imaging during realistic operating conditions.

Campaign 4 utilized both engines to acquire experimental data that could be utilized to calibrate a 1-D engine model to be used for deeper analyses. Deviating results from previous campaigns raised the hypothesis that trapped residual gasses, undetected, might obscure the measured dilution rates in terms of air-dilution. The single-cylinder engine was fitted with additional sensors to acquire high load lean combustion data. The multi-cylinder engine was instrumented in a similar manner and utilized to acquire low load combustion data.

The following sections describe the experimental hardware in more detail.

## *3.2 Experimental Hardware*

### 3.2.1 Turbocharged Multi-Cylinder Engine

The multi-cylinder engine utilized in campaign 1 and 4 was a modified Volvo Cars two-liter in-line four-cylinder direct injected spark-ignited turbocharged engine rated to 187

kW and 350 Nm. Details of the engine are provided in Table 1 and a schematic layout is presented in Figure 14. The engine was self-sustaining in the sense that it did not require any auxiliary power input nor external air supply to operate.

*Table 1. Specifications of the multi-cylinder engine*

| | |
|---|---|
| Engine type | VEP4 MP Gen I |
| Number of cylinders | Four, in-line |
| Displaced volume | 1969 cc |
| Bore / Stroke | 82 mm / 93.2 mm |
| Compression ratio | 10.8:1 |
| Valve train | DOHC, 16 valves |
| Intake camshaft phasing | Electro-hydraulic, variable 0-48° CA advance |
| Exhaust camshaft phasing | Electro-hydraulic, variable 0-30° CA retard |
| Valve actuation | Direct, mechanical lash adjuster |
| Ignition system | DCI, standard J-gap spark plugs |
| Fuel system / Injection pressure | DI / 200 bar |
| Start of injection | -308° to -340° ATC |
| Boosting system | 2-stage regulated turbocharger |
| Rated power/ Rated torque | 187 kW / 350 Nm |

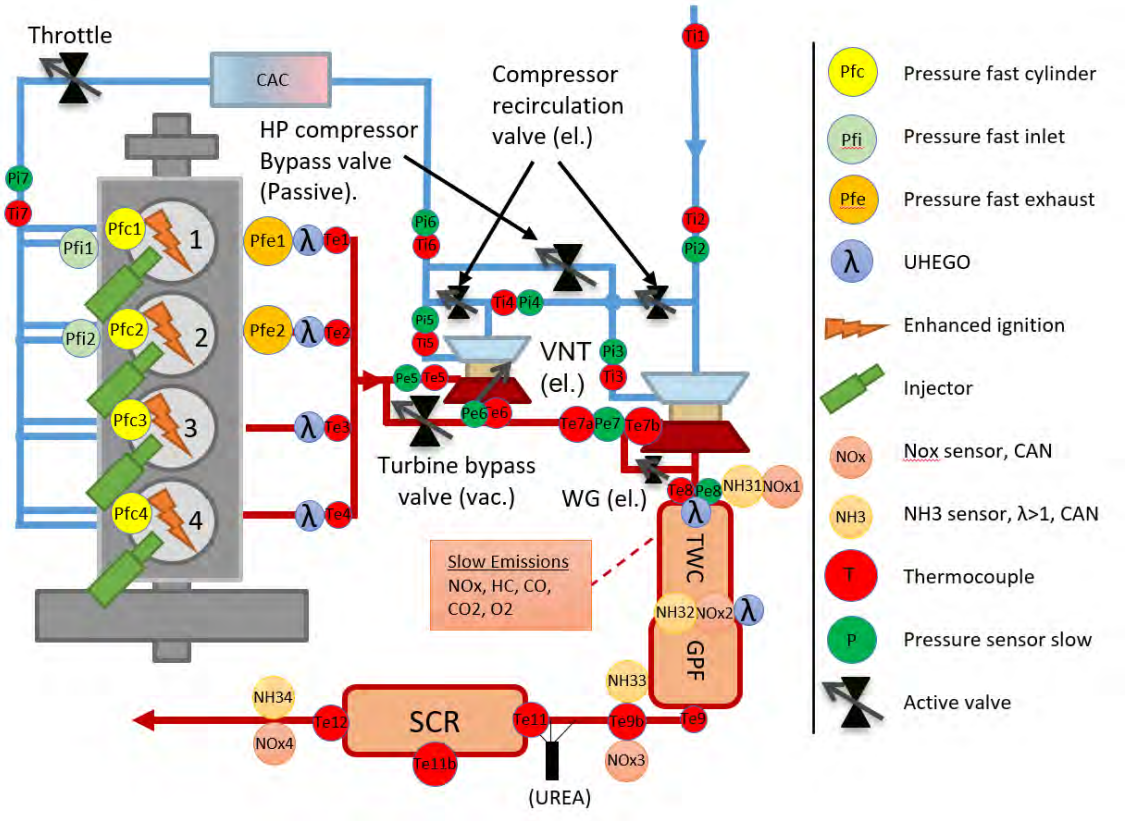


*Figure 14 . Schematic overview of the multi-cylinder engine setup.*

The multi-cylinder engine was equipped with a prototype regulated two-stage serial turbocharger with a high-pressure stage consisting of a variable nozzle turbine (VNT), and a low-pressure stage consisting of a waste-gated (WG) turbine. The high-pressure stage turbine was equipped with an active bypass valve, equivalent to an external waste-gate, to control exhaust flow between the two turbine stages at various conditions. The turbocharger system was designed to meet the high demands on air mass flow to achieve highly diluted lean combustion exceeding lambda 2 at low engine speed between low torque levels up to maximum torque. At peak power, the turbocharger was designed to deliver an approximate air mass flow sustaining lambda 1.4. The VNT high-pressure turbine was primarily optimized to operate at the challenging intermediate torque levels above 6 bar NMEP (where a naturally aspirated engine normally reaches its lean torque limit) and 11-13 bar NMEP where the main turbocharger normally starts to deliver significant boost. The two turbines could both operate in series, parallel or as single stage, depending on the engine operating point. At higher engine speeds, the VNT turbine had to be bypassed to avoid excessive restriction of the exhaust. The dimensioning of the system was conducted by Volvo Cars, hence the design and assessment of the turbocharger system itself is out of scope of this thesis. The turbocharger is visualized in Figure 15.

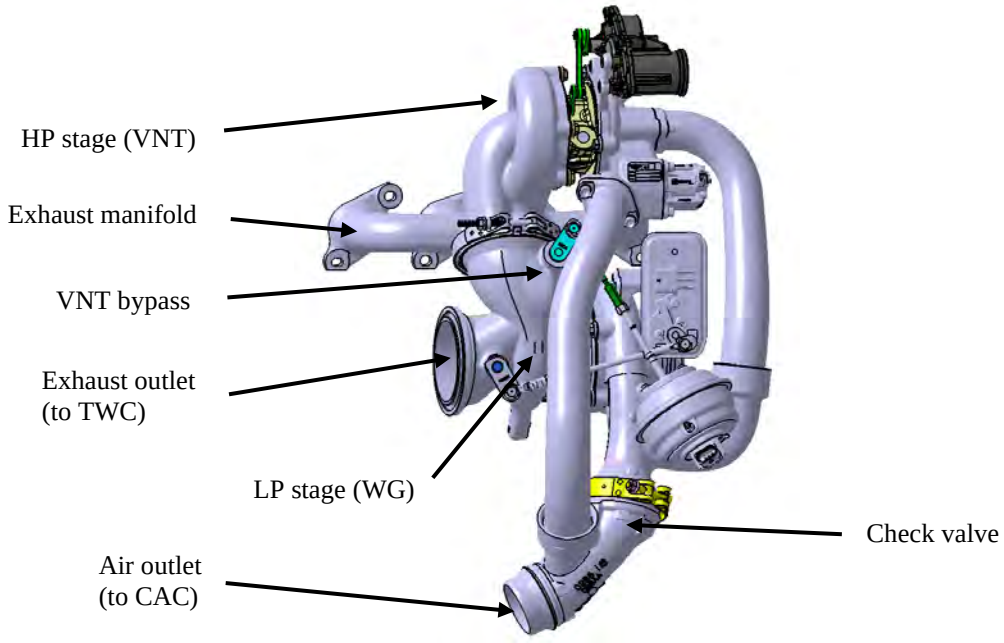


*Figure 15. CAD-image of the turbocharger fitted to the multi-cylinder engine which was used to increase air mass flow rates to extend lean combustion capabilities.*

A high energy ignition system from Borg Warner utilizing dual coils was fitted to the engine to increase spark energy and spark duration to improve the ignition quality of lean charges. The reader is referred to Alger. et. al for more details on dual coil systems [90]. The main working principal of the system is that the two parallel coils work in series to sustain a continuous, pulsating arc between the spark plug electrodes. After discharge of the first coil and before all available coil energy is emitted, the second coil discharges while the first coil is reloaded.

The engine was fitted with a complete exhaust aftertreatment system for realistic pressure drop and to characterize aftertreatment conditions during lean operation. The aftertreatment system consisted of a standard three-way catalyst (TWC) close-coupled to

the second, low-pressure turbine, and a downstream active urea-SCR. The SCR-system was not activated during measurements but served only to achieve realistic exhaust conditions in terms of back-pressure. In campaign 4, a gasoline particulate filter (GPF) was added to the exhaust aftertreatment system.

The engine was fitted with a variety of sensors to sample temperature, gas exchange system- and in-cylinder pressures signals. The engine was positioned in a test cell and connected to an AVL Elin 315 static dynamometer to control and measure engine speed and load during tests. An emission sample was extracted after the second turbine to retrieve engine out raw emissions and these emissions were analyzed using a standard emission rack. More details about the measurement equipment are provided in Table 2. Cylinder 1 and 2 were equipped with piezoresistive, fast response, pressure transducers in the inlet and exhaust ports which were used to acquire calibration data for consecutive simulations of the gas-exchange process. The multi-cylinder engine was equipped with a parallel-inlet-port cylinder head, which meant that each cylinder had two parallel inlet runners, inlet ports and valves, but only one of the ports of cylinder 1 and 2 was fitted with a pressure-transducer.

*Table 2. Specifications of the acquisition system of the multi-cylinder engine*

| | |
|---|---|
| Cylinder pressure sensors | Kistler 6045AU20 |
| Cylinder pressure amplifiers | Kistler 5011 |
| Exhaust port pressure sensors | Kistler 4007BA20FA0 |
| Inlet port pressure sensors | Kistler 4007C005FDS1-2.0 |
| Crank angle decoder | AVL 365C |
| Indicating acquisition hardware | AVL Indimaster 670 |
| Indicating acquisition software | AVL Indicom 1.6 |
| General pressure transducers | Trafag CMP 8270 |
| Temperature probing | Thermocouples type K |
| $CO_2$ | Non-dispersive infrared detector |
| CO | Non-dispersive infrared detector (0-500ppm + 0-5%) |
| $O_2$ | Paramagnetic oxygen analyser |
| HC | Flame ionization detector |
| $NO_x$ | Two channel chemiluminescence detector ($NO+NO_x$) |
| Lambda | OEM Broadband exhaust gas oxygen sensor |
| Lambda | Bosch LSU 4.9 (runner lambda) |
| Fuel mass flow | Micromotion Coriolis mass flow meter |

Each exhaust runner was fitted with a broad band universal heated exhaust gas oxygen (UHEGO) sensor (lambda-sensor) to monitor the air-fuel ratio of each cylinder individually. This was a necessary act since it was early proven that there was a significant maldistribution of air and fuel amongst the cylinders, which is why each cylinder had to be calibrated individually to make the cylinders perform equally. Measuring lambda using UHEGO sensors proved to be difficult. The sensors are commonly pre-heated prior to startup of the engine, but at startup there are often

condense droplets expelled from the exhaust port during the first seconds. These droplets hit the UHEGO probe cracking the warm zirconia elements inside the UHEGO. This is why runner mounted UHEGO sensors are preferably not preheated nor activated until a minute after engine start up.

Emission species were measured to assess combustion efficiency and the influence of air-dilution on noxious emissions of $NO_x$, HC and CO. Consequently, the emission species were used to compute the Brettschneider lambda to validate the broadband lambda-sensor readings.

### 3.2.2 Single-Cylinder Research Engine

The single-cylinder research engine utilized in campaigns 2 to 4 was an AVL 5411, fitted with a custom cylinder head designed for single cylinder engine prototype usage, provided by Volvo Cars. The single-cylinder engine provides unlimited calibration access to all engine settings and also eliminates potential issues associated with managing multiple cylinders simultaneously. The single-cylinder engine also allows complete decoupling of the hot and cold parts of the gas-exchange system which allows extended studies on gas-exchange phenomena. Details of the engine are listed in Table 3 and a schematic overview of the setup is presented in Figure 16.

*Table 3. Specifications of the single-cylinder research engine*

| | |
|---|---|
| Engine type | Single-cylinder research engine, AVL 5411 |
| Displaced volume | 475 cc |
| Bore / Stroke | 82 mm / 90 mm |
| Cylinder head | Single-cylinder VEP MP Gen III |
| Compression ratio | 10:1 |
| Combustion chamber | Pent roof |
| Tumble ratio | 1.5/ 2.5 at open/ closed flap |
| Variable tumble | Tumble Flap, 0/50% blocked area |
| Valve train | DOHC, 4 valves |
| Valve actuation | Roller finger followers, hydraulic lash adjusters |
| Camshaft phasers | Mechanical, fixed |
| IVC | -141° ATC @ 1 mm lift |
| EVO | 137° ATC @ 1 mm lift |
| Overlap | 23° CA @ 0 mm lift |
| Ignition system #1 | DCI, standard J-gap spark plug |
| Ignition system #2 | HFI, 5-electrode igniter |
| Ignition system #3 | SCI, standard J-gap spark plug |
| Start of injection | -310° ATC |
| Boosting system | 2 bar gauge, external supply |

To sustain high load lean operation, the engine was connected to an external air-supply delivering a maximum of 2 bar gauge boost pressure and maximum mass flow far exceeding the requirements. The boost pressure was accompanied by an exhaust pressure valve that could simulate turbine pressure drop of a turbocharger. Imposing a realistic backpressure (exhaust pressure) is particularly important to avoid unrealistic scavenging and positive pump work which would otherwise bias the net efficiency of the combustion cycle. Throughout the experiments performed in the single-cylinder engine, the exhaust pressure was maintained equal to the inlet pressure, unless stated otherwise.

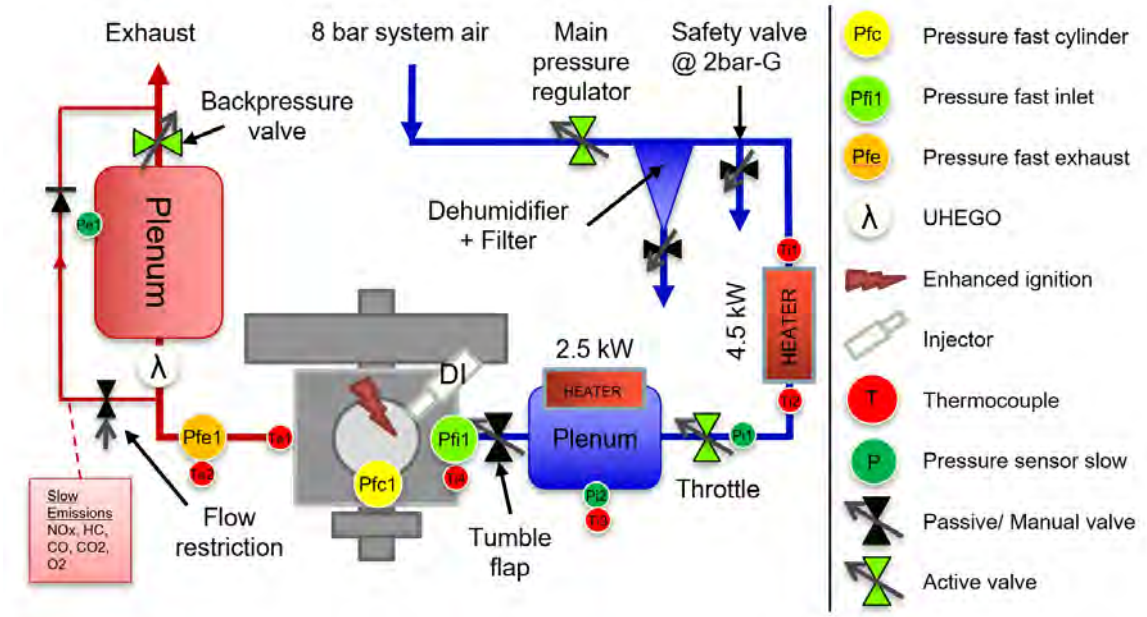


*Figure 16 . Engine layout of campaign 2*

The engine was fitted with a variable tumble device consisting of a divider plate inserted into the inlet ports, where the lower half of the ports could be blocked by a valve to target the top side of the valves and increase gas velocity. The device was previously illustrated in Figure 13.

Three different ignition systems were utilized with the single-cylinder engine. The very same dual-coil ignition system utilized in the multi-cylinder engine was utilized in campaign 2 and 4. Additionally, a Borg Warner EcoFlash high-frequency ignition system (HFI) was utilized in campaign 3 together with a regular single transistor coil ignition system for comparison with the HFI system.

Details of the acquisition system are listed in Table 4. Similar to the acquisition system of the multi-cylinder engine, the main emissions species from the exhaust were measured to assess influence of lean combustion on emission characteristics. The concentrations of emission species were also used to estimate combustion efficiency and to compute the Brettschneider lambda value to establish redundancy.

*Table 4. Specifications of the acquisition system of the single-cylinder engine*

| | |
|---|---|
| Cylinder pressure sensor | AVL GH14DK (M5) |
| Cylinder pressure amplifier | Kistler 5011 |
| Exhaust port pressure sensor | Kistler 4049A5SP22 (water cooled) |
| Inlet port pressure sensor | Kistler 4007C005FDS1-2.0 |
| Crank angle decoder | AVL 365C |
| Indicating acquisition hardware | AVL IndiModul |
| Indicating acquisition software | AVL Indicom 2.6 |
| Pressure transducers | Trafag 8862 + 8863 |
| Temperature probing | Thermocouples type K |
| $CO_2$ | Non-dispersive infrared detector |
| CO | Non-dispersive infrared detector (0-5000ppm + 0-5%) |
| $O_2$ | Paramagnetic oxygen analyser |
| HC | Flame ionization detector |
| $NO_x$ | Two channel chemiluminescence detector ($NO+NO_x$) |
| Lambda | Broadband UHEGO, Horiba MEXA110 |
| Fuel mass flow | Micromotion Coriolis mass flow meter |

### 3.2.3 Fuels and Injection Systems

A standard test fuel of gasoline containing 10% ethanol with an octane rating of 95 was used throughout all experiments. The fuel is representative of the pump-fuel found in European gas stations. One exception occurred in the third experimental campaign, where also direct injected methane was utilized in the single-cylinder engine. Direct injected methane was utilized to assess the impact of an alternative fuel on high load lean combustion. Both the multi-cylinder engine and the single-cylinder engine used fuel injection systems with the same type of injector and main characteristics when operated on gasoline. The properties of each fuel and the corresponding fuel injection systems are described in Table 5.

*Table 5. Fuels and corresponding fuel injection systems utilized*

| Fuel and fuel injection | Gasoline E10, RON95E10S | Methane, $CH_4$ |
|---|---|---|
| Fuel composition | 90% m/f Gasoline<br>10% m/f Ethanol | 100% methane |
| Octane number (RON) | 95 | >120 |
| Methane number (MN) | - | 100 |
| AFR stoichiometric | 14.01:1 | 17.19:1 |
| Lower heating value (MJ/kg) | 42.79 | 50.01 |
| H/C atomic ratio | 1.94:1 | 4:1 |
| O/C atomic ratio | 0.033:1 | 0:1 |
| Injection type | Direct Injection | Direct Injection |
| Injector position | Central | Central |
| Injector type | Solenoid | Solenoid |
| Injection pressure (bar) | 200 | 40 |
| Number of nozzle holes | 6 | 10 |
| Start of injection | 310° BTC | 310° BTC |
| Injector manufacturer | Denso | GDTech |

### 3.2.4 Optical Setup of the Single Cylinder Research Engine

In campaign 3, optical access to the combustion chamber of the single-cylinder engine was established by utilizing an endoscope fitted through the combustion chamber pent-roof wall. An additional cylinder head of the single-cylinder research engine was therefore acquired and modified accordingly. The optical access was necessitated by the need for further insight into the combustion that could not be determined from measured in-cylinder pressure nor other probed quantities. Figure 17 illustrates the optical access accomplished and Figure 18 presents the engine with endoscope and camera setup. Images were acquired using a high-speed color video camera. The camera used was an Ametec Vision Research Phantom Miro M310 highspeed color video camera equipped with a Carl Zeiss 85 mm f/2 lens. The endoscope was a LaVision Hybrid Camera Endoscope. Images were acquired with 512 x 464 pixels resolution, an exposure time of 50 microseconds and a sample rate of 12000 frames/second. The camera was equipped with a Bayer-format single CMOS-sensor, meaning that the true resolution for each color is reduced. The capturing of images was gated during each combustion cycle to only capture visible spark and early combustion. This resulted in that the internal memory of the camera allowed storage of images during approximately 91 consecutive combustion cycles at a time. The previously presented Figure 9, Figure 10 and Figure 11 visualize examples of images acquired from the combustion chamber using the utilities described.

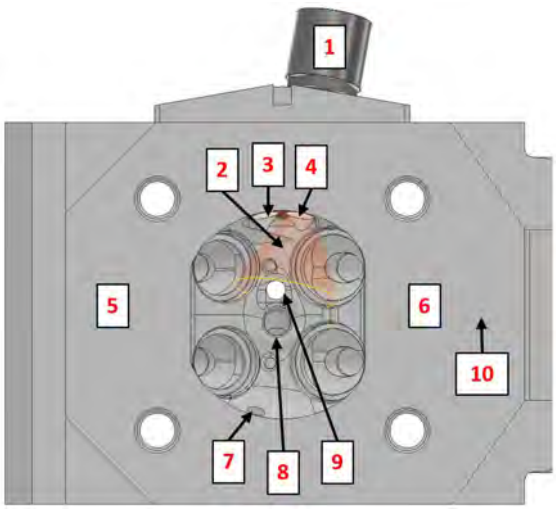


*Figure 17. CAD-rendering of the bottom side of the cylinder head (front of engine). 1 – endoscope magnifying lens; 2 – projected view of the endoscope; 3 – alternative endoscope/ light entry; 4 – endoscope shield lens; 5 – exhaust side; 6 – intake side; 7 – pressure transducer location; 8 – spark plug location; 9 – injector location; 10 – cylinder head deck.*

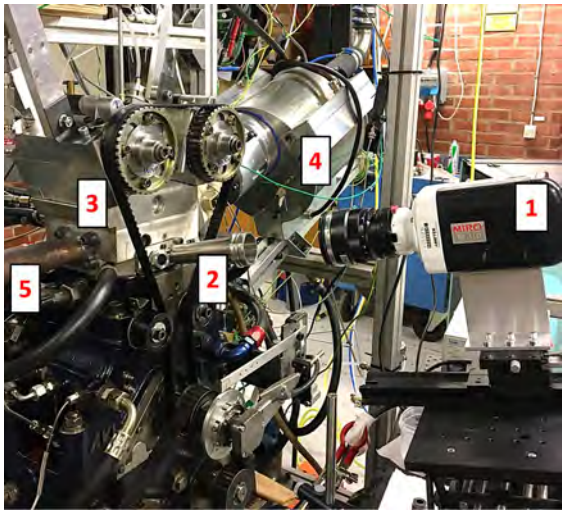


*Figure 18. Optical setup with endoscope: 1 - high speed video camera; 2 - endoscope connected to cylinder head; 3 - engine cylinder head; 4 - air intake manifold; 5 - exhaust gas runner.*

The images were primarily used to assess the flame development post ignition. To assess the large quantities of images, a post-processing routine was developed based upon the approach developed by Dahlander and used by Melaika et al. [129]. The main working principals rely upon separating flame luminosity from the background noise. This was done by a gaussian filter combined with various pass-band filters. The images were ultimately binarized by a threshold value to determine the flame contours. Each flame contour from a corresponding combustion cycle could then be overlayed in an ensemble image of which, when normalized, corresponded to the relative frequency of the whereabout of the flame at a certain crank angle. These images were used to assess the dispersion of the flame development during experiments conducted with the single cylinder research engine. The details of the post-processing routine were described in appended Paper III. The main steps of the image processing and an example image of the ensemble result are visualized in Figure 19.

Three major drawbacks are accompanied by the use of combustion chamber image acquisition using a color camera. First, since the sensor is of the Bayer format, the effective resolution of the images is reduced. Second, significant luminosity of the flame front is emitted in the ultraviolet spectrum, and therefore, it is not certain that the actual flame front is detected by the use of a color camera since the color camera is limited to detection of light in the visible spectrum. Third, it is more difficult to discriminate undesired light such as reflections and glow. The spark from the spark plug sometimes produces strong broadband light emissions that obscures the initial flame completely. This has necessitated the use of extensive filtering during postprocessing to eliminate the undesired quantities that manifests on some of the acquired images.

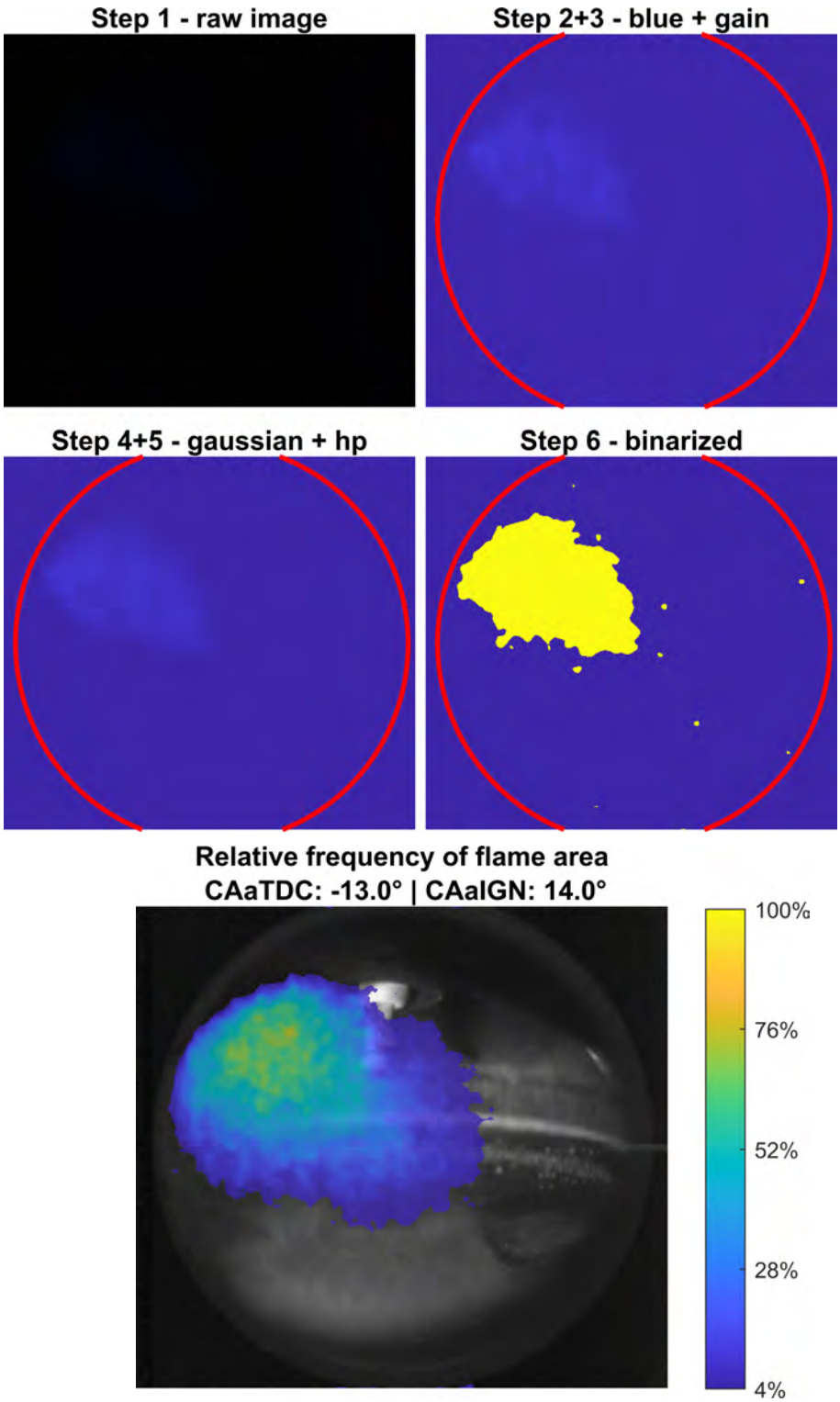


*Figure 19. Illustration of the main steps of image post processing utilized, from raw RGB-image (step 1), extracted blue matrix and gained (step 2+3), gaussian filtration and high-pass (step 4+5), and binarization of the result resulting in the flame contour/ flame area (step 6). An additional image is provided illustrating the ensemble relative frequency of flame area. As can be seen from the frequency image, the flame is rarely in the same position between the cycles (<100%).*

The use of an endoscope was chosen in favor of a fully transparent (optical) engine setup. The endoscope allows engine operating conditions similar to real operating conditions,

i.e., high cylinder temperatures and pressures and high engine speeds. Additionally, the combustion chamber remains virtually unchanged compared to the standard one, which means that the engine will be able to reproduce the same results as a full metal engine. The drawback of using endoscopic access to the combustion chamber is that the view is limited, and the image is distorted due to the wide-angle lens of the endoscope. A fully optical engine, using an optical liner and/ or a Bowditch piston with a transparent piston crown, can accomplish orthogonal optical access to the major parts of the combustion chamber without distortion. However, a fully transparent optical engine implies heavily restricted operating conditions to avoid failure of the optical components and the piston extension. Additionally, large optical elements affect the heat conduction characteristics of the combustion chamber which influence combustion. It is also questionably if the operating conditions investigated in campaign 3, with engine speeds of 2500 rpm and peak cylinder pressures of 90-100 bar, could be sustained in a conventional optical engine.

## *3.3 Data Acquisition and Evaluation*

Measurements were exclusively conducted under steady state conditions. Before each measurement, temperatures were verified to be stable. Temperature readings are subject to high inertial effects and are therefore appropriate indicators of a steady state. By acquiring data during steady state conditions, statistical quantities such as CoV and LNV can be appropriately determined from each sample without considering drifts. If the conditions are non-steady, i.e., transient, it will likely influence the stability of the combustion thus impairing the statistical quantities.

Measurements were acquired by simultaneously measuring the indicating system, i.e., the high frequency crank angle resolved acquisition system, and the time-resolved, low frequency data. The indicating system utilized with the multi-cylinder engine recorded 300 consecutive cycles and time-resolved data were sampled during the same time frame. The indicating system of the single-cylinder research engine sampled 500 consecutive cycles, and the time-resolved data was recorded over 30 seconds. 30 seconds approximately corresponds to the maximum measurement duration of the indicating system at an engine speed of 1000 rpm. The time-resolved data was averaged to discriminate against signal noise.

The indicating systems recorded pressure signals at 0.1°crank angle (CA) resolution in the window of -50° to 90° CA after top center (ATC), and with a resolution of 1° CA during the remining part of the combustion cycle. High resolution in the combustion window is necessary to capture the higher frequencies obtained by knocking combustion, where literature suggests at least 0.25° CA resolution. Additionally, higher resolution improves accuracy of heat release determination.

Drifts and dispersion of the measurement setup were accounted for by daily measuring a reference engine load-point. Various reference points were utilized, depending on the nature of the corresponding experiments. In campaign 1 when using the multi-cylinder engine, a load-point of 1500 rpm and 10 bar BMEP was chosen, which also served as warm-up. In the single cylinder engine, both a motored measurement and a fired one were acquisitioned after each start-up. The reference load-point of the single cylinder engine was 1500 rpm and 5.5 bar NMEP. The single-cylinder engine was pre-heated by its auxiliary rig-system which made any warm-up running obsolete. Additionally, daily calibration of the exhaust gas analyzers was conducted using zero- and span-gases to account for any drifts and potential accumulation of contaminants in the instruments.

Ideally, all measurements are repeated at least three times to estimate the measurement errors. This is however sometimes impractical due to cost and time-constraints if many experiments are to be performed. During the experiments conducted to produce this thesis, strategic repeated measurements at chosen, representative conditions, were used to estimate the repeatability and corresponding errors of the setup and measurement devices. An example of such repetitions, contained within a measurement series that is a sweep of the parameter lambda, is illustrates in Figure 20. The measurements of the repeated daily reference operating points were additionally used to assess measurement errors when applicable and could also be used to monitor variations from day to day and long-term drifts. The use of selected repetitions of reference conditions is a simplification, since the reference operating condition cannot be guaranteed to represent the dispersion of other conditions, but the practice is commonly used in experimental methodology to decrease experimental effort.

Measurements were generally conducted by performing so called lambda sweeps. A lambda sweep includes a measurement at stoichiometry, followed by increments of lambda in increasing order, until the stability limit is exceeded. Where appropriate, the order of tested increments of lambda was randomized. It should be noted however that randomizing the order of measurement increases the duration of stabilization- and tuning. An advantage of the parameter sweep of lambda is that the stoichiometric point is included, which means that the results of lean combustion can be compared relatively to stoichiometric combustion. As could be seen in Figure 20, the measurement dispersion compared to the effect of lambda was very small.

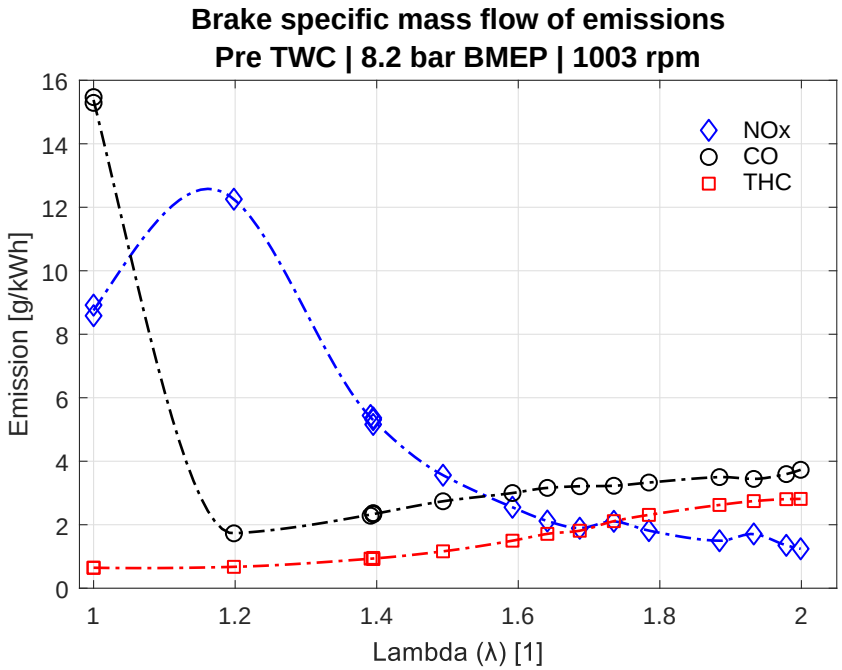


*Figure 20. Resulting emissions from a lambda-sweep of the multi-cylinder engine. Repetitions have been included at lambda = 1 and lambda = 1.4 to visualize the dispersion. This is to assure that the variance of measurement noise is not dominating the desired parameter-induced variance. As can be seen, the dispersion relative to the large changes in emission with respect to lambda is small.*

## *3.4 Combustion Diagnostics*

From the acquired in-cylinder crank angle resolved pressure signals, it is possible to compute the heat released from combustion of fuel inside the cylinder. The heat release characteristics ought to be one of the most used diagnostic tools when assessing combustion in reciprocating engines. The online software of the acquisition units provided online computation of the heat release with corresponding extraction of various combustion angles, on a cycle resolved basis, based upon simplified approaches. The online results were used for online calibration during the experiments. The online software also accounted for pegging of the cylinder pressure transducers, which was conducted by using the thermodynamic approach. Pegging is necessary to determine the zero offset on a combustion-cycle basis of the drifting signals from the piezo-electric in-cylinder pressure transducers. When the specific heat capacity of the in-cylinder charge is changed, due to addition of air-dilution or other diluents, the thermodynamic properties of the cylinder charge changes, which is not accounted for in the computations of release of heat by online software. Therefore, measured cylinder pressures obtained from experiments were postprocessed using more refined computational methods to obtain the combustion attributes. Since lean combustion is strongly related to unsteady phenomena, it is important to accurately capture the characteristics of each combustion cycle during a measurement interval and not only ensemble average quantities.

### 3.4.1 Heat Release

By using the first law of thermodynamics, assuming no mass-transfer over the combustion chamber control volume boundaries, the chemical rate of heat release, $Q_{ch}$, or rate of gross heat release can be computed as:

$$\frac{dQ_{ch}}{d\theta} = \frac{\gamma}{\gamma - 1} P \frac{dV}{d\theta} + \frac{1}{\gamma - 1} V \frac{dP}{d\theta} + \frac{dQ_{ht}}{d\theta} \tag{18}$$

Assuming no mass-transfer means that blow by, the leakage of through the piston rings into the crankcase, in neglected. For the formula to succeed one must know the pressure, volume, and ratio of the specific heats, of the gasses within the combustion chamber, and the corresponding losses of heat to the cylinder walls, in the crank angle domain. Heat losses can be approximated by means of modelled correlations or more complex simulations. One may also simplify the formula by disregarding the heat loss, $Q_{ht}$, and only compute the net heat release, $Q_{net}$:

$$\frac{dQ_{net}}{d\theta} = \frac{\gamma}{\gamma - 1} P \frac{dV}{d\theta} + \frac{1}{\gamma - 1} V \frac{dP}{d\theta} \tag{19}$$

The net release of heat is also known as the apparent heat release. When computing the net heat release, an adiabatic process is assumed, and the resulting heat release will be directly proportional to the measured quantities of pressure and volume. The net heat is not representative of the actual gross release of heat inside the combustion chamber, but it is representative of the useful heat converted into work. During all experimental campaigns, the net heat release was utilized as the measure of heat release rate.

The ratio of specific heats, gamma, must be known in order to compute the heat release. The ratio of specific heats is dependent on the properties of the gasses inside the combustion chamber and the corresponding temperatures. For quick assessments, the ratio of specific heats may be set to a constant value of approximately 1.32 for pre-mixed, stoichiometric SI-engines, for a more detailed analysis, the ratio of specific heats should be determined appropriately.

### 3.4.2 Estimation of Ratio of Specific Heats

***The polytropic approach***

Various proposals have been presented in the literature of how to estimate the ratio of specific heats. By assuming adiabatic compression and expansion, the ratio of specific heats equals the polytropic coefficient. The polytropic coefficient may consequently be computed from the compression and expansion curves respectively. This may be accomplished by using a least squares method to estimate the polytropic constant $C$. This method was proposed by Dahl [130], which in turn was derived from the method proposed by Tunestål [131]. The polytropic coefficient $\kappa$ can be determined from the following equation:

$$P \cdot V^{\kappa} = C \tag{20}$$

However, the polytropic relation does not hold during the combustion due to the corresponding addition of heat. This can be managed by interpolating the polytropic coefficient between start and end of combustion. Since the polytropic coefficient is computed from the measured pressure, it automatically incorporates changes in the specific heats from altering the air-fuel ratio. This method was used during campaign 1 to compute the heat release. During rapid combustion, the interpolated polytropic coefficient has little influence on the resulting heat release calculation, such as HCCI combustion. However, if the combustion is slow, like spark-ignited homogeneous lean combustion, a deviating estimation of gamma during the combustion may have larger influence on the computed results. Another disadvantage of the method is that the heat flux to the cylinder walls influence the polytropic coefficient which in reality is not constant during compression nor expansion. Additionally, the polytropic coefficient is only equal to the ratio of specific heats at the so-called inversion point at which the heat flux to the cylinder walls is zero.

***Ceviz-Kaymaz***

Another method of estimating the ratio of specific heats has been proposed by Ceviz and Kaymaz [132]. The ratio of specific heats is computed separately for unburned and burned gasses respectively, as a so-called two-zone model. The dependencies of the burned and unburned ratios of specific heats in relation to gas temperatures and air-fuel ratio are given by algebraic expressions defined by Ceviz and Kaymaz. The average ratio of specific heats of both burned and unburned gasses can then be computed accordingly:

$$\gamma = MFB \cdot \gamma_b + (1 - MFB) \cdot \gamma_u \tag{21}$$

Where $MFB$ corresponds to mass fractions burned, and subscripts $b$ and $u$ are burned and unburned respectively. By averaging, the two zones are merged into a single zone computation. To compute the ratio of specific heats of the two zones, the cylinder temperature needs to be known. Assuming consistency of the ideal gas law, one can estimate the average cylinder temperature on a crank angle basis as:

$$T_{cyl}(\theta) = T_{cyl,ivc} \frac{P_{cyl}(\theta) \cdot V_{cyl}(\theta)}{P_{cyl,ivc} \cdot V_{cyl,ivc}} \tag{22}$$

Computing the cylinder temperature as a single zone cylinder average temperature is a simplification, since the temperature of the unburned and burned gasses are different. From equation 22, it can be concluded that reference conditions at inlet valve closing (IVC) must be known to estimate the gas temperatures. The pressure is given by the in-cylinder pressure measurement and the volume is known from the position of the piston.

However, the temperature at IVC must be estimated. This can be accomplished by measuring the inlet air temperature just before it enters the combustion chamber. During the intake stroke the fresh charge will interact with the combustion chamber walls and residual gasses hence resulting in convection of heat presumably increasing the final charge temperature in relation the admitted fresh air. Another implication is that if the engine is direct injected, the cooling effect of the vaporization of the fuel also affects the temperature of the charge. Computation of heat transfer and vaporization is however complicated and may be considered as excessive. Small temperature variations have negligible influence on the resulting estimation of specific heats. Grandin suggested the use of a fixed value of a temperature increase of 40K, added to the measured inlet air temperature [133]. This approach has been utilized to estimate the cylinder temperature and corresponding ratio of specific heats by the method presented by Ceviz-Kaymaz to determine the rate of heat release in the experimental campaigns 2 to 4. The Ceviz-Kaymaz approach was chosen in these three campaigns instead of the previously discussed polytropic approach since Ceviz-Kaymaz was considered more accurate during slow combustion. A drawback of the Ceviz-Kaymaz approach is that the effective compression ratio must be known, and sometimes carefully tuned, in order to eliminate apparent heat release during compression and expansion. The polytropic approach automatically cancels these effects.

To compute the resulting ratio of specific heats using the approach of Ceviz-Kaymaz, the mass fractions burned must be known first. This means that the heat release must be iteratively computed. A constant ratio of specific heats was used in the first iteration to estimate an initial heat release, which was then used as a starting value for two consecutive iterations of the Ceviz-Kaymaz approach.

## *3.5 One-Dimensional Engine Simulation using TPA*

Observations made from the experimental campaigns 1 to 3 resulted in unanswered questions regarding the influence of trapped residual gasses. This led to a fourth measurement campaign being conducted to investigate the impact of residual gasses on lean combustion. Residual gasses are difficult to measure. Due to the heat flux between cylinder walls and the fresh charge, and the heat brought by the unknown amounts retained residual gasses, the temperature inside the cylinder is difficult to determine. If the temperature is unknown, the density and the corresponding total trapped cylinder mass cannot be computed from regular acquisition data such as cylinder pressure, volume, fuel and air flow, and port temperatures. Determination of residual gasses may however be accomplished by the use of one-dimensional modelling and simulation of the gas-exchange process and the corresponding combustion. A specific type of one-dimensional modelling is called three-pressure analysis (TPA). This method was utilized in campaign 4 to complement the experimental measurements. TPA is a mostly non-predictive simulation approach that utilizes crank angle resolved intake port, cylinder, and exhaust port pressure signals to calibrate the model which eliminates the need for modelling of the external gas-exchange system and the combustion. The TPA is therefore reliant upon experimentally acquired data and cannot be used for predictive simulations. The use of experimental data reduces modelling errors and uncertainties accompanied by a fully predictive one-dimensional model. What is left to predict by the model are primarily the mass flows through the ports and valves, and the heat flux between the gasses and the various walls. The TPA approach is an established method and is provided as a template by software developers such as Gamma Technologies. The very same developer provided the software, GT-power, that was used in campaign 4 to establish TPA models.

A TPA simulation reproduces the experimental results and in doing so, estimates additional quantities such as in-cylinder temperature and residual gas fraction. Only temporal, spatially averaged, values from within the cylinder can be estimated using the one-dimensional approach. To determine the spatial in-cylinder distribution, more advanced methods such as three-dimensional CFD or optical diagnostics in necessary. However, the target of the investigation in question was to assess the influence of the total amounts of trapped residual gasses, why the influence of any spatial distribution was considered redundant.

TPA is a convenient method since it requires no additional intrusion in the combustion chamber. The inlet and exhaust port pressure transducers can be mounted in the walls of the runners or mounted in sandwich plates fitted between the cylinder head and inlet/ exhaust manifold flanges. The pressure transducers are robust and allows full range of engine operating conditions. Additionally, the required data and corresponding experimental setup needed to acquire data for a TPA is similar to that used for regular combustion diagnostics and engine assessment. This means that no additional, adapted measurement procedures must occur, and that the corresponding simulation results can be linked to combustion characteristics. Other methods, such as in-cylinder probing of gasses which can used to physically measure the residual gasses, often require interruptions or intrusions in the measurement, such as skip firing or significant bleeding of the cylinder, to conduct the extraction of gasses properly [134, 135].

Apart from the precision of the experimental measurements, the quality of a TPA is solely reliant upon the accuracy of the model that is established. Characteristics of the combustion system such as geometry, heat transfer properties, and discharge coefficients of the valves must be known to achieve a successful model. The software solves the unsteady compressible flow equation which means that the mass flow through the system is determined, and therefore the trapping efficiency of the cylinder. By finite elements, the gradients of heat in, and heat flux to, the combustion chamber walls can be solved. If the correct mass of air, residual gasses, and fuel, is determined, the experimental high-pressure combustion loop pressure can be reproduced in the simulation by a fitted Wiebe-function which represents the heat release. If the prediction of trapped mass is incorrect, the resulting high-pressure loop pressure will be incorrect. An example of the agreement between the simulated- and the experimentally acquired data is provided in Figure 21.

During the fourth experimental campaign, both of the two test-engines were utilized to acquire experimental calibration data and simulated using TPA. The single-cylinder engine was utilized to assess high load lean combustion with various inlet and exhaust pressures that would not be possible with the multi-cylinder engine which is limited to its turbocharger characteristics. The multi-cylinder engine was utilized to acquire data from low load engine operation, primarily since the multi-cylinder featured stock electro-hydraulic camshaft phasers that could be utilized in a convenient manner to manipulate the valve timings and therefore the gas exchange process which was used to vary the amounts of trapped residual gasses inside the combustion chamber. The corresponding schematics of the models of each engine are illustrated in Figure 22.

A TPA is modelled using primarily a single cylinder at a time. Technically, the boundaries imposed by the experimentally acquired port pressures could be extended further from the cylinder and include more cylinders, but the further away from the cylinder, the lower the accuracy. Cylinder 1 of the multi-cylinder engine was used as reference for the corresponding TPA model. It was assumed that the other three cylinders would behave reasonably similar as cylinder 1, and therefore, that cylinder 1 could represent the whole

engine. Geometry and other engine characteristics were provided by Volvo Cars for both engines. Various valve timings were utilized for both engines. The valve timings of the single-cylinder engine were set manually by phasing the camshaft sprockets as opposed to the multi-cylinder engine that could adjust the timings electronically. The corresponding valve-lift profiles of both engines, with the various phasing angles utilized, are presented in Figure 23 and Figure 24.

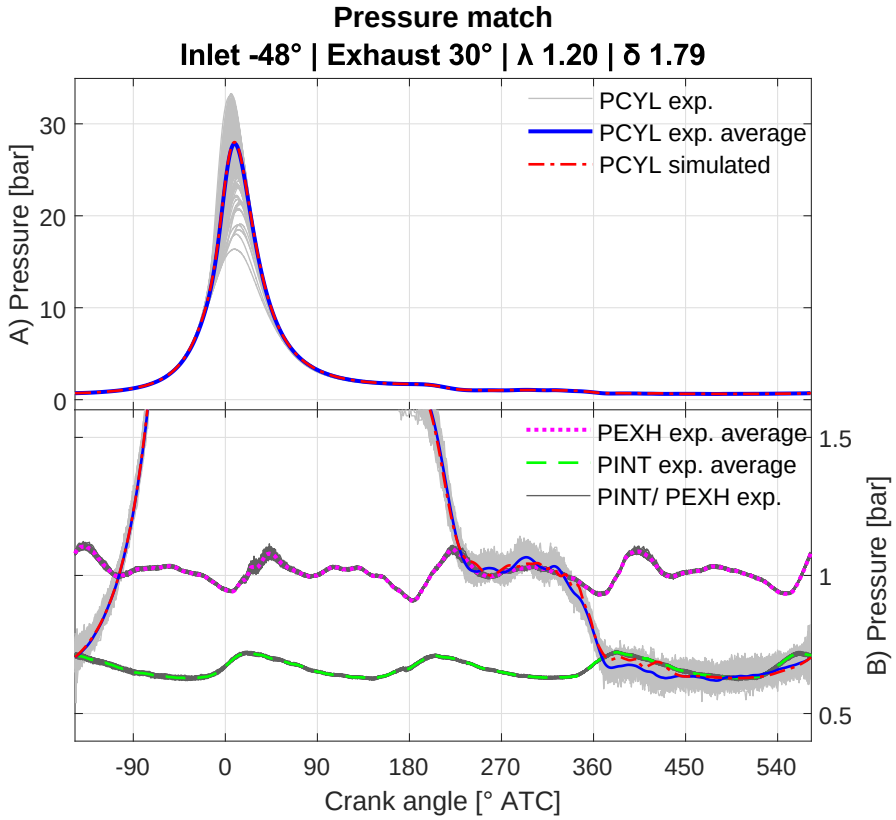


*Figure 21. Example of simulated versus experimental pressure traces, called "pressure match", of the multi-cylinder engine with maximum valve overlap (-48° and +30° CA), and Lambda = 1.2. *exp: denotes experimental data. *PCYL: Pressure cylinder. *PEXH: Pressure exhaust. *PINT: Pressure intake.*

The simulations were conducted as ensemble averaged. This meant that the crank angle resolved pressures from several consecutive combustion cycles acquired during a measurement were merged into one averaged crank angle resolved sample. It is possible to conduct cycle-resolved simulations as well. The three crank-angle resolved pressure signals are by default cycle resolved. However, additional cycle resolved measurements of the injected fuel and emissions are required to produce meaningful cycle-resolved results. The knowledge of the exact amount of injected fuel is necessary to compute the total trapped in-cylinder mass and to determine the available chemical energy inside of the cylinder. The need for cycle resolved fuel injection measurements may be eliminated if the fuel injection event can be repeated exactly from cycle to cycle, which is theoretically possible with a high-precision injector which operates with a constant duty-cycle. Measurements of cycle resolved fuel injection quantities were not possible using the single-cylinder engine nor the multi-cylinder engine in the experimental work included in this thesis. Consequently, it was not possible to analyze cycle-resolved variations of the mass of residual gasses. More details of the TPA modelling approach are covered in the fourth appended paper of this thesis.

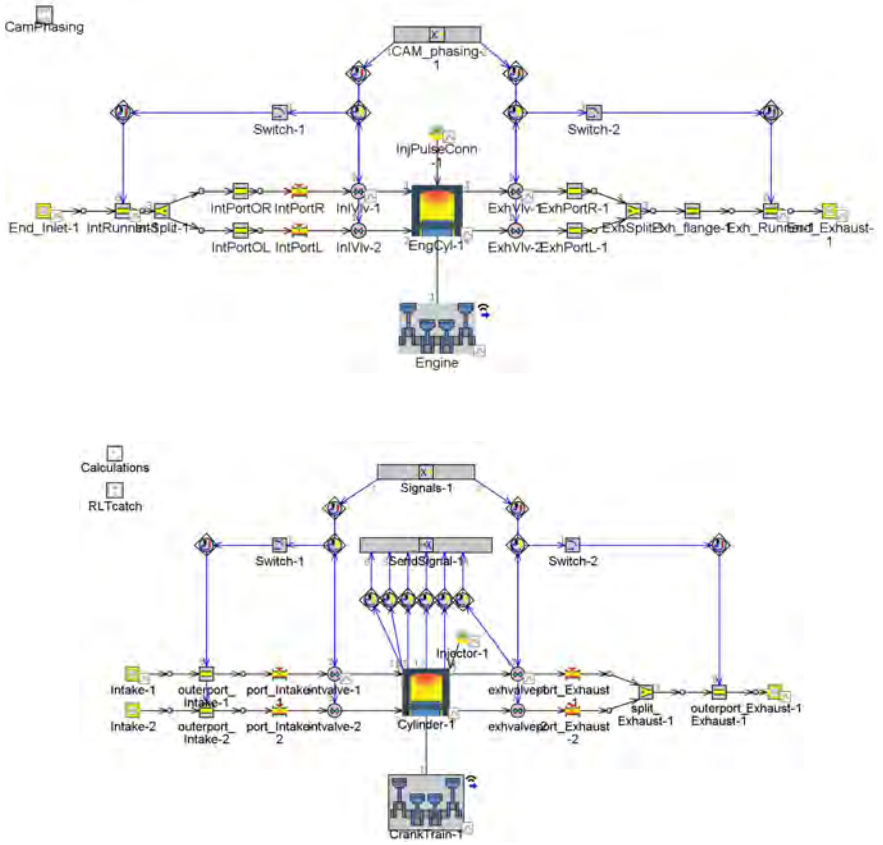


*Figure 22. Top: GT-power schematic of the single-cylinder engine TPA-model. Bottom: GT-power schematic of the multi-cylinder engine TPA-model.*

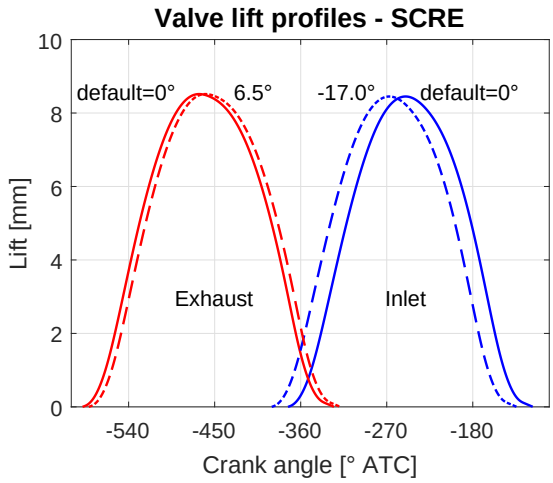


*Figure 23. Valve lift profiles, including lash, of the single-cylinder research engine (SCRE), at two camshaft phasing angles for each camshaft respectively. Both camshafts were phased simultaneously, resulting in a default minimum overlap setting and a second "increased" overlap setting.*

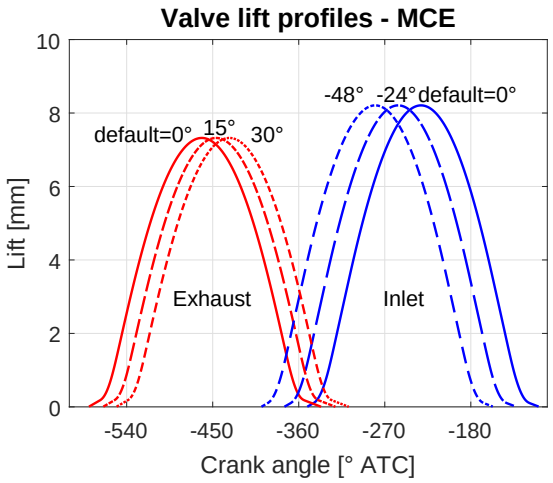


*Figure 24. Valve lift profiles, including lash, of the multi-cylinder engine (MCE) at various camshaft phasing angles. Three increments were implemented of each camshaft independently, including the default 0° phasing angle.*

## 3.6 Knock Characterization

The undesirable occurrence of knocking combustion due to the auto-ignition of the end-gas manifests as pressure waves inside of the combustion chamber with high frequencies. To evaluate the knock, it is useful to separate the corresponding high frequency knock signal from the low frequency signals related to the regular combustion cycle. It may also be beneficial to exclude the knock signal from the pressure trace when performing heat release estimations since the high-frequency shockwaves caused by knock do not necessarily represent release of heat. The knock signal received by the combustion chamber pressure transducer has an approximate frequency band of 5 kHz to 50 kHz and may be extracted using band-pass filters. Band-pass filters are not perfect, however. Some of the corresponding challenges of using filters are to construct one that provides minimum ripple, sharp cut-off and imposes no phase shift to the signal. The lowest frequencies of the knock signal tend to be similar to the highest frequencies of the combustion process, why it sometimes can be difficult to separate knock and combustion completely. Since the frequencies are similar or may overlap, a sharp cut-off of the filter is desirable. An example of two frequency spectrums from lean combustion with one combustion cycle with no detectable knock, and one cycle with heavy knock, originating from the same sample, is shown in Figure 25. The corresponding knocking combustion cycle is illustrated in the time (crank-angle) domain in Figure 26, which shows the separation of signals by filtration.

Two different types of filters have been utilized in this thesis. In campaign 1, a Butterworth filter of the fourth order was utilized to filter the signals during post processing. Since the signal was finite, it could be filtered two times in opposite directions to eliminate the phase distortion otherwise introduced by a single-pass Butterworth filter. In campaigns 2 to 4, a finite impulse response filter based upon a Hanning window was utilized. The finite impulse response filter provides a steeper cut-off compared to the Butterworth one, and due to the symmetry of the filter, no phase shift is introduced.

The multi-cylinder engine features built in knock-mitigation routines which successively retards the spark advance to reduce the peak cylinder pressure. This is done on each cylinder individually, based upon a signal from an engine block-mounted accelerometer. Therefore, no excessive knock occurred during any experiments with the multi-cylinder engine. The corresponding knock boundary in terms of maximum applicable spark advance and corresponding combustion phasing at high loads was therefore solely determined by the online mitigation algorithm of the multi-cylinder engine. The single-cylinder research engine featured no online knock-mitigation routine, which was why the engine had to be manually calibrated to avoid excessive knocking. The spark-timing was swept at each operating condition to determine the position of the knock boundary. The exact angle of the knock boundary was determined during post processing using the filtration routines described.

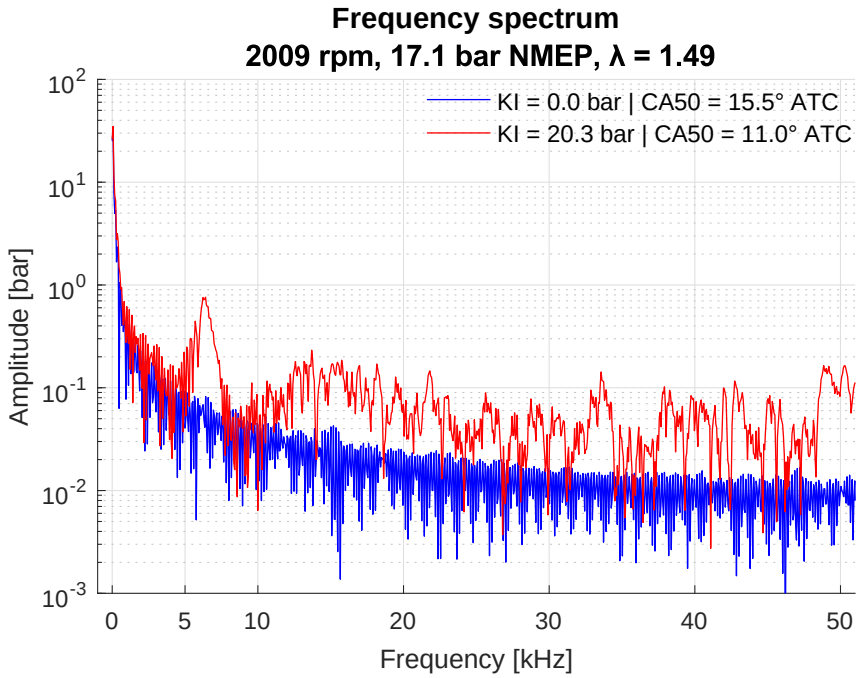


*Figure 25. Fourier transformed pressure signals of a knocking combustion cycle and a non-knocking combustion cycle from the same 500-cycle sample. As can be seen, the lowest knock amplitudes start at approximately 5kHz, which is close, or interacts with, the frequencies obtained from the heat release.*

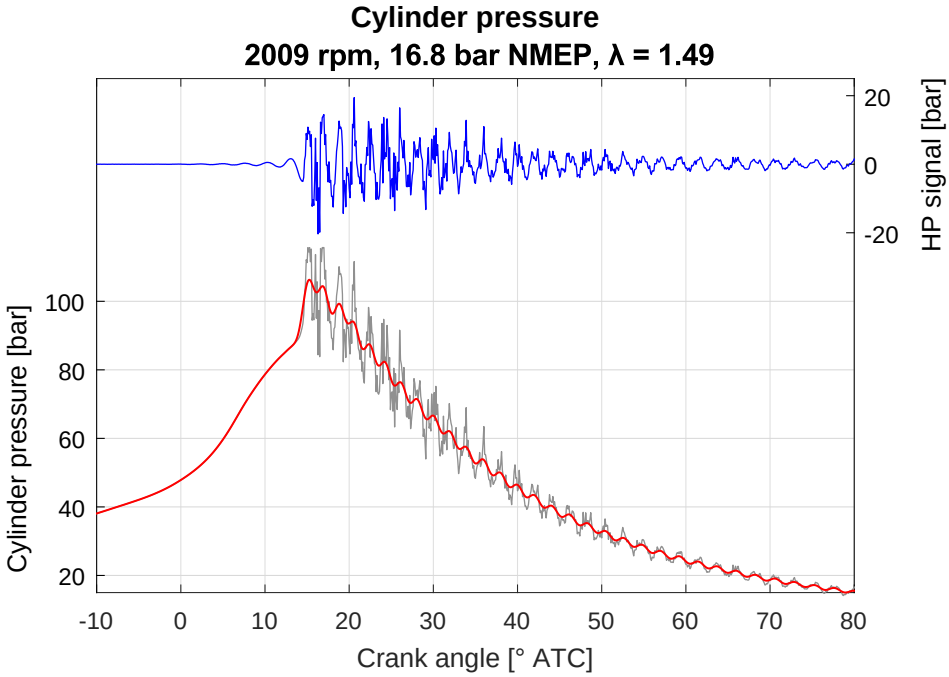


*Figure 26. Example of cylinder pressure with heavy knock, corresponding to the knocking combustion cycle presented in Figure 25. The original pressure trace is presented, with an overlayed low-passed signal. Additionally, the high pass filtered knock signal is visualized separately. As can be seen, the low-pass signal still present low-frequency oscillations despite that the high-frequency knock signal has been separated.*

The knock boundary was defined as a maximum knock intensity (KI) of 5 bar and a maximum knock tendency (KT) of 10%. The knock intensity is the halved amplitude of the knock signal, while the knock tendency is the frequency of detected knocking combustion cycles in a sample. A knock limit of 5 bar in KI is high compared to accustomed limits which vary in the range between 0.5-1 bar. However, most conditions investigated in this thesis considered lean combustion. During lean combustion, the natural increase of dispersion leads to a few combustion cycles with strong knock due to early, fast combustion, while other cycles experience little or no knock due to later, slower combustion. The natural dispersion of combustion therefore decreases the chance of a "runaway-knock" scenario. Runaway knock is described as several combustion cycles in a row, at or beyond the knock boundary, of which the severity of knock increases incrementally due to consecutive build-up of heat, which ultimately leads to engine failure if not addressed [136]. Therefore, occasional high intensity knock cycles are less harmful and may be tolerated to a larger extent, if the acoustic noise itself can be accepted. It may be noted that the single-cylinder engine in question occasionally was operated with continuous knock intensities of between 10-20 bar during the corresponding experiments with lean combustion, without causing engine failure.

The damage potential from knock is difficult to determine solely from the pressure-based knock signal [123]. Additionally, to the best of the authors knowledge, the damage potential of knocking combustion at very lean conditions has not been investigated. The damage caused by excessive knocking originates from strong heat flux to the piston and combustion chamber walls, leading to reduced material integrity and ultimately failure [19]. Combustion of a lean charge produces lower flame temperatures and consequently lower cylinder temperatures. This raises the question if knock during very lean conditions may be less harmful, compared to knock during stoichiometric operation, and therefore may be tolerated to a larger extent. A lean charge results in a lower speed of sound, that in turn shifts the frequency spectrum to lower orders, which in turn may increase the low-order knock intensities [95]. At certain conditions, the autoignition can be controlled and utilized to improve combustion. The intended use of spark-ignited combustion combined with non-harmful end-gas autoignition has been investigated and termed mixed-mode combustion by Sjöberg and He [137]. As they pointed out, mixed mode combustion is similar to spark assisted compression ignition, which in turn is similar to homogeneous charge compression ignition (HCCI). Evidently, auto-ignition can be harmless at certain conditions if the reactions in the end-gas are sufficiently slow not to cause severe pressure waves. It may be that the corresponding end-gas autoignition at very lean conditions at high loads enter another regime due to the different low temperature reactions taking place in the end-gas from air-dilution. High load lean end-gas auto-ignition is therefore an interesting topic for future research.

# 4 Results and Discussion

This chapter presents an overview of selected pieces of the results that have been achieved throughout the work to produce this thesis and the appended publications. This section also includes additional discussions of the results.

## 4.1 Mapping of the Turbocharged Multi-Cylinder Engine –Campaign 1

In the first experimental campaign, one of the world's first downsized SI-engines equipped with a prototype 2-stage turbocharger, designated to sustain ultra-lean (lambda > 1.6) air-dilution rates with homogeneous combustion over a wide range of loads and speeds, was developed and assessed. The prototype turbocharger allowed assessment of engines loads combined with very lean combustion. Something that had previously been difficult to achieve without using external supercharging. Extension of the lean operating conditions allows for increased utilization of lean combustion which in turn improves the engine fuel efficiency during real driving. The target was to extend the lean operating conditions of the multi-cylinder test-engine fitted with the prototype turbocharger to a specific engine load of at least 16 bar BMEP. Reaching this load would enable the engine to utilize lean combustion during approximately 90% of the worldwide harmonized light vehicle test cycle (WLTC).

The engine in question was operated and mapped at various engine load points determined by engine speed and BMEP. At each load point, a sweep of lambda was conducted. The maximum amount of air-dilution that could be achieved without exceeding the defined combustion stability criterions at each operating point was assembled into a lean map, which is visualized in Figure 27.

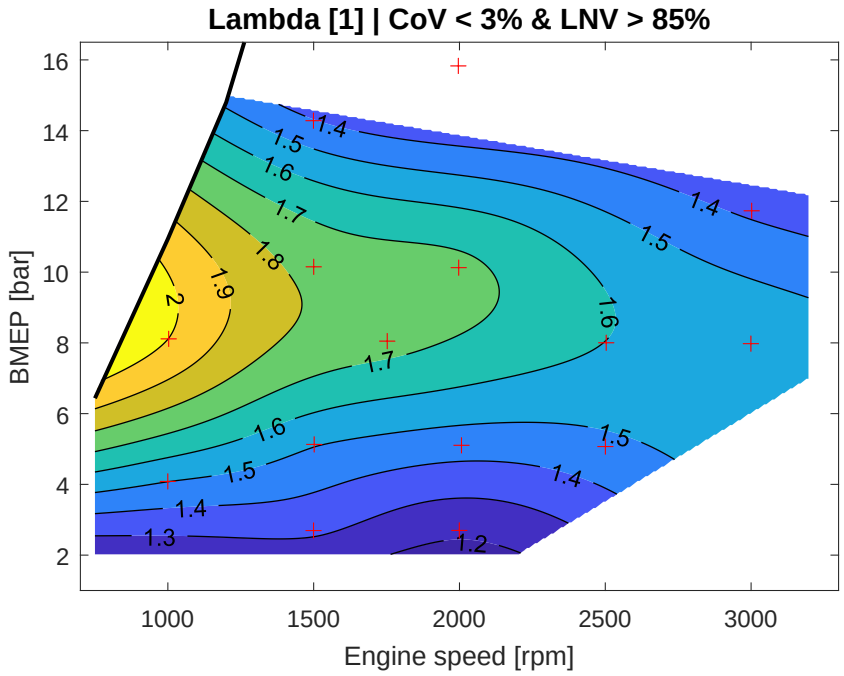


*Figure 27. Maximum achieved air-dilution (air-dilution tolerance) at given stability criterions of the multi-cylinder engine, called the "lean-map". Markers denotes the tested operating points.*

*The limitation of torque due to the surge-line of the turbocharger is visualized as a black solid line.*

From the lean map presented in Figure 27, several conclusions have been made. With a two-stage turbocharger, it was possible to extend homogeneous lean combustion operation beyond the naturally aspirated limit of the engine. However, the targeted load of 16 bar BMEP could not be achieved. When operating with lean combustion, a maximum load of 14 bar BMEP was obtained at 1500 rpm. The corresponding maximum air-dilution was a moderate lambda = 1.4. The maximum applicable air-dilution varied substantially over the map. The peak air-dilution of lambda = 2 was obtained at an engine operating condition of approximately 9 bar BMEP and 1000 rpm. Moving away from this point resulted in reduced air-dilution tolerances. Evidently, the air-dilution tolerance was heavily influenced by both engine speed and load and there appeared to be an optimum engine load that resulted in the maximum air-dilution tolerance.

The corresponding engine out $NO_x$-emissions of the lean map are presented in Figure 28. When the results visualized in Figure 28 were compared to the air-dilution rates presented in Figure 27, it became evident that the produced $NO_x$-emissions were not proportional to air-dilution. The map visualizing the $NO_x$-emissions was comparatively flat below 10 bar BMEP, while the $NO_x$-emissions increased drastically at higher engine loads. However, the amounts of air-dilution were similar at both 14 bar and 2.62 bar BMEP respectively. Therefore, the discrepancy in terms of $NO_x$-emissions between high and low load was contradictory. From the $NO_x$-map, it could also be concluded that the minimum produced levels of $NO_x$-emissions were in the range of approximately 2 g/kWh.

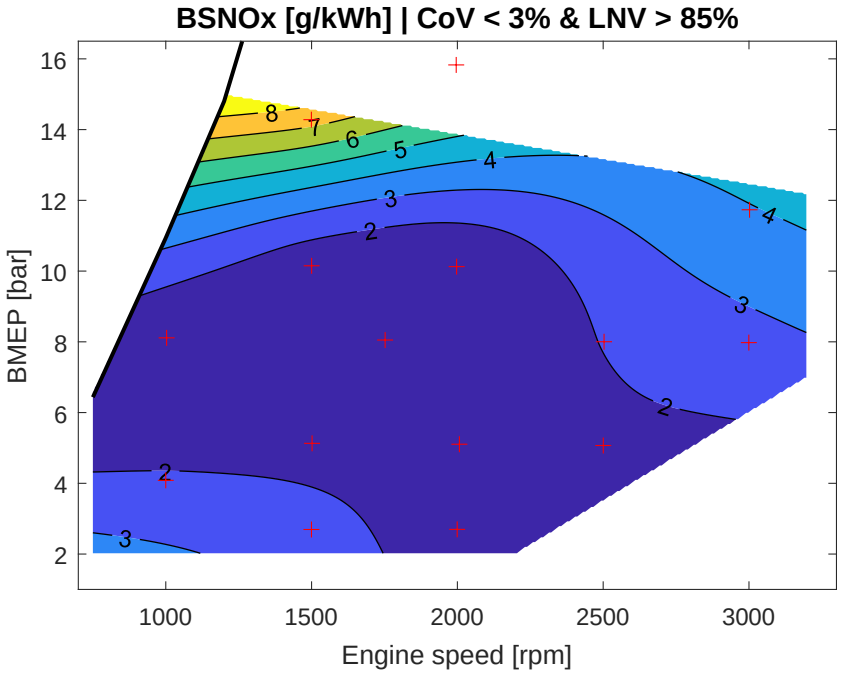


*Figure 28. Corresponding NOx emissions of the lean map of the multi-cylinder engine. Markers denotes the tested operating points.*

Figure 29 presents the performance of the turbocharger in terms of accomplished energy transfer from exhaust to inlet in units of pressure, from a selected load point of 10 bar BMEP and 1500 rpm. Figure 29 clearly illustrates the necessity of using a two-stage turbocharger. Between lambda = 1 and 1.4, the low-pressure stage was sufficient to

compress and displace the required amount of charge air. Beyond lambda = 1.4, the waste-gate of the low-pressure stage was fully closed, and the pressure could not be increased further. However, thanks to the second high-pressure stage, the pressure could be increased further, beyond lambda = 1.4 and up to lambda = 1.95. From the results presented in Figure 29, it was also observed that the turbocharger produced a higher exhaust pressure compared to the inlet pressure, indicating inefficient operation, leading to increased pumping losses of the engine. Hence, there were no pumping loss advantages gained from air-dilution at boosted operation. This in contrast to low load operation, at or below the naturally aspirated limit, where de-throttling reduces pumping losses. Despite some additional pumping losses, it was concluded that the turbocharger could produce sufficient air mass-flow to sustain ultra-lean combustion at the operating conditions investigated. But, due to the combustion instabilities obtained at high loads, not all intended operating conditions could be assessed at ultra-lean conditions.

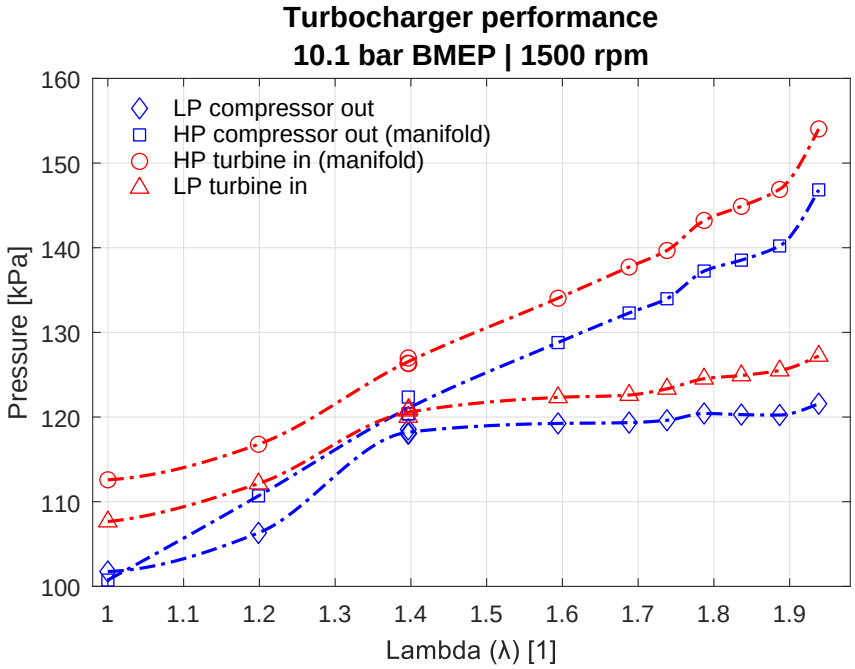


*Figure 29. Pressure of inlet air and exhaust gasses at the various stages of the turbocharger system. LP = low pressure, the waste-gate turbocharger. HP = high pressure, the VNT turbocharger.*

Figure 30 presents the combustion phasing angle (CA50), the crank angle of 10% mass fractions burned (CA10), and CoV of NMEP versus lambda, at an engine load of 10 bar BMEP and 1500 rpm. This is the very same load point that was depicted in Figure 29. At stoichiometric combustion, the combustion phasing angle was delayed to mitigate knock. The obtained combustion phasing angle was approximately 17° ATC, as opposed to the peak efficiency angle which would occur at 8° ATC. When the air-dilution was increased, the combustion phasing and corresponding spark advance could be advanced due to reduced tendency of knocking combustion. The substantial advancement of the combustion phasing angle led to the extraction of more energy during the expansion stroke. This contributed to an increase of the thermal efficiency of approximately 12%, at the engine load point in question. The clear effect from the optimized combustion phasing angle verified the hypothesis that air-dilution can be used to mitigate knock.

The operating point of 1500 rpm and 14 bar BMEP was the highest engine load that could sustain lean combustion and is illustrated in Figure 31. This figure presents the same parameters that were shown in Figure 30, but due to the increased load, the tendency of knocking combustion increased which resulted in a further delayed combustion phasing angle. A delay of the combustion phasing angle at stoichiometric operation was expected. However, despite the addition of air-dilution, the combustion phasing could not be advanced during lean combustion. Additionally, the dispersion of combustion in terms of CoV of NMEP increased rapidly and exceeded the chosen limit of 3% already at lambda = 1.4. This observation rather contradicted the hypothesis that air-dilution could mitigate knock, as compared to the observation that was made at an engine load of 10 bar BMEP. The observed deterioration of stability and knock also contradicted results and conclusions made by previous researchers such as Doornbos et al. [95].

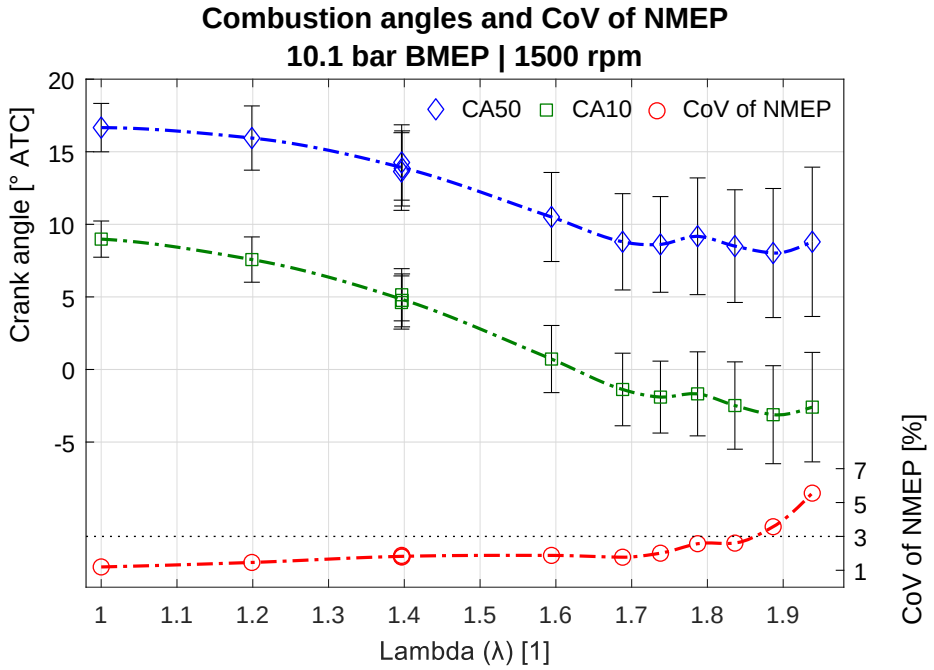


*Figure 30. Cylinder average (knock limited) combustion angles CA50 (50% MFB), CA10 (10% MFB) and corresponding CoV of NMEP at intermediate engine load. Error bars denote the standard deviation of the dispersion of the corresponding combustion angles. A measurement repetition is included at lambda = 1.4.*

The mixed results obtained from exploring the lean combustion capabilities of the modified multi-cylinder engine fitted with the prototype turbocharger raised several new questions. Firstly, and most evident, was a question regarding why the engine failed to sustain ultra-lean combustion at loads higher than 14 bar BMEP. The second question that was raised was why the air-dilution tolerance at low loads appeared to be very limited. Despite the moderate air-dilution rates achieved at low loads, comparatively low $NO_x$-emissions were obtained. Thirdly, it was unclear why the air-dilution tolerance appeared to the negatively affected by increased engine speeds.

Clearly, air-dilution was not sufficient to achieve necessary mitigation of end-gas autoignition at the highest engine loads investigated. The insufficient mitigation of knock did not permit any noteworthy advancement of the combustion phasing angle. The resulting late combustion phasing angles are not necessarily an obstacle to introduce lean combustion at high loads in itself. However, the absence of combustion phasing

advancements at lean operation appeared to be linked to increased dispersion of combustion. It was originally hypothesized that high engine loads, which are accompanied by higher temperatures, pressures, and turbulence, would result in faster flame development and reduced dispersion, leading to more stable combustion and less sensitivity to the combustion phasing angle. This did not seem to be the case, considering the very disperse combustion experienced when investigating lean combustion at 14 bar BMEP.

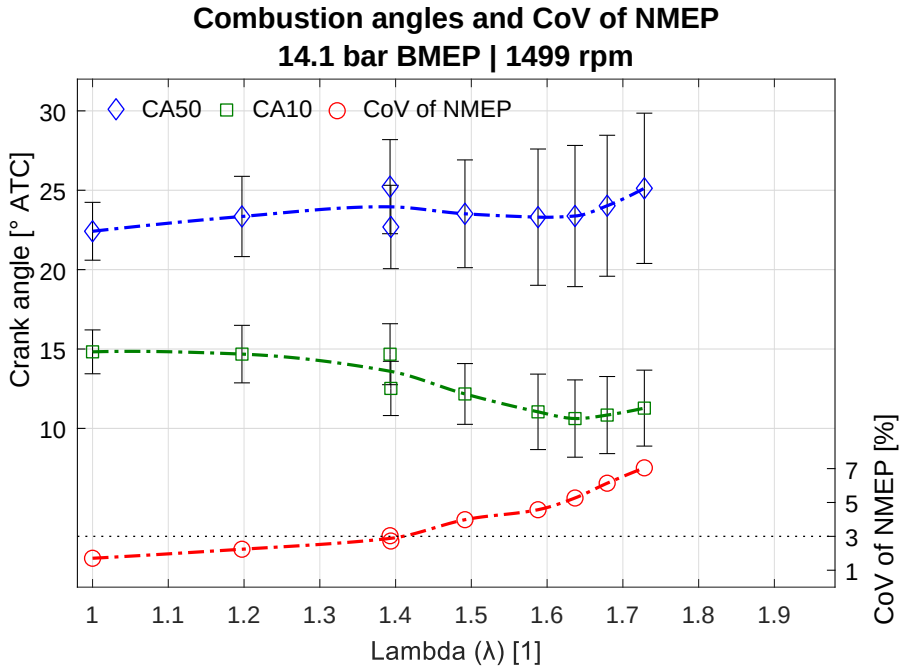


*Figure 31. Cylinder average (knock limited) combustion angles CA50 (50% MFB), CA10 (10% MFB) and corresponding CoV of NMEP at the highest load point with lean combustion. Error bars denote the standard deviation of the dispersion of the corresponding combustion angles. A measurement repetition is included at lambda = 1.4.*

## 4.2 Investigation of the Lean Load Limit –Campaign 2

Further experiments were conducted using a single-cylinder research engine. This was done to continue investigating high load lean combustion and thereby attempting to answer the remaining questions from the first measurement campaign. To sustain ultra-lean combustion at high loads, the engine was modified with a boosting system capable of supplying 2 bar gauge boost pressures and sufficient air mass-flow.

Parameter sweeps of the ignition timing (ignition sweeps) were conducted to investigate the influence of the corresponding combustion phasing angle on the combustion dispersion. The results from an ignition sweep are visualized in Figure 32. When the relation between NMEP and combustion phasing angle of each individual combustion cycle is plotted as a scatter plot, the scatter forms a pattern which resembles a second-degree polynomial curve. This curve corresponds to the combustion phasing angle efficiency curve. The peak of this curve determines the corresponding angle at which the point of highest efficiency is yielded. This angle is also commonly known as the maximum brake torque (MBT) angle. From the scatter plot visualized in Figure 32 it could be concluded that the individual dots were scattered along the curve rather than being grouped to each corresponding increment of the average combustion phasing angle.

The cyclic dispersion of heat release, resulting in a corresponding dispersion of the combustion phasing angle, was much larger than the intentional phasing of combustion due to changed ignition timings. Shown in Figure 32, later ignition timing, and therefore later combustion phasing, resulted in a larger dispersion of NMEP which is seen from the vertical error bars. The increase in dispersion of NMEP could partly be attributed to that the dispersion of CA50 increased when the ignition timing was delayed. However, most of the increase in dispersion of NMEP appeared to be linked to the steep gradient of the efficiency curve, which resulted in a higher correlation between dispersion of combustion and NMEP. In other words, if there was a certain amount of combustion dispersion at a certain operating condition, the dispersion measured in NMEP would increase with a delayed mean combustion phasing angle. This observation offered an explanation to why the combustion stability apparently suffered from delayed combustion phasing angles due to knock limitations when air-dilution was added. The dependence of the stability upon the ignition timing imposes a "latest permissible ignition timing limit" if the combustion stability criterions are not to be exceeded.

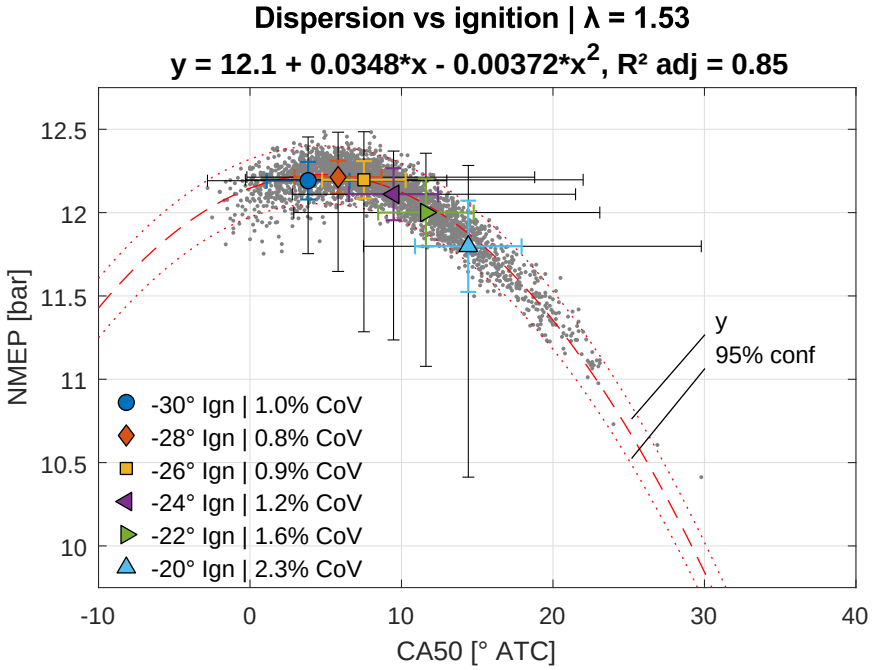


*Figure 32. Scatter plot of cycle resolved NMEP versus combustion phasing (CA50) of an ignition sweep at 1500 rpm. The scatter denotes each individual cycle of all six ignition timings combined. Thick colored error bars denote standard deviation. Thin black error bars denote max/min.*

On low engine loads, the ignition timing may be adjusted rather freely since the peak pressure of the combustion chamber is low and do not cause any harmful end-gas autoignition. However, introduction of higher loads imposes a knock boundary when auto-ignition start to occur. Knocking combustion generally increases in severity when advanced ignition and corresponding combustion phasing angles are applied since this leads to an increase of combustion chamber pressure and temperature. This results in the occurrence of an "earliest permissible ignition timing" due to knocking combustion. If the limit of combustion stability and limit of knock is plotted in terms of combustion phasing angle (CA50), versus lambda, a graph that denotes the operating window can be illustrated. An example of such graph is shown in Figure 33. The gray shaded area in Figure 33 shows the operating window which is enclosed by the upper knock boundary

and the lower stability boundary. During the corresponding operating conditions of Figure 33, in terms of engine speed and load, the two boundaries of knock and stability respectively do not intersect. Since the boundaries do not intersect, valid combustion could be maintained up to relative air-dilution of lambda = 1.75. Beyond lambda = 1.75, the combustion stability deteriorated. Figure 34 illustrates the very same parameters as in Figure 33, but at an increased engine load. From Figure 34, it was concluded that the knock boundary was substantially delayed which in turn narrowed the operating window. Beyond lambda = 1.5, the two boundaries intersected which rendered the combustion characteristics corresponding to higher amounts of air-dilution invalid. This intersection was termed as the lean load limit.

Hypothetically, the operating window should widen if either the dispersion of combustion is reduced, and/ or the tendency of knock is mitigated, thereby separating the two boundaries. To investigate this hypothesis, several operating conditions were tested using the single-cylinder research engine. In addition to different engine loads and speeds, the influence of the intensity of the in-cylinder tumble motion was assessed by utilizing a tumble flap inserted to the inlet port of the engine cylinder head. Previous research has shown that increased tumble both can decrease the dispersion of combustion and reduce the tendency of knock.

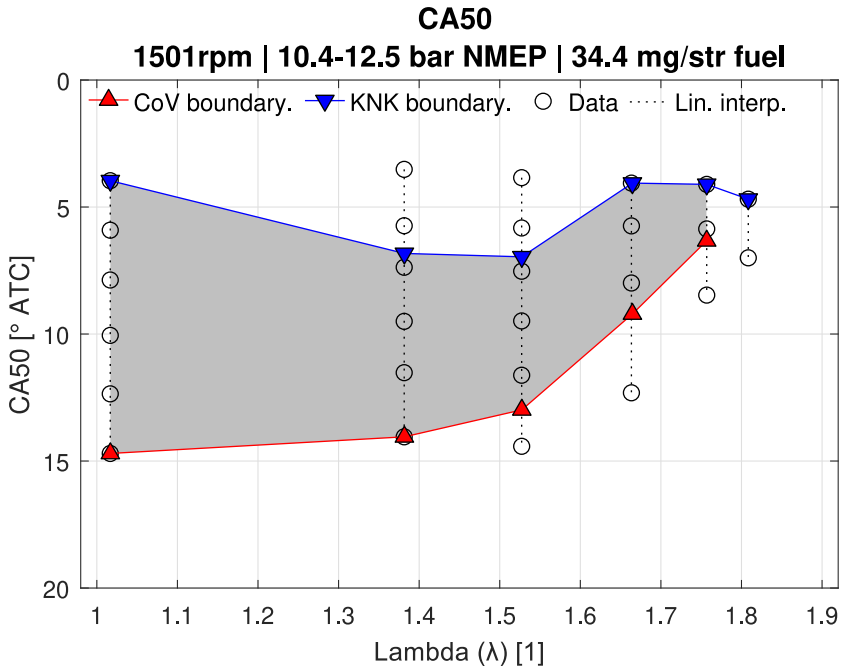


*Figure 33. Operating window in terms of combustion phasing CA50, determined by the lower stability limit and the upper knock limit. Each vertical dotted line with markers represents an ignition sweep. At some increments of lambda, excessive delay of the combustion phasing was not investigated.*

Figure 35 presents resulting engine loads in terms of NMEP, obtained at various engine speeds, with both default low tumble and increased tumble. The injected quantity of fuel was similar amongst the various operating conditions, maintained within a range of +/- 1%. From the visualized results in Figure 35, it was observed that the engine load increased with increased air-dilution. This was due to that constant fuel injection was utilized during each sweep of air-dilution. Therefore, the engine torque output increased when air-dilution was added, caused by the ability of lean combustion to improve thermal

efficiency. From the results presented in Figure 35, it could be concluded that increased tumble had a substantial positive effect on the air-dilution tolerance. The effect of increased tumble was prominent at engine speeds of 1500 and 2000 rpm. However, at 2500 rpm the effect was comparatively small. When comparing the various results obtained using default low tumble levels, it was concluded that the 2000 rpm case performed remarkably poor in terms of maximum air-dilution compared to the results obtained at other engine speeds. Therefore, a repeated measurement was conducted (pentagon markers) which confirmed the preliminary results.

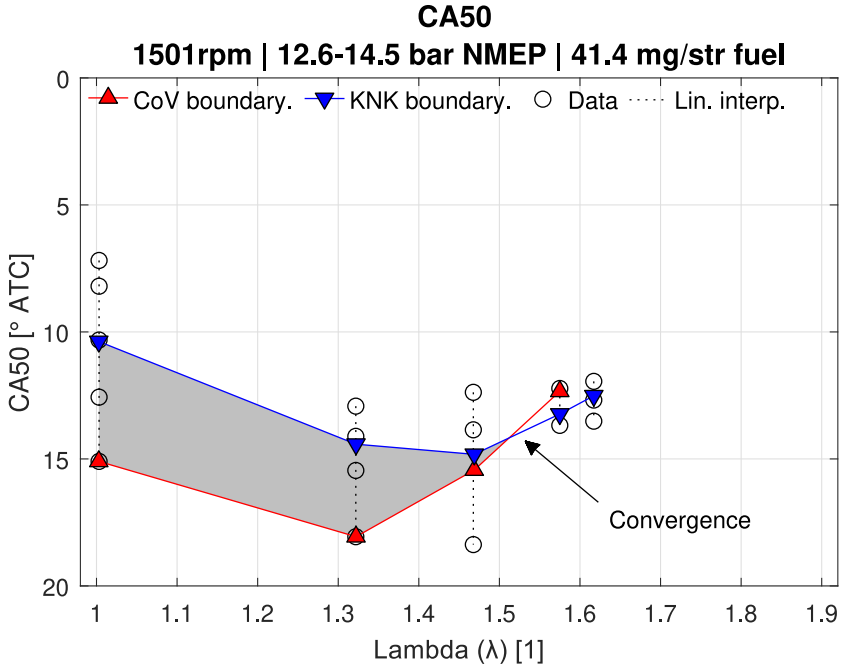


*Figure 34. Operating window in terms of combustion phasing CA50, determined by the lower stability limit and the upper knock limit. Each vertical dotted line with markers represents an ignition sweep. At some increments of lambda, excessive delay of the combustion phasing was not investigated.*

Next, the influence of engine load and tumble was investigated at a constant engine speed of 2000 rpm. The corresponding results in terms of NMEP are presented in Figure 36. The two cases denoted 13-15 bar that are included in Figure 36 are the very same as the 2000 rpm cases earlier presented in Figure 35.

The results illustrated in Figure 36 led to the conclusion that the use of increased tumble resulted in the extension of maximum applicable engine load sustaining lean combustion up to a load of approximately 16 bar NMEP. As comparison, when using default tumble, it was difficult to exceed 13 bar NMEP in load and lambda = 1.3 in air-dilution rates. The results corresponding to low tumble of the single-cylinder engine were worse compared to the ones achieved using the multi-cylinder engine from the first experimental campaign. The multi-cylinder engine achieved lambda = 1.4 at an engine load of 14 bar BMEP (Approximately 14.7 bar NMEP). However, using increased in-cylinder tumble, the single-cylinder research engine could sustain ultra-lean combustion, lambda = 1.7, at an engine load of 16 bar NMEP.

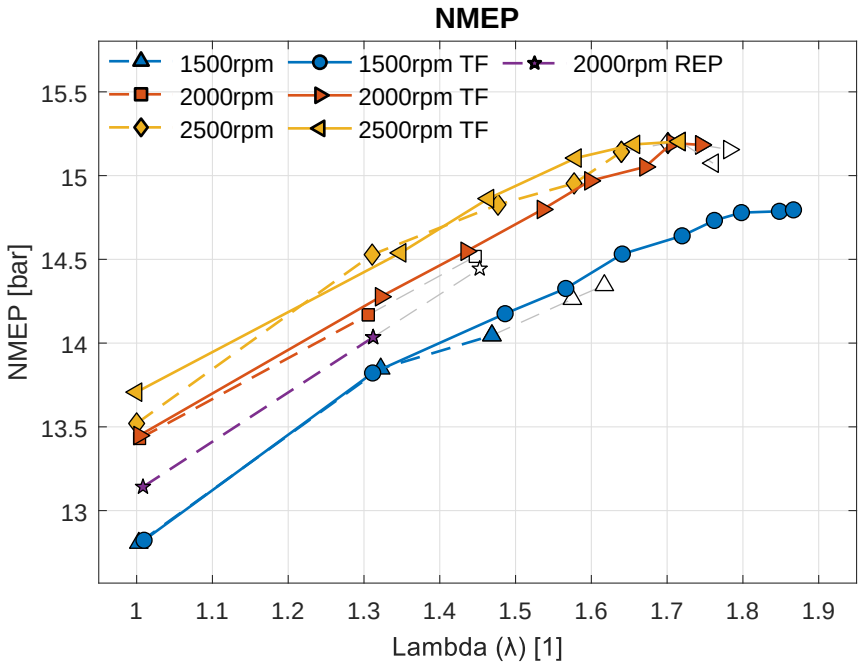


*Figure 35. NMEP versus lambda for various engine speeds and default and increased tumble by engaging the tumble flap (TF). Gray lines and open markers denote points with combustion dispersion exceeding the limit.*

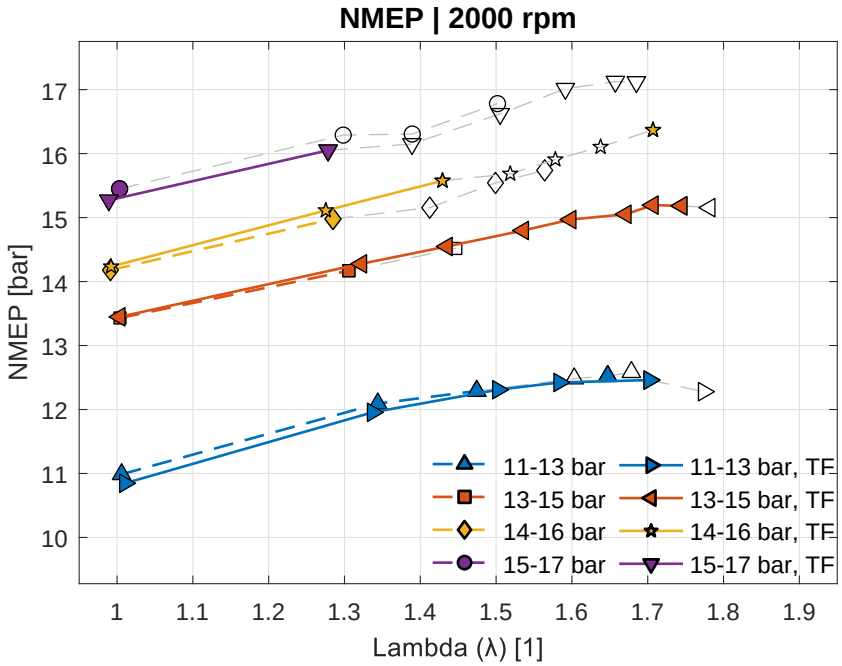


*Figure 36. NMEP versus lambda for various engine loads and default and increased tumble by engaging the tumble flap (TF). Gray lines and open markers denote points with combustion dispersion exceeding combustion stability criterions.*

The experimental effort of campaign 2 provided an answer to the previous question of why the maximum loads were limited when operating the multi-cylinder engine with lean combustion: the lean load limit, determined by the convergence of the stability limit and knock limit, was heavily impeding the maximum applicable air-dilution.

New observations during the second experimental campaign, that investigated high load lean combustion, resulted in new questions. Similar to the results obtained using the multi-cylinder, it appeared that the air-dilution tolerance of the single-cylinder engine was reduced by increasing the engine speed. Increased tumble offered little improvement in extending the maximum air-dilution at 2500 rpm. On lower engine speeds, increased tumble had a substantial positive effect on air-dilution tolerance. Additionally, the dilution tolerance at 2000 rpm corresponding to default, low tumble was exceptionally poor at all of the four different engine load ranges investigated. These new questions and observations sparked continued experimental activities.

## 4.3 Influence of Alternative Fuel on the Lean Load Limit –Campaign 3

Previous investigations conducted in the first and second experimental campaigns were conducted using gasoline with an octane rating of 95. The choice of fuel affects the corresponding tendency of knocking combustion. Higher resistance of the fuel to auto-ignite allows for higher pressures and temperatures without the occurrence of knock. Therefore, increasing the octane rating of the fuel could theoretically be utilized to mitigate the knock limited boundary of the combustion phasing angle, which in turn could widen the lean combustion stability window and therefore extend the lean load limit. To investigate the influence of a fuel with increased octane rating on the lean load limit, direct injected methane was utilized in the third experimental campaign. Methane has an octane rating that is above 120 which means that it seldomly auto-ignites in a regular spark-ignited engine that is built for combustion gasoline. As comparison, regular gasoline fuels do not exceed an octane rating of 100. An additional advantage of methane is that it can be extracted from renewable sources as a biogas, making it an interesting fuel for future low-carbon emission combustion engine applications. Methane also has a higher hydrogen to carbon ratio, which means that it produces less carbon emissions when combusted, compared to other fuels such as gasoline.

Direct injected methane and direct injected gasoline were utilized as fuels during several experiments at an engine speed of 2500 rpm and with loads ranging from 11.5 to 13 bar. These experiments were performed utilizing the same single cylinder research engine as in the previous experimental campaign. Two different ignition systems were utilized in the single cylinder engine: a standard single coil ignition system and a high-frequency ignition system. Similar to the previous campaign, the engine load varied when lambda was changed, due to that constant fuel injection was used during each sweep. To gain further insight into the combustion characteristics, a cylinder head with endoscopic optical access to the combustion chamber was fitted to the engine. The endoscopic access allowed the acquisitioning of in-cylinder images of the combustion by means of a high-speed color camera.

Figure 37 presents the resulting dispersion of NMEP in terms of CoV versus relative air-fuel ratio lambda. The figure includes results from eight different engine configurations in terms of fuel, tumble, ignition system and combustion phasing strategy. The results visualized in Figure 37 led to the conclusion that direct injected methane clearly outperformed gasoline in terms of overall combustion stability. It should be noted that the results presented in Figure 37 were obtained using single-coil ignition (SCI), which provides substantially reduced ignition energy as opposed to the dual-coil system that was used in campaign 1 and 2. Evidently, the reduction in ignition energy was clearly unfavorable to the combustion stability of gasoline, since the obtained dispersion of combustion was far worse in the third campaign when compared to the corresponding

dispersion of combustion at similar operating conditions of the previous experimental campaigns.

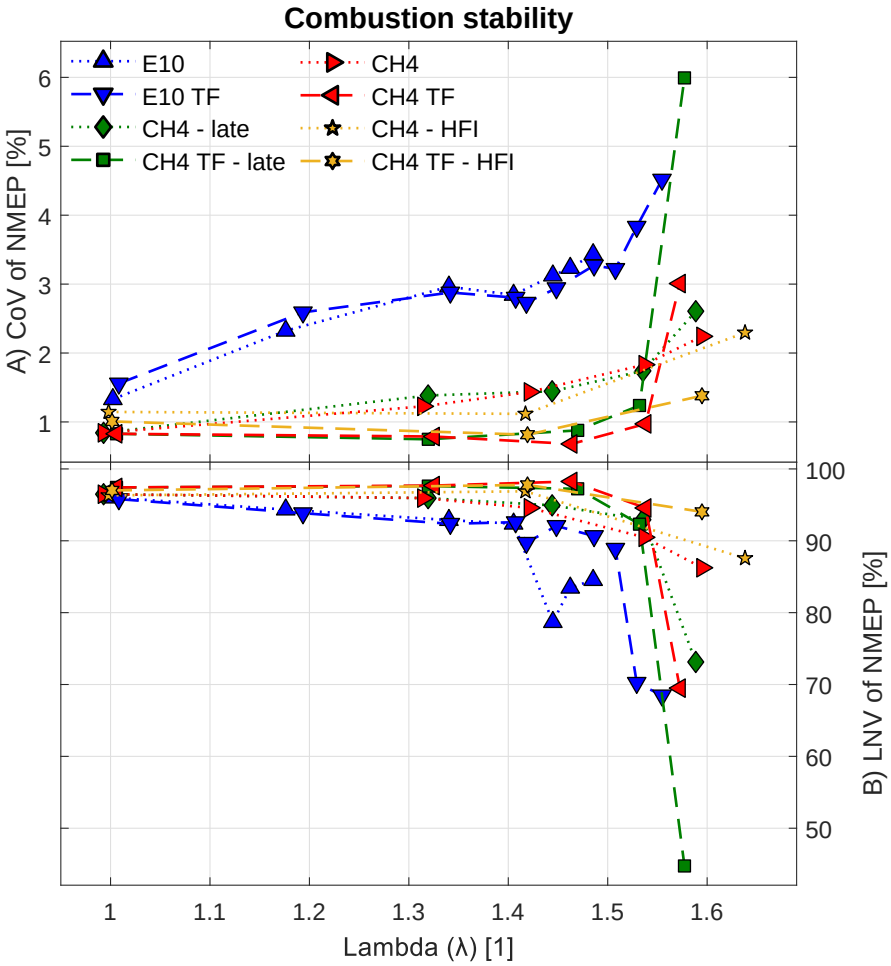


*Figure 37. CoV and LNV of NMEP at 2500 rpm and loads ranging from 11.5 to 13 bar NMEP (constant fuel injection). *E10: Gasoline. *CH4: Methane. *TF: Engaged tumble flap (increased tumble) (all other are default, low tumble). *late: Delayed combustion phasing. *HFI: High frequency ignition (all other are SCI, single coil).*

Compared to gasoline, direct injected methane appeared to be less affected by the lower ignition energy. The use of methane resulted in substantially lower combustion dispersion in the range of lambda = 1 up to 1.55. Due to absence of end-gas autoignition when operating the engine on methane, the ignition timing and combustion phasing angle could be adjusted freely. To assess the influence of the combustion phasing angle on the combustion quality, a comparison was made between early and late combustion phasing (green versus red lines/ markers). Early combustion phasing corresponded to the maximum brake torque (MBT) angle, while the setting named “late” was delayed approximately 5 crank angle degrees from MBT. From the resulting graphs in Figure 37, it was concluded that the difference between the early and late combustion phasing angle configurations had little influence on the combustion stability. The difference in combustion phasing between early and late phasing was however rather small. Since the overall combustion stability of methane was surprisingly high, it was hypothesized that the small delay in combustion phasing angle simply was insufficient to cause any increase in dispersion.

The influence of ignition energy upon combustion stability was investigated further by assessing the results obtained when the high-frequency ignition (HFI) system was utilized. When excluding the deviating results obtained when using, it could be concluded that the resulting CoV of NMEP of HFI and SCI were very similar in the intermediate range of lambda = 1 to 1.55. This was unpredicted, since the HFI system provides substantially higher amount of energy to the charge during the ignition event. The result indicated that the minimum ignition energy (MIE) requirement of methane was already exceeded by the SCI system and that further increases in ignition energy from the HFI system had little influence.

The third engine feature that was investigated included increased in-cylinder tumble using a tumble flap. Compared to changing ignition systems, the introduction of increased tumble resulted in significant differences in terms of dispersion of NMEP. Increased tumble could push the combustion dispersion in terms of CoV of NMEP below 1% up to a relative air-fuel ratio of lambda = 1.5. Similarly, LNV of NMEP could be maintained above 95% with increased tumble. Beyond lambda = 1.5 however, most of the cases started to deteriorate in stability. Most distinct deterioration was obtained with the high tumble cases with methane. The high frequency ignition could partly suppress the deterioration of combustion stability beyond lambda = 1.5. Further increments of lambda using the HFI system were not investigated due to peak pressure limitations of the engine cylinder, which was imposed by the endoscope. However, it was anticipated that had lambda been increased further by an increment of 0.1 it would have resulted in similar deterioration of stability as with the other configurations.

Another important observation was made when the HFI system was utilized in combination with lean combustion, namely that HFI caused increased complexity during the experiments. The HFI system is very sensitive to the impedance of the combustion chamber gasses. If the impedance is exceeded, a flash-over occurs depleting the energy of the igniter (Previously shown in Figure 11). The impedance of the combustion chamber is proportional to the combustion chamber pressure. At very lean conditions, due to slower combustion, the ignition timing must be advanced to phase the combustion accordingly so that the major heat release occurs close to TDC. When the ignition timing is advanced, the corresponding combustion chamber pressure at the timing of ignition is reduced, leading to a reduction in impedance. A consequence is that the igniter voltage of the HFI system must be reduced, resulting in slower initial combustion, urging further ignition timing advancement, and therefore a negative spiral is obtained. This causes very sudden limits in applicable levels of dilution when using the HFI system, when early ignition timings are enforced beyond an arbitrary crank angle degree that depends upon the in-cylinder conditions. For this reason, it was often difficult to achieve any larger increase in air-dilution than increments in the range of 0.1 units of lambda compared to other ignition systems. This despite that the HFI system on paper promises significant increases in energy and ignition volume which should result in higher combustion stability and therefore substantial increases of the air-dilution tolerance.

The difficulties in extending the lean stability limit, air-dilution tolerance, beyond lambda = 1.6 at 2500 was unexpected. Particularly surprising was the lack of positive effects from increased tumble, which previously had been proven beneficial at other operating conditions. Additionally, both tumble and HFI had been proven to be beneficial when investigating lower amounts of air-dilution, below lambda = 1.5. This raised the hypothesis that the turbulence intensity of the in-cylinder flow, obtained at 2500 rpm, reached such levels that the turbulence started to impede flame development due to quenching. This hypothesis was investigated by analyzing the in-cylinder images of the

combustion that were acquired during the experiments, corresponding to the results previously presented in Figure 37. Four chosen images at representative conditions, all acquired when the engine was operated at the highest implemented increment of relative air-dilution lambda, are presented in Figure 38. All four images represent the relative frequency of the binarized flame area. In other words, the frequency represents the number of appearances of the flame at a specific location, divided by the total sample size (number of combustion cycles acquired). The flame area, or contour, was determined at a specific crank angle at each combustion cycle included in the continuous sample acquired during each measurement (approximately 92 cycles). Yellow, 100%, denotes that the flame is present at the corresponding location at all sampled combustion cycles. The lower the frequency, the fewer is the number of cycles of which the flame is present at a certain location. All four images are acquired from a crank angle that is approximately 2-3° crank angle before 2% mass fractions burned (CA02). CA02 is the combustion angle of which the heat release may barely be observed to start. The images corresponding to CA02 were chosen specifically since they represent the early, slow progression of the developing flame and its corresponding dispersion.

The images of the upper row of Figure 38 were acquired when the single coil ignition system was utilized in combination with methane. The left image of the top row represents high tumble, and the right image low tumble (default). Two conclusions were made from the comparison of these two images: Firstly, increased tumble led to a more consistent deflection of the developing flame, generally to the left, exhaust, side of the combustion chamber. The flame development using low tumble was more disperse, developing to either side of the combustion chamber. Secondly, despite that increased tumble appeared to produce more consistent deflection of the flame, the corresponding flames were generally smaller and weaker compared to the low tumble flames judging from the larger share of blue, low frequency, shade of the image. The absence of a 100% frequency zone in the upper left image also reveals that not all flames overlap each other in terms of their contour between the individual combustion cycles.

The lower row of Figure 38 illustrates the corresponding results obtained using high frequency ignition and direct injected methane. The absolute crank angle relative to top dead center of the two images of the lower row with HFI is similar to the corresponding absolute crank angle of the upper row with SCI. However, due to the much higher ignition energy provided by the HFI system, the corresponding initial flame developments are faster. This results in that the number of crank angle degrees between ignition and the crank angle degree of the flame images is less when using HFI, compared to SCI. The analysis of the images acquired from using HFI led to the conclusion that the influence of the level of tumble was similar to the results obtained with SCI. High tumble resulted in higher consistency of the deflection of the flame towards the exhaust side, but also produced generally weaker and smaller flames. The low tumble setting resulted in increased tendency of flame deflection to the upper right intake side of the combustion chamber. Due to the 5-electrode igniter of the HFI system, the flame kernels were larger and more centralized and overlapping compared to the SCI system, partly explaining the more stable combustion obtained from using HFI.

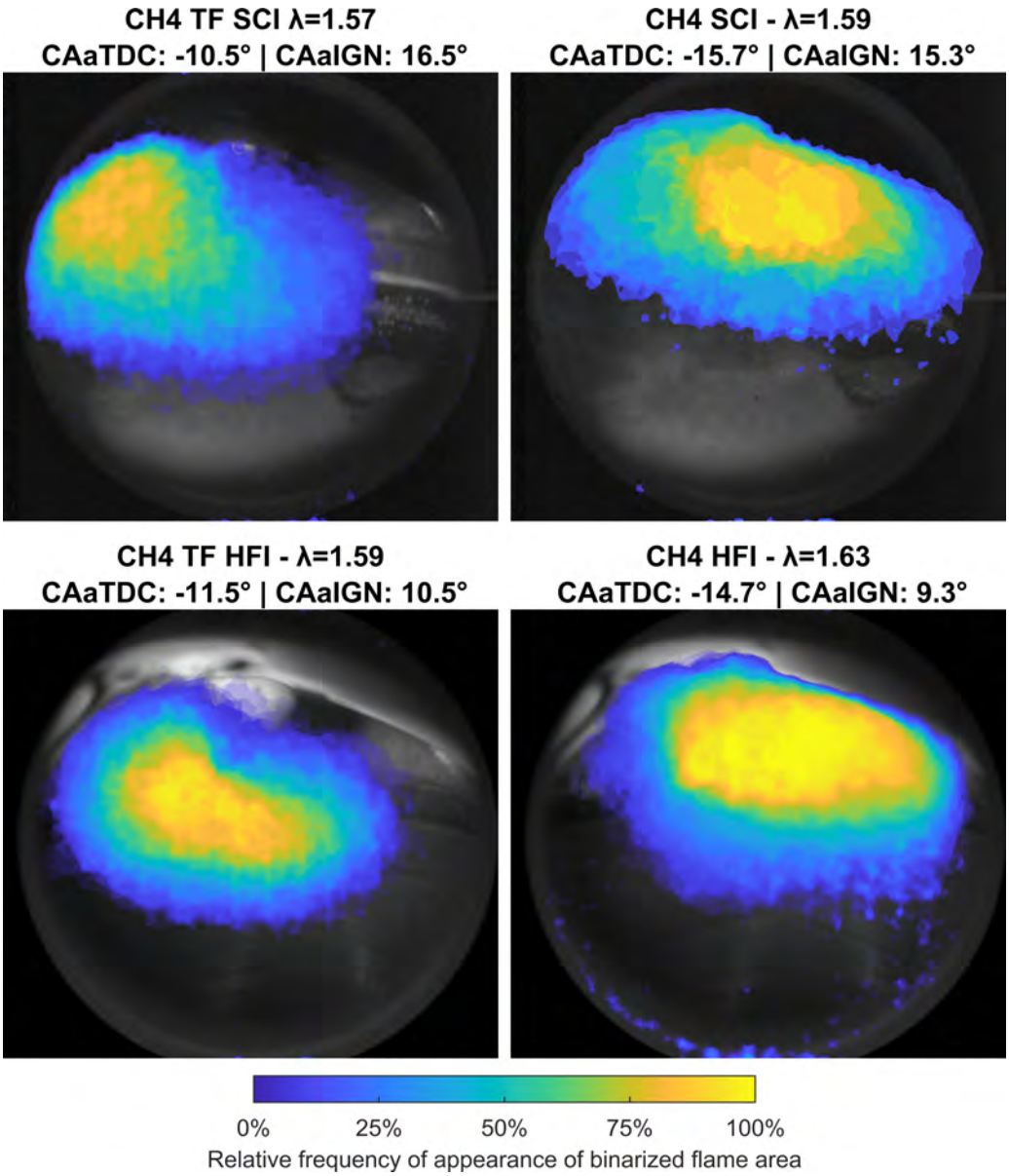


*Figure 38. Relative frequency of the appearance of the binarized flame area (flame contour) at four different conditions using methane as fuel, an engine speed of 2500 and approximately 13 bar NMEP. *SCI: single coil ignition. *HFI: High frequency ignition. *TF: Engaged tumble flap (increased tumble) (other are default, low tumble).*

From the four images combined that were presented in Figure 38, it could be concluded that indeed, increased tumble appeared to increase the turbulence to such levels that the development of the flame kernels was challenged. Whether this could be termed as quenching or not could not be concluded, but excessive turbulence was likely the cause behind the apparently weak developments of the flames. It appeared that the default tumble and turbulence generated by the inlet ports themselves were sufficient to suppress the development of the flame at the highest increments of lambda, at an engine speed of 2500 rpm. Therefore, despite resulting in a more consistent deflection, little or no improvement in air-dilution tolerance could be obtained from further increasing the tumble by utilizing the tumble flap. Similar results were obtained by Ogink and Babajimopoulos when they investigated the utilization of a tumble device with very similar hardware as the one with the single cylinder research engine included in this thesis

[110]. They concluded that an optimum level of tumble existed, since only moderate improvements were made by increasing it, at certain conditions. To highlight the importance of engine speed upon the generation of in-cylinder tumble, the results obtained at 2500 rpm may be compared to previous results acquired at 1500 rpm in the second experimental campaign. Engaging the tumble flap at 1500 rpm, and thereby increasing the tumble, resulted in an increase of the maximum air-dilution tolerance from a modest lambda = 1.5, up to lambda = 1.85.

The observations made from analyzing the flame images offered a potential answer to one of the questions raised from the first experimental campaign, regarding the reason to why the air-dilution tolerance appeared to decrease with increased engine speed: The turbulent kinetic energy of the in-cylinder bulk flow increases with increased engine speed, which likely causes increased tendency of extinction of the developing flame with increased engine speed. Hypothetically, switching to inlet ports that produce less tumble, i.e., filling ports, could potentially reduce this issue, and thereby increase the maximum engine speed with very lean combustion.

The analysis of the flame images also resulted in the conclusion that increased tumble resulted in more consistent spatial development of the flame from cycle to cycle inside the combustion chamber. This conclusion offered an explanation to why increased tumble often is accompanied with greater combustion stability, except for the cases when the turbulence intensities become excessive. Dispersion of combustion is sometimes explained by slow initial flame development, and it is therefore easy to draw the conclusion that the corresponding enhancement of the initial combustion, i.e., shortened flame development duration, is the reason behind better combustion stability at higher levels of tumble. However, it is also possible that the increased repeatability of the combustion, progressing flame, due to a more consistent pattern of the flow of the bulk contributes to better stability of combustion on a cycle-to-cycle basis. Similar observations have previously been made by Wang et al. [79, 80]. They investigated lower engine loads and speeds as opposed to the experiments included in this thesis, but the engine properties and obtained results were very similar. Wang et al. also noted that the flames tended to develop at either direction inside the combustion chamber. They attributed the flames that were developing in a counter-flow direction, i.e., towards the intake side, to increased flame-wall interaction and corresponding slower flame development which led to poorer combustion. The effect of increased tumble points to that increased kinetic energy of the bulk flow is important to achieve a consistent flow during the late compression stroke, when ignition normally occurs. A weak tumble vortex appears to dissipate at an earlier stage during the compression stroke, which causes more unsteady fluctuations of the flow due to the tumble breakdown.

The introduction of direct injected methane resulted in substantial improvements in combustion stability as compared to the results obtained from direct injected gasoline. Due to the stable combustion, it was difficult to analyze the influence of mitigating the knock boundary by a non-knocking fuel and the corresponding influence on the lean load limit. Additionally, the poor combustion stability obtained with gasoline using the single coil ignition system made it difficult to compare gasoline and methane in the same context. Due to that methane provided both non-knocking combustion and improved stability, the lean load limit could not be elicited at the conditions investigated. This is not to be confused with the lean stability limit, which occurred due to decreased flame speeds and excessive turbulence beyond lambda = 1.55. The lean stability limit is a partial burn or misfire phenomena occurring due to poor early flame development and corresponding unsteady combustion. The reason behind the improved combustion

stability by direct injected methane could not be determined, but it was suspected that the high-pressure direct injection of methane at 40 bar contributed. The high-pressure injection may induce turbulence in the combustion chamber which in turn causes rapid mixing of fuel and air, improving mixture homogeneity. The injection could also aid mixing of any residual gasses remaining in the combustion chamber. It was however unclear how the high-pressure injection of gas interacted with the bulk flow. The start of injection occurred early during the intake stroke, at a crank angle of 310° before top dead center which meant that much of the injection of methane preceded the main admission of fresh charge air. If the injection would be timed to a later crank angle, it is possible that the flow of the injected gas could interact with the bulk flow and increase the turbulent kinetic energy. It is also possible that much of the injected gas intersects the upward flowing portion of the tumble vortex with could decrease the turbulent kinetic energy and increase dissipation. Most work found in the literature that considers high-pressure injection of gas have utilized poppet valve injectors. These injectors create a different injection plume as compared to the multi-hole injectors utilized in this thesis. Using poppet valve injectors, researchers such as Song et al. and Moon et al. have shown that direct injection of gas indeed enhances turbulence, but it is uncertain whether this conclusion applies to multi-hole injectors [138-140]. Another factor related to methane that may have significant impact is the minimum ignition energy. Methane has a substantially lower minimum ignition energy (MIE) requirement which may explain why it produced such high combustion stability despite using a the standard single-coil ignition system. The influence of minimum ignition energy has been investigated extensively by researchers such as Shy et al. and Jiang et al. [57, 141]. From their experiments, it may be concluded that methane both has a significantly lower MIE and that the corresponding MIE is less dependent upon the turbulence intensity, compared to a liquid fuel such as isooctane which closely resembles gasoline.

## 4.4 Investigation of the Influence of Residual Gasses –Campaign 4

In the first experimental campaign it was concluded that the multi-cylinder engine experienced comparatively poor air-dilution tolerances at low engine loads. Despite modest amount of air-dilution, the corresponding $NO_x$-emissions were found to be surprisingly low. During the second experimental campaign, a discontinuity at an engine speed of 2000 rpm in the trend of air-dilution tolerance of the single-cylinder engine was found. Due to the remaining gap of knowledge, a fourth research campaign was conducted to investigate the influence of residual gasses. It was hypothesized that the deviating results observed in both campaign 1 and 2 was a result of circumstances that increased the trapping of internally retained residual gasses within the corresponding cylinder/ cylinders. To quantify the amounts of trapped residual gasses, an approach that utilized both physical engine experiments and engine simulations were chosen. Both the multi-cylinder- and single-cylinder research engine were utilized to acquire experimental data. Subsequently, both engines were modelled and simulated one-dimensionally using a commercial software. The multi-cylinder engine was chosen and utilized for experiments at a low load condition of 2.62 bar BMEP and 2000 rpm. This engine was chosen since it featured a well-tuned OEM software that allowed it to operate smoothly at low load conditions with a constant torque output. Additionally, the multi-cylinder engine was equipped with dual camshaft phasers that could be utilized to manipulate valve-timings which in turn influenced the gas-exchange process. The single-cylinder engine was chosen and utilized at higher engine loads. The single-cylinder engine allowed free choice

of the boosting pressure and exhaust pressure since it utilized external, artificial, supercharging. This feature was suitable to eliminate the influence on the gas exchange that would otherwise occur when using a regular turbocharger. The single-cylinder engine additionally provided the opportunity to increase the tumble by means of the featured tumble flap. The engine operating conditions investigated using the single-cylinder engine ranged between speeds of 1500, 2000 and 2500 rpm and various loads ranging from 11 bar NMEP up to almost 18 bar.

The engines were modelled using the so called three-pressure analysis (TPA) approach. In TPA, crank angle resolved inlet, cylinder and exhaust pressures are imposed in the model as boundaries and references respectively. The utilization boundary and references originating from experimental data minimizes the need for model predictions such as air and exhaust routing and combustion models. A TPA-model conducts a reproduction of the experimental results. To do so, the mass flow over the valves and corresponding capturing efficiency of the cylinder must be determined. These are the quantities that are missing from the experiments and that inhibit the determination of the residual gasses. If the determination of the trapped mass inside the cylinder is correct, an accurate reproduction of the heat release is obtained from the model which should match the experimentally acquired release of heat. A drawback is that a TPA model cannot be used to simulate a condition that lacks experimental data.

The purpose of the fourth experimental campaign was to assess the influence of additional dilution by trapped residual gasses, on combustion with air-dilution. To analyze and compare these two different types of diluents, the relative dilution factor was proposed and used.

$$Dilution_{relative} = \frac{\left(m_{gas}/m_{fuel}\right)_{actual}}{\left(m_{air}/m_{fuel}\right)_{stoichiometric}} \tag{23}$$

The relative dilution factor that was computed when all trapped gasses of the combustion chamber were included in $m_{gas}$ was denoted the relative total dilution factor, or simply total dilution. The Greek letter delta was assigned to the total dilution factor.

A design of experiments consisting of a three-by-three full factorial design was chosen and executed using the multi-cylinder engine. The two factors were inlet and exhaust camshaft phasing angles respectively. The design and corresponding factors were chosen to investigate the influence of valve timings on the air-dilution tolerance. At each combination of camshaft phasing angles, a sweep of lambda was performed starting at stoichiometry and swept beyond the corresponding combustion stability limit. At each increment of lambda, a sweep of the ignition timing was performed, ranging from excessively late to excessively early. This resulted in a final test matrix consisting of approximately 900 measurements.

Figure 39 visualizes the highest relative air-dilutions obtained at each combination of camshaft phasing angles, with maintained combustion stability above 75% LNV of NMEP and below 5% CoV of NMEP. The engine operating point was 2000 rpm and 2.62 bar BMEP. From the results presented in Figure 39, it could clearly be observed that increased valve overlap (upper right corner) resulted in the lowest amount of air-dilution. In the first experimental campaign, the very same operating point at 2000 rpm and 2.62 bar BMEP was investigated. The corresponding camshaft phasing angles utilized then were 40° phasing of the intake camshaft and 30° of the exhaust camshaft. This meant that during the first experimental campaign, the multi-cylinder engine was operated with camshaft phasing angles corresponding to the upper right corner of Figure 39, which

verifies the poor air-dilution tolerances that were obtained at low engine loads. However, the results presented in Figure 39 could not explain why the corresponding air-dilution tolerances were exceptionally poor when a high degree of valve overlap was utilized.

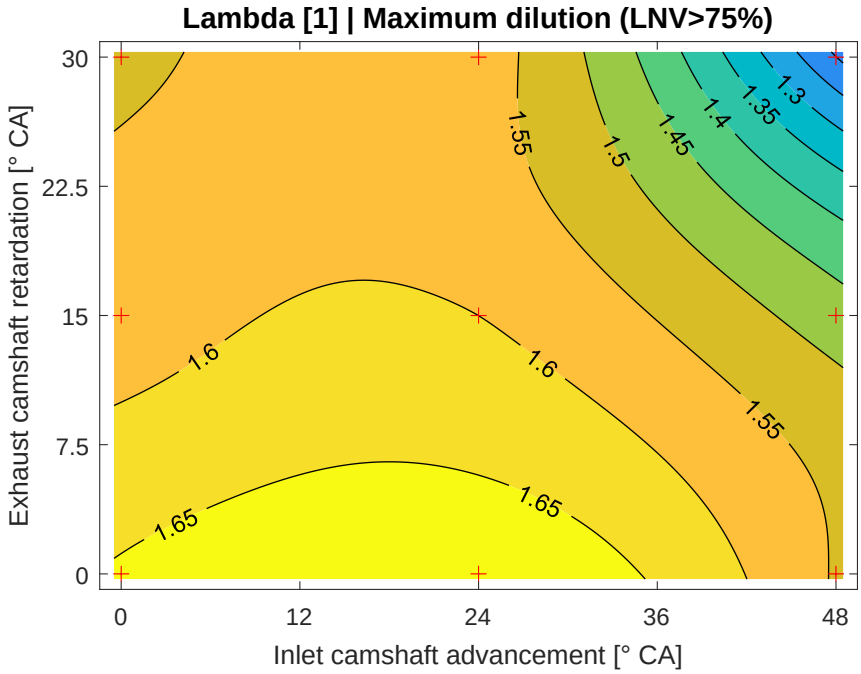


*Figure 39. Maximum relative air dilution, lambda, versus various camshaft phasing angles, at an engine speed of 2000 rpm and 2.62 bar BMEP.*

Figure 40 presents the corresponding total dilution, the combination of air-dilution and residual gas dilution. The colormap of Figure 40 has the same scaling as the one in Figure 39. The total dilution map of Figure 40 showed something completely different as opposed to the air-dilution map. Compared to the air-dilution map, the total dilution map appeared to be almost flat. Clearly, there were significant, hidden, diluent gasses present during combustion. These additional diluents consisted of residual gasses which claimed a share of the charge dilution why the corresponding air-dilution tolerance was reduced. Thus, it was concluded that the actual dilution obtained when running the multi-cylinder engine at low loads during the first experimental measurement campaign was in reality much higher than the amount of dilution that were indicated by measuring relative air-dilution, lambda. This also explained why the corresponding $NO_x$-emissions during low load operation could be reduced to low levels, despite modest air-dilution.

The results presented in Figure 40 were not expected. It had been anticipated that the introduction of residual gasses would result in a lower dilution tolerance compared to dilution by air. This due to that residual gasses are mostly inert. Dilution by recycled exhaust gasses is known to produce lower flame temperatures and lower flame speeds compared to dilution by air. This is due to that an increased share of exhaust gasses results in a lower concentration of oxygen in the cylinder charge [142]. However, internally recycled exhaust gasses, residual gasses, have high temperatures that resembles the exhaust temperatures. Depending on the amount of retained residual gasses, the corresponding enthalpy may increase the total unburned charge temperature by 100 K or more. The additional heat brought by internally trapped residual gasses may explain why the residual gasses did not result in any additional significant reduction of the dilution tolerance, compared to air-dilution. Additionally, if air-dilution and residual gas dilution

is mixed, the residual gasses will contain excess oxygen which reduces the corresponding oxygen depletion otherwise caused by dilution by residual gasses.

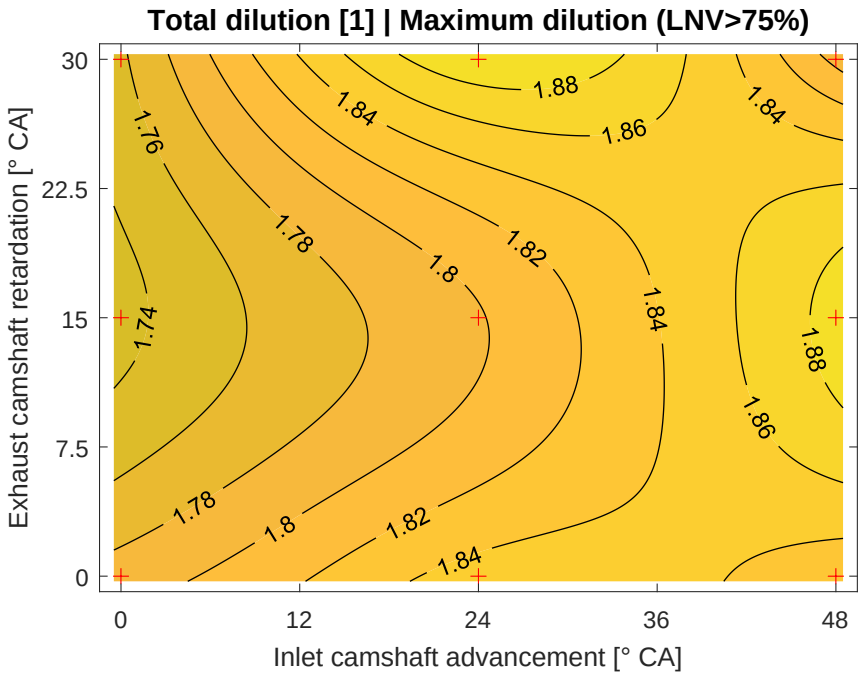


*Figure 40. Maximum relative total dilution, delta, versus various camshaft phasing angles, at an engine speed of 2000 rpm and 2.62 bar BMEP.*

The results that were presented in Figure 40 led to the conclusion that the total dilution tolerance was similar regardless of the blend of air and residual gas dilution. There was however one exception from this conclusion. When there was no excess oxygen present during the combustion, the dilution tolerance became significantly lower. With stoichiometric combustion, solely diluted by internally trapped residual gasses, a maximum relative dilution ratio of 1.6 was obtained. Solely diluting the combustion with residual gasses also resulted in very low NOx-emissions, despite lower amounts of relative dilution.

The corresponding $NO_x$-emissions versus total dilution are presented in Figure 41. The results presented in Figure 41 show that there is a clear correlation between total dilution, i.e., the arbitrary blend of residual gasses and air-dilution, and the corresponding indicated specific $NO_x$-emissions. This holds true except for the stoichiometric cases, which are highlighted in the figure as blue cross-marks. A regression of the points corresponding to lean combustion was performed, from which the stoichiometric operating points containing only residual gas dilution were excluded. The resulting regression line is visualized in Figure 41 together with the r-square value that indicates a high degree of correlation. The smallest amount of relative air-dilution applied amongst the results presented in Figure 41 was lambda = 1.2 (stoichiometric points excluded). It was concluded that the addition of a minimum of lambda = 1.2 in air-dilution significantly increased the $NO_x$-emissions compared to the stoichiometric points. This resulted in two separate groups. What was more interesting was that in terms of $NO_x$-emissions, once an air-dilution of lambda = 1.2 was added to the charge, it did not seem to matter whether further dilution was accomplished by the addition of more air or residual gasses. Despite that all of the lean combustion points shown in Figure 41 contained an arbitrary mix of residual gasses and air, they all correlated to a high degree as the regression of the $NO_x$-

emissions indicated. Therefore, the conclusion was made that it was the amount of total dilution, and not air-dilution, that determined the resulting $NO_x$-emissions from lean combustion, as long as there is some amount of excess air present in the charge. This result also correlates to the previous conclusion that various blends of air and residual gas dilution appeared to result in similar dilution tolerances. It should be noted that no increments of air-dilution rates between lambda = 1 and 1.2 were investigated. Therefore, it could not be determined if lambda = 1.2 was the amount of excess air which saturated the enhancement of air-dilution upon $NO_x$-emissions. It is therefore possible that lower amounts of air-dilution results in similar encouragements upon the $NO_x$-emissions.

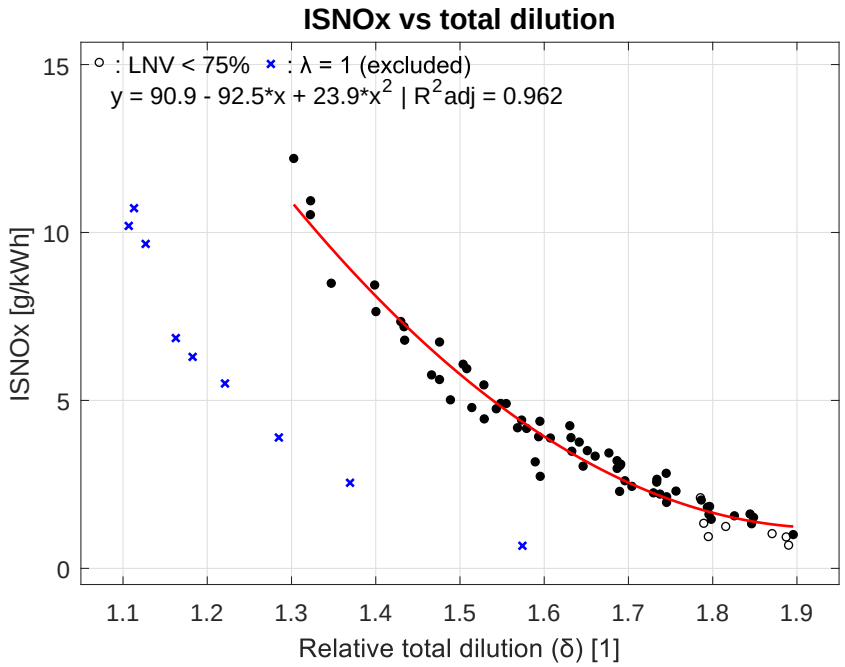


*Figure 41. Correlation plot between indicated specific NOx emissions and relative total dilution. The stoichiometric points are excluded from the curve-fit due to the shift of the second derivative between lambda 1 and 1.2. Engine speed 2000 rpm, 2.62 bar BMEP engine load, CA50 = MBT.*

Interestingly, the data points picked to represent the scatter plot in Figure 41 each represented a combustion phasing angle of maximum brake torque (MBT). The angle of MBT shifts significantly when dilution is added to a stoichiometric charge due to the changes in flame speed and thermodynamic properties. The combustion phasing angle is well known to have a significant influence on $NO_x$-emissions since it influences the peak pressure and therefore peak temperature. The combustion phasing angle also influence the time frame in which the charge remains at a high temperature before expansion which affect available time for chemical reactions. Since the combustion phasing angle should have a strong impact on the $NO_x$-emissions, it was surprising that the results presented in Figure 41 correlated so well. The results presented in Figure 41 represents various combustion pashing angles determined by MBT. Therefore, it was possible that the obtained correlation might have been a coincidence. To investigate the additional influence of the combustion phasing angle upon $NO_x$-emissions, a two-dimensional regression was made. The two-dimensional regression included all available data points of the experimental design matrix including all combustion phasing angle sweeps (ignition sweeps) at each operating conditions. The corresponding results are visualized in Figure 42.

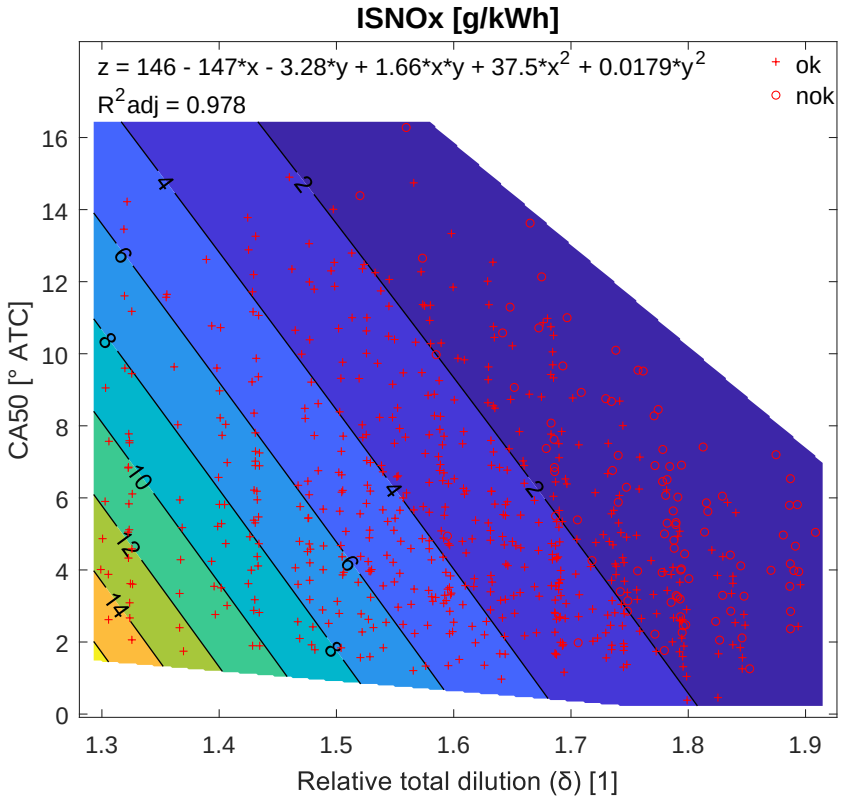


*Figure 42. Regression model of ISNOx versus relative total dilution (δ) and combustion phasing (CA50), at 2000 rpm and 2.62 bar BMEP of the multi-cylinder engine. *ok: combustion within stability criterions. *nok: combustion exceeding stability criterions. Stoichiometric combustion is excluded. The map and corresponding regression are derived from approximately 650 measurements.*

The resulting two-dimensional regression model visualized in Figure 42 improved the correlation even further. The high degree of correlation with an adjusted R-square value of 0.978 led to the conclusion that total dilution and combustion phasing angle combined could accurately predict $NO_x$-emissions. The same approach of regression was used to establish a second regression model of the high engine load $NO_x$-emissions produced by the single-cylinder engine. The regression of the single-cylinder engine data resulted in a similar degree of correlation as the low load multi-cylinder regression model. An attempt was made at reproducing the results of the regression models by replacing total dilution with air-dilution, which resulted in a substantially lower correlation.

The resulting regression models of $NO_x$ were different between the two engines. Therefore, it was not possible to establish one universal model that could predict the emissions of both engines without including more dimensions. This was likely caused by the large difference in engine loads between the multi-cylinder engine, operated at 2.62 bar BMEP (3.5 bar NMEP), and the single-cylinder engine, operated between 11 and 17 bar NMEP approximately. The large differences in engine loads affects the corresponding combustion temperatures which may explain the different $NO_x$-emissions that were obtained.

The single-cylinder research engine was utilized to acquire experimental data at various high load lean combustion operating conditions which were consecutively simulated. The investigation of high load conditions was conducted to determine if there were significant amounts of trapped residual gasses present during high load lean combustion, and if these

gasses had any detrimental effect upon the combustion stability. It was suspected that one reason behind the poor high-load performance of the multi-cylinder engine discovered in the first experimental campaign was due to excessive exhaust throttling by the turbocharger that in turn caused high amounts of residual gasses to be trapped in the cylinders. An overview of various results corresponding to various engine configurations of the single-cylinder engine is presented in Figure 43. Figure 43 represents a chosen operating point of 2000 rpm and approximately 16 bar NMEP.

Six different cases are illustrated in Figure 43 where each one represents an engine configuration which is indicated on the x-axis. All six cases correspond to the highest achieved charge dilution without exceeding a stability limit of 3% CoV of NMEP and 85% LNV of NMEP. The results presented in Figure 43A) revealed that there were significant amounts of trapped residual gasses present in the cylinder which offset the air-dilution during engine operation at 2000 rpm. In the second experimental campaign, it was observed that the single-cylinder research engine experienced poor air-dilution tolerances at this particular engine speed, compared to the other engine speeds investigated. The discovery of additional dilution by residual gasses offered some explanation to the poor combustion stability at 2000 rpm. The trapping of residual gasses of the engine was investigated at engine speeds of 1500 and 2500 rpm as well which were found to be lower compared to 2000 rpm. The reason why the single-cylinder engine trapped increased amounts of residual gasses at 2000 rpm was concluded to be a consequence of the exhaust runner length and its corresponding exhaust pulse frequencies at 2000 rpm, which resulted in a pressure peak prior to the closing of the exhaust valves.

The results presented in Figure 43A) revealed that the total amounts of trapped residual gasses were significant, but rather small, compared to the low load cases which were investigated with the multi-cylinder engine. The multi-cylinder engine could retain residual gasses equivalent to relative dilution factors of up to 1.6 with remained combustion stability. The single-cylinder engine on the other hand retained a maximum in residual gasses corresponding to a dilution factor of 1.17 at the operating conditions and configurations investigated. Therefore, at high loads, the residual gasses did only offset the total dilution factor from the corresponding air-dilution factor in small extents. It was expected that higher engine loads would result in lower amounts of residual gasses, since the difference in pressure between intake and exhaust becomes more equal at loads at or above the naturally aspirated limit, as opposed to low loads with sub-atmospheric inlet pressures.

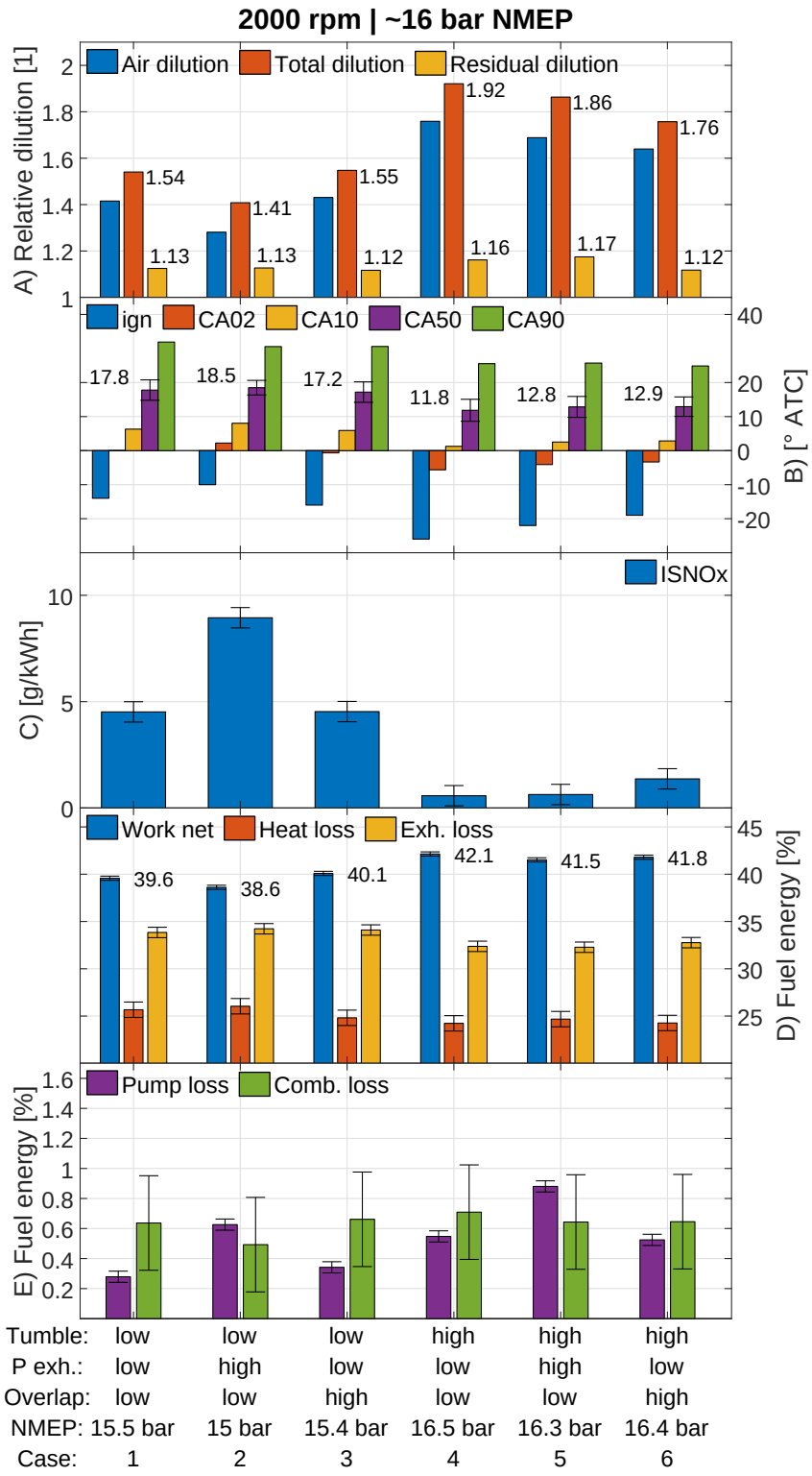


*Figure 43. Measurement- and simulation results of the single cylinder research engine at 2000 rpm and approximately 16 bar NMEP, using various configurations as indicated on the x-axis. *Comb.: Combustion. *Exh.: Exhaust. *P exh.: Pressure exhaust. *ign.: Ignition. B) Error bars denote std of CA50. C-E) Error bars denote std of repeated reference measurements.*

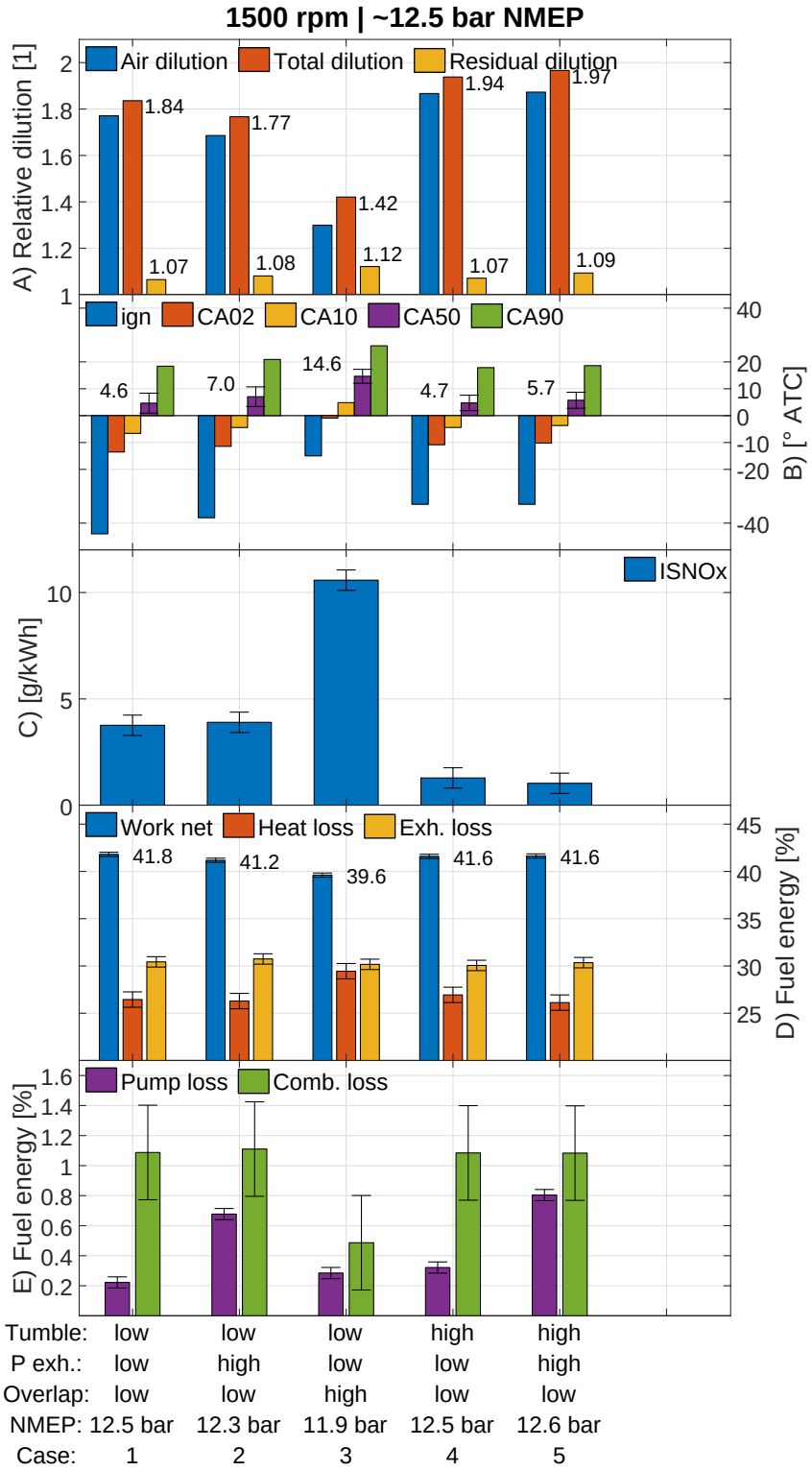


*Figure 44. Measurement- and simulation results of the single cylinder research engine at 1500 rpm and approximately 12.5 bar NMEP, using various configurations as indicated on the x-axis. *Comb.: Combustion. *Exh.: Exhaust. *P exh.: Pressure exhaust. *ign.: Ignition. B) Error bars denote std of CA50. C-E) Error bars denote std of repeated reference measurements.*

Despite that the single-cylinder engine trapped comparatively small quantities of residual gasses at high loads, the residual gasses seemed to have a negative influence on the combustion stability. Figure 44 presents the corresponding results of an engine operating

point of 1500 rpm and 12.5 bar NMEP. It contains the very same engine configurations as were presented in Figure 43, except for the sixth configuration that was omitted from the experimental campaign. The first three cases shown in Figure 44A) show that the amounts of residual gasses increased successively when the exhaust pressure and valve overlap were increased. Simultaneously, the corresponding combustion phasing angles, shown in Figure 44B), were delayed further and the dilution tolerances, both in terms of air-dilution and total dilution, were reduced. Due to the increased delay of the combustion phasing angle, it was clear that the lean load limit was elicited. The lean load limit in turn originates from the increased propensity of knock. Residual gasses are known to increase tendency of end-gas autoignition, knock. The hot gasses increase the end-gas temperature and any unburned oxygen and fuel remining in the residual gasses increase local reactivity. Additionally, previous research has indicated that NO may be an auto-ignition promoter, a species which is brought to the end-gas by the residual gasses [143, 144]. Knock-promotion by heat and chemistry from residual gasses offered a potential explanation to the obtained results in which small amounts of residual gasses appeared to have a detrimental impact on combustion stability at some of the investigated conditions. A similar conclusion regarding the correlation of NO from residual gasses and knock was made by Doornbos et al. [95]. They investigated knock during lean combustion at similar conditions.

Figure 43B) indicated that the resulting combustion phasing angles of case 1 to 3 were delayed from TDC, more than 17° ATC. The results of case 4 to 6, presented in Figure 43 and Figure 44, featured increased tumble. As shown in Figure 43, the increase of the in-cylinder tumble at 2000 rpm led to a clear advancement in the combustion phasing angle and the corresponding dilution could be increased. Increased tumble provided increased dilution tolerance at 1500 rpm as well, but the contrast in terms of combustion phasing angle advancement was less clear. This may be explained by the lower engine load at 1500 rpm which meant that the tendency of knocking was lower. Due to the resulting increase in dilution from increased tumble, the $NO_x$-emissions could be suppressed to 1 g/kWh levels. Since the engaged tumble flap blocked a part of the inlet ports, it resulted in an increased pressure drop through the inlet ports. This resulted in increased pumping losses, which could be seen in Figure 43E) corresponding to 2000 rpm. Furthermore, the throttling of the inlet port resulted in increased amounts of trapped residual gasses, as was illustrated in Figure 43A). However, despite the increase of trapped residual gasses, as compared to default low tumble, the additional residual gasses appeared not to overcome the positive effects of increased tumble. The same increase in pumping losses and residual gasses were not observed for the 1500 rpm operating point of Figure 44. This was likely a consequence of the overall lower mass flow due to the lower power at 1500 rpm. This caused less pressure drop in the inlet port when the tumble device was engaged.

The observation that increased levels of tumble could counteract negative influence on the combustion stability due to trapped residual gasses is important. In a self-sustaining multi-cylinder engine, relying upon a turbocharger to deliver the required air mass-flows, there will likely be many scenarios where the cylinder traps increased amounts of residual gasses due to increases in exhaust pressure from the turbine(s). As the example visualized in Figure 29 showed, the turbocharger caused a pressure difference between exhaust and inlet of 15 kPa (150 mbar). If residual gasses have a detrimental influence on lean combustion stability at high loads, as the low-tumble cases of Figure 44 showed, it will raise concern regarding turbocharged high load lean operation. If increased tumble can mitigate this negative influence, as has been demonstrated in this work, it is more likely

that a turbocharged high load operating lean burn engine can succeed in achieving high dilution rates and corresponding low $NO_x$-emissions.

# 5 Conclusions

The research questions have been addressed by four major research campaigns that have provided insights into homogeneous lean combustion. The obtained results have led to the following conclusions:

- Homogeneous lean combustion does not unconditionally benefit from increased engine loads. Increased engine loads, with corresponding changes of the in-cylinder conditions, did not diminish the cycle-to-cycle variations of the heat release. However, higher engine loads led to shorter combustion duration which reduced the impact of disperse heat release (cycle-to-cycle) and in turn allowed later combustion phasing angles compared to lower loads.
- Homogeneous lean combustion, air-dilution, can be used to suppress end-gas autoignition at high loads, to a limited extent. In the intermediate range of air-dilution, lambda = 1 to 1.4, the tendency of autoignition, knocking combustion, tends to increase. If knocking combustion is prominent, and dispersion of combustion high, a narrow operating window exist of which its boundaries will converge at some degree of dilution. The point of convergence between the knock and stability boundaries was termed the lean load limit. By decreasing either the tendency of knocking or dispersion of combustion, or both, the operating window can be widened, and the dilution increased. This could be accomplished by increased kinetic energy of the in-cylinder tumble flow. At very lean conditions, lambda > 1.6, the tendency of knock decreases which allows earlier combustion phasing angles. The influence of even greater amount of air-dilution, lambda > 2, could not be investigated since the utilized combustion systems did not support such air-dilution rates. From the conditions investigated however at lambda = 1 to 1.9, it was clear that knock during lean combustion experienced similar problems as stoichiometric combustion, the tendency of knock generally increased with increased engine loads.
- It is possible to suppress engine out $NO_x$-emissions down to levels of 1-2 g/kWh by means of air-dilution. During the conducted experiments, it was observed that air-dilution rates exceeding lambda = 1.7 were generally required to achieve such $NO_x$-emission levels. However, these levels of $NO_x$-emissions could only be obtained using high tumble in-cylinder flow in the single-cylinder research engine. The corresponding $NO_x$-emissions of the multi-cylinder engine, with lower levels of tumble, produced 2 g/kWh $NO_x$-emissions or higher.
- It is possible to sustain high load lean combustion using a purposedly designed turbocharger system. Due to limitations of the combustion system of the multi-cylinder engine utilized to conduct the experiments, combustion instabilities limited applicable engine loads with very lean combustion. A maximum of 14 bar BMEP and lambda = 1.4 could be achieved. The engine could be operated at 14 bar BMEP and lambda = 1.7, but with unacceptable combustion dispersion. The prototype turbocharger system did not show any signs of limitations at the conditions investigated, why it is believed that it would have been possible to operate at engine loads of the targeted 16 bar BMEP with air-dilutions exceeding lambda = 1.6. Experiments using the single-cylinder research engine with external boosting and increased tumble could sustain ultra-lean (lambda > 1.6) combustion up to a load of approximately 17 bar NMEP, which roughly equals 16 bar BMEP. This indicates that, with a combustion system with the appropriate characteristics,

it is possible to operate at ultra-lean conditions at 16 bar BMEP using a turbocharger.

- It has been concluded that residual gasses have significant influence on air-diluted combustion. Influence of residual gasses are often overlooked, something that may be explained by that residual gasses are difficult to measure. Three-pressure analysis simulations of engine experiments showed that substantial amounts of residual gasses were trapped in the corresponding engine cylinders during operation, particularly at low loads. The trapped residual gasses resulted in additional dilution which caused the corresponding air-dilution tolerance to decrease. Despite being a different mix of gasses, as opposed to diluent air, internally trapped residual gasses appeared to have similar effect on $NO_x$-emissions as air-dilution, as long as there was some amount of excess oxygen present. Therefore, increasing the share of dilution by residual gasses in a lean mixture did not offer any advantage in terms of $NO_x$-suppression. Similarly, it could be concluded that the relative total dilution, an arbitrary blend of all diluent gasses inside the combustion chamber, determined the ultimate dilution tolerance at low load engine operation. At higher loads, the presence of residual gasses was lower, and they were primarily linked to increased propensity in knocking combustion, rather than adding to the total dilution. However, increased levels of in-cylinder tumble could be utilized to mitigate the negative influence of residual gasses at high loads. Since the share of internally retained residual gasses generally decreases with increased engine load, a larger share of air-dilution is tolerated why it appears that the air-dilution tolerance increases with increased engine load. This is believed to be one of the major factors behind the correlation between engine load and air-dilution tolerance in the range between very low and intermediate loads. The total dilution remains similar throughout this range of engine loads.
- The work has shown that residual gasses are an important parameter that deserves more attention in order to perform better analyses of lean combustion. Consequently, the total dilution rate comprising residual gasses is an important measure for evaluating performance of engine operation with charge dilution by air and other diluents. This research has shown that important correlations cannot be made by only considering the rate of air-dilution.

# 6 Future work

All experimental work conducted to produce this thesis has been conducted using standard engines. The only modifications to the corresponding combustion systems have been high-energy ignition systems, boosting and a tumble-flap. There exist various promising techniques that could further improve the results, such as modified piston bowls, increased direct injection pressure or port injection, and longer stroke, to mention a few alternatives. Another limiting factor of the conducted experiments was peak cylinder pressure, that was limited to 120 bar in the multi-cylinder engine and 100 bar in the single-cylinder engine. A high load lean combustion system may easily obtain peak pressures of 150 bar in the investigated ranges of engine loads.

High load lean combustion is to a large extent limited by knocking combustion. As was demonstrated, the issue of knocking combustion can be partially solved by using other fuels. All engine experiments conducted to produce this thesis were implemented using gasoline with an octane rating of 95 (RON), with the exception of the third experimental campaign where direct injected methane was utilized. Another interesting fuel that may solve some experienced issues is ethanol. Ethanol has a substantially higher resistance to end-gas autoignition, which is why it hypothetically would be an ideal fuel for a high load lean combustion high-efficient zero net carbon engine. It is suspected by the author that, had the multi-cylinder engine been fueled with ethanol rather than gasoline, it could have achieved all the desired goals in terms of high load lean combustion.

Another interesting topic is the potential future application of lean combustion. A lean combustion system can be accomplished in several ways. The system can either be optimized, using cutting edge, expensive, technology to achieve extremely low engine out $NO_x$-emissions that would render the need for lean $NO_x$ aftertreatment obsolete. It may also be realized by cheaper options of technology relying upon conventional spark ignition and few combustion system modifications, combined with lean $NO_x$ aftertreatment to realize clean tailpipe emissions. Either option increases cost of the combustion system. Simultaneously, the very high demands on overall powertrain fuel efficiencies raises the question if it will be possible to produce a car without hybridization in the future. If hybridization is enforced, it adds additional cost to the propulsion system. The combination of an expensive prime mover, a lean combustion engine, and an electric-hybrid system is questionable. This is a complicated optimization problem that deserves attention to determine the future role of lean combustion engines as the primary source of propulsion in cars.

# 7 Summary of Papers and Contributions

This chapter provides a brief overview of the appended articles, their respective research contribution, and the corresponding efforts of the author of this thesis. Additionally, the contribution to knowledge and uniqueness in doing so is addressed.

## 7.1 Paper I

*Clasén, K., Koopmans, L., and Dahl, D., "Homogeneous Lean Combustion in a 2lt Gasoline Direct Injected Engine with an Enhanced Turbo Charging System", SAE Technical Paper 2018-01-1670.*

This paper presented results from an experimental investigation of the world's first self-sustaining two-stage turbocharged homogeneous lean combustion multi-cylinder engine. The results provided insights of the nature of an extended lean map, in terms of engine load and speed. The experiments could verify that it was possible to sustain high load lean combustion using a purposedly designed turbocharger. However, high load lean limitations due to combustion instabilities were obtained, which sparked further research effort in the consecutive experiments.

The author was responsible of conducting the engine experiments, analysis of the data, conclusions, and the writing of the manuscript. The co-authors provided fruitful discussions of the results and assisted in improving the manuscript. The paper was presented as SAE Fuels & Lubricants meeting in Heidelberg, September 2018.

## 7.2 Paper II

*Clasén, K. and Koopmans, L., "Investigation of Homogeneous Lean SI Combustion in High Load Operating Conditions", SAE Int. J. Advances & Current Practices in Mobility 2(4):2051-2066, 2020.*

The apparent load limitation with lean combustion previously experienced was investigated further in this paper. It presented results from an experimental investigation utilizing a single-cylinder research engine with a modified boosting system, allowing high load lean combustion. Experiments with the engine could reveal that there exists a lean load limit, which was defined as the convergence of the combustion stability boundary, denoting the latest permissible spark timing, and the knock boundary, denoting the earliest permissible spark timing. The results explained the lean load limitation obtained in the previous research campaign. Additionally, it could be concluded that increased in-cylinder tumble flow had a substantial positive effect on both combustion stability and mitigation of knock, which could be used to widen the operating window and mitigate the lean load limit. Loads up to 17 bar NMEP, with very lean combustion, could therefore be achieved.

The author was responsible for the research question and the corresponding effort to plan and conduct the experiments to test its hypothesis. The author designed the boosting system, which was manufactured by the research engineers of the engine laboratory. The author conducted all experiments and corresponding analysis of the results. He was also the first author of the paper who wrote the manuscript, with assistance from the co-author.

The paper was submitted to the SAE World Congress, April 2020, in Detroit. Due to its significant contribution, the paper was transformed into a journal article.

## 7.3 Paper III

*Clasén, K., Melaika, M., Koopmans, L., and Dahlander, P., "High Load Lean SI-combustion Analysis of DI Methane and Gasoline using Optical Diagnostics with Endoscope", SAE Technical Paper 2021-24-0046.*

The effect of non-knocking, direct injected methane, on the high load lean limit was investigated in this paper. Additionally, imaging of the flame development was acquired using optical access to the combustion chamber through an endoscope. The use of methane resulted in a significant improvement in combustion stability and the corresponding non-knocking combustion led to the conclusion that the lean load limit was mitigated. Flame images revealed that at higher engine speeds, 2500 rpm, and high tumble, the early flame tends to weaken which led to the conclusion that there exists a maximum applicable kinetic energy of the tumble flow which, when exceeded, may result in the extinguishing of the developing flame at very lean conditions.

The author was responsible for the design of the engine cylinder-head modifications to fit an optical endoscope through the combustion chamber wall. He was also responsible for planning the experiments and analyzing the results. Engine experiments were conducted jointly by the author and Dr. Melaika. Prof. Dr. Dahlander provided image analysis code that was used to develop a new image analysis routine by the author. The author was the main author of the paper, responsible for writing the manuscript, with support from the co-authors. The paper was submitted to the 15$^{th}$ international conference on engines and vehicles in Capri, September 2021.

## 7.4 Paper IV

*Clasén, K. and Koopmans, L., "Influence of Trapped Residual Gasses in Air-Diluted Spark Ignited Combustion", manuscript accepted by SAE International Journal of Engines, 2022.*

The influence of trapped residual gasses on lean combustion was investigated in this paper by the use of combined engine experiments and engine simulations using three-pressure analysis. Two different engines were used to acquire experimental data. Amongst several results, it could be concluded from the simulation results that there existed significant amounts of residual gasses at most operating conditions that influenced the corresponding combustion characteristics. At low loads, it was found that residual gasses contributed greatly to the total dilution, which resulted in relative total dilution factors of up to 1.9. This, in contrast to the maximum applicable air-dilution observed at low loads in the firs paper published, of lambda = 1.3. It could also be concluded that the relative total dilution, consisting of an arbitrary mix of diluent air and residual gas, could accurately predict $NO_x$-emissions, both at low and high engine loads.

The author was responsible of conducting the experimental activities. He designed equipment that allowed the installation of fast pressure-sensors in the single cylinder engine to acquire necessary experimental data. Additionally, the author established two TPA-models, one for each engine, and conducted the consecutive simulations, using a commercial software, of which the results were used to investigate the influence of

residual gasses on lean combustion. The author was the first author of the corresponding manuscript with support of the co-author.

## 7.5 Contribution to Knowledge and Uniqueness

This thesis has contributed with knowledge about high load spark-ignited homogeneous lean combustion operation that has previously not been deeply investigated. In this thesis, it has been shown that it is possible to sustain high load lean combustion by a customized two-stage turbocharger, which proves that it is possible to design a production engine with high load lean combustion capabilities that does not have to rely upon a mechanical supercharger nor an E-booster (electric supercharger). It has been shown that there exists a lean load limit that determines the maximum applicable load and corresponding air-dilution. The lean load limit was identified as the convergence of the knock and stability limits. Using a regular spark plug combined with a high energy ignition system and intensified tumble, engine loads with ultra-lean combustion of 17 bar NMEP could be achieved using RON95 gasoline. By endoscopic imaging of the flame development, using novel high-pressure direct injection with a multi-hole injector of methane and an advanced ignition system, the nature of high load lean flame development has been demonstrated and the influence of the charge motion assessed. Also, this thesis has presented clear evidence about the importance of the total dilution factor and that it dictates both $NO_x$-emissions and combustion stability, rather than the air-dilution solely.

# References


[1] Wing, S. E., Larson, T. V., Hudda, N., Boonyarattaphan, S., et al., "Preterm Birth among Infants Exposed to in Utero Ultrafine Particles from Aircraft Emissions", *Environmetal Health Perspective* 128(4), 2020, doi:10.1289/EHP5732.

[2] "CO2 emissions from cars: the facts," Transport & Environment 2018. Available: https://www.transportenvironment.org/sites/te/files/publications/2018_04_CO2_emissions_cars_The_facts_report_final_0_0.pdf.

[3] P. Mock, Ed., "European Vehicle Market Statistics". International Council on Clean Transportation, 2020.

[4] Our World in Data, "Energy", 2020. Available: https://ourworldindata.org/electricity-mix

[5] "BP Statistical Review of World Energy," British Petroleum, bp.com 2021, vol. 71. Available: https://www.bp.com/en/global/corporate/energy-economics/statistical-review-of-world-energy.html.

[6] ASME, "Advancing Battery Technology for Modern Innovations ", 2021. Available: https://www.asme.org/topics-resources/content/advancing-battery-technology-for-modern-innovations

[7] Møller, K. T., Jensen, T. R., Akiba, E., and Li, H.-w., "Hydrogen - A sustainable energy carrier", *Progress in Natural Science: Materials International* 27:34-40, 2017, doi:10.1016/j.pnsc.2016.12.014.

[8] Berg, H., Nyman, J., Erlandsson, P., Johansson, P., et al., "Direct Ethanol Fuel Cells: Ethanol for our future fuel cells?," Energiforsk 2015, vol. 137. Available: https://energiforskmedia.blob.core.windows.net/media/18529/direct-ethanol-fuel-cells-ethanol-for-our-future-fuel-cells-energiforskrapport-2015-137.pdf.

[9] Kargul, J., Stuhldreher, M., Barba, D., Schenk, C., et al., "Benchmarking a 2018 Toyota Camry 2.5-Liter Atkinson Cycle Engine with Cooled-EGR", *SAE Int. J. Advances & Curr. Prac. in Mobility* 1(2):601-638, 2019, doi:10.4271/2019-01-0249.

[10] Bae, C. and Kim, J., "Alternative fuels for internal combustion engines", *Proceedings of the Combustion Institute* 36:3389-3413, 2017, doi:10.1016/j.proci.2016.09.009.

[11] www.acea.auto, "New Passenger Car Registration By Fuel Type In The European Union 2020", 2021. (Accessed 2021, 11-02). Available: https://www.acea.auto/fuel-pc/fuel-types-of-new-cars-electric-10-5-hybrid-11-9-petrol-47-5-market-share-full-year-2020/

[12] www.acea.auto, "New Passenger Car Registration By Fuel Type In The European Union Q3 2021", 2022. (Accessed 2022, 01-09). Available: https://www.acea.auto/fuel-pc/fuel-types-of-new-cars-battery-electric-9-8-hybrid-20-7-and-petrol-39-5-market-share-in-q3-2021/

[13] Statista, "Breakdown of global car sales in 2019 and 2030, by fuel technology", 2021. (Accessed 2022, 01-10). Available: https://www.statista.com/statistics/827460/global-car-sales-by-fuel-technology/

[14] International Council on Clean transportation, "CO2 Emission Standards for Passenger Cars and Light-Commercial Vehicles in the European Union", 2019. (Accessed 2020, 05-27). Available: https://theicct.org/sites/default/files/publications/EU-LCV-CO2-2030_ICCTupdate_201901.pdf

[15] Kiyota, Y., Akishino, K., and Ando, H., "Concept of Lean Combustion by Barrel-Stratification", SAE Technical Paper 920678, 1992, doi:10.4271/920678.

[16] Johansson, A. N., Hemdal, S., and Dahlander, P., "Experimental Investigation of Soot in a Spray-Guided Single Cylinder GDI Engine Operating in a Stratified Mode", SAE Technical Paper 2013-24-0052, 2013, doi:10.4271/2013-24-0052.

[17] International Council on Clean transportation, "Real-Driving Emissions Test Procedure for Exhaust Gas Pollutant Emissions of Cars and Light Commercial Vehicles in Europe", 2017. (Accessed 2021, 11-02). Available: https://theicct.org/sites/default/files/publications/EU-LCV-CO2-2030_ICCTupdate_201901.pdf

[18] Ogink, R. and Golovitchev, V., "Gasoline HCCI Modeling: An Engine Cycle Simulation Code with a Multi-Zone Combustion Model", SAE Technical Paper 2002-01-1745, 2002, doi:10.4271/2002-01-1745.

[19] Heywood, J. B., "Internal Combustion Engine Fundamentals". McGraw-Hill inc., 1988.

[20] Keck, J. C., Heywood, J. B., and Noske, G., "Early Flame Development and Burning Rates in Spark Ignition Engines and Their Cyclic Variability", SAE Technical Paper 870164, 1987, doi:10.4271/870164.

[21] Baritaud, T. A., "High Speed Schlieren Visualization of Flame initiation in a Lean Operating S.I. Engine", SAE Technical Paper 872152, 1987, doi:10.4271/872152.

[22] Hopkinson, B., "The Effect of Mixture Strength and Scavenging upon Thermal Efficiency", *Proceedings of the Institution of Mechanical Engineers* 74(1):417-489, 1908.

[23] Ricardo, H. R., "Some Experiments on Supercharging in a High-Speed Engine", *Proceedings of the Institution of Automobile Engineers* 15(1):717-770, 1920.

[24] Dunstan, A. E. and Thole., F. B., "Aviation Spirit - Past, Present and Future," in *International Air Congress*, London, 1923.

[25] Bolt, J. A. and Holkeboer, D. H., "Lean Fuel/Air Mixtures for High-Compression Spark-Ignited Engines", SAE Technical Paper 620524, 1962, doi:10.4271/620524.

[26] Bolt, J. A. and Harrington, D. L., "The Effects of Mixture Motion Upon the Lean Limit and Combustion of Spark-Ignited Mixtures", SAE Technical Paper 670467, 1967, doi:10.4271/670467.

[27] Environmental Protection Agency, "Timeline of Major Accomplishments in Transportation, Air Pollution, and Climate Change". (Accessed 2020, May 19, 2020). Available: https://www.epa.gov/transportation-air-pollution-and-climate-change/timeline-major-accomplishments-transportation-air

[28] Lee, R. C. and Wimmer, D. B., "Exhaust Emission Abatement by Fuel Variations to Produce Lean Combustion", SAE Technical Paper 680769, 1968, doi:10.4271/680769.

[29] Tanuma, T., Sasaki, K., Kaneko, T., and Kawasaki, H., "Ignition, Combustion, and Exhaust Emissions of Lean Mixtures in Automotive Spark Ignition Engines", SAE Technical Paper 710159, 1971, doi:10.4271/710159.

[30] Yagi, S., Date, T., and Inoue, K., "NOx Emission and Fuel Economy of the Honda CVCC Engine", SAE Technical Paper 741158, 1974, doi:10.4271/741158.

[31] Noguchi, M., Sanda, S., and Nakamur, N., "Development of Toyota Lean Burn Engine", SAE Technical Paper 760757, 1976, doi:10.4271/760757.

[32] Scussel, A. J., Simko, A. O., and Wade, W. R., "The Ford PROCO Engine Update", SAE Technical Paper 780699, 1978, doi:10.4271/780699.

[33] Germane, G. J., Wood, C. G., and Hess, C. C., "Lean Combustion in Spark-Ignited Internal Combustion Engines - A Review", SAE Technical Paper 831694, 1983, doi:10.4271/831694.

[34] "General Motors Believes it has an Answer to the Automotive Air Pollution Problem," in *The Blade: Toledo*, ed, 1974.

[35] Engh, G. T. and Wallman, S., "Development of the Volvo Lambda-Sond System", SAE Technical Paper 770295, 1977, doi:10.4271/770295.

[36] Volvo Car Sverige AB, Newsroom, "The prize winner - Lambda Sond", 2002. (Accessed 2020, 05-19). Available: https://www.media.volvocars.com/se/sv-se/media/pressreleases/5249

[37] Ingesson, G., Yin, L., Johansson, R., and Tunestal, P., "Evaluation of Nonlinear Estimation Methods for Calibration of a Heat-Release Model", *SAE Int. J. Engines* 9(2):1191-1200, 2016, doi:10.4271/2016-01-0820.

[38] Stokes, J., Lake, T. H., Christie, M. J., and Denbratt, I., "Improving the NOx/Fuel Economy Trade-Off for Gasoline Engines with the CCVS Combustion System", SAE Technical Paper 940482, 1994, doi:10.4271/940482.

[39] Kuwahara, K., Ueda, K., and Ando, H., "Mixing Control Strategy for Engine Performance Improvement in a Gasoline Direct Injection Engine", SAE Technical Paper 980158, 1998, doi:10.4271/980158.

[40] Kano, M., Saito, K., Basaki, M., Matsushita, S., et al., "Analysis of Mixture Formation of Direct Injection Gasoline Engine", SAE Technical Paper 980157, 1998, doi:10.4271/980157.

[41] Wirth, M., Mayerhofer, U., Piock, W. F., and Fraidl, G. K., "Turbocharging the DI Gasoline Engine", SAE Technical Paper 2000-01-0251, 2000, doi:10.4271/2000-01-0251.

[42] Ortmann, R., Arndt, S., Raimann, J., Grzeszik, R., et al., "Methods and Analysis of Fuel Injection, Mixture Preparation and Charge Stratification in Different Direct Injected SI Engines", SAE Technical Paper 2001-01-0970, 2001, doi:10.4271/2001-01-0970.

[43] DieselNet Technology Guide, "NOx Adsorbers", 2020. (Accessed 2020, 05-20). Available: https://dieselnet.com/tech/cat_nox-trap.php

[44] Chambon, P., Huff, S., Norman, K., Edwards, K. D., et al., "European Lean Gasoline Direct Injection Vehicle Benchmark", SAE Technical Paper 2011-01-1218, 2011, doi:10.4271/2011-01-1218.

[45] Enderle, G. V., Merdes, N., Kreitmann, F., and Weller, R., "The new 2.0l turbo engine from the MercedesBenz 4-cylinder engine family," presented at the 2nd Aachen Colloquium China, 2012, 2012.

[46] Pauly, T., Franoschek, S., Hoyer, R., and Eckhoff, S., "Cost and Fuel Economy Driven Aftertreatment Solutions -for Lean GDI-", SAE Technical Paper 2010-01-0363, 2010, doi:10.4271/2010-01-0363.

[47] Inoue, T., Matsushita, S., Nakanishi, K., and Okano, H., "Toyota Lean Combustion System - The Third Generation System", SAE Technical Paper 930873, 1993, doi:10.4271/930873.

[48] Zelenyuk, A., Wilson, J., Imre, D., Stewart, M., et al., "Detailed characterization of particulate matter emitted by lean-burn gasoline direct injection engine", *Int. J. Engine Research* 18(5-6):560–572, 2016, doi:10.1177/1468087416675708.

[49] Parks, J. E., Storey, J. M. E., Prikhodko, V. Y., Debusk, M. M., et al., "Filter-Based Control of Particulate Matter from a Lean Gasoline Direct Injection Engine", SAE Technical Paper 2016-01-0937, 2016, doi:10.4271/2016-01-0937.

[50] Clasén, K., Melaika, M., Koopmans, L., and Dahlander, P., "High Load Lean SI-combustion Analysis of DI Methane and Gasoline using Optical Diagnostics with Endoscope", SAE Technical Paper 2021-24-0046, 2021, doi:10.4271/2021-24-0046.

[51] Newhall, H. K., "Kinetics of engine-generated nitrogen oxides and carbon monoxide", *Symposium (International) on Combustion* 12(1):603-613, 1969, doi:10.1016/S0082-0784(69)80441-8.

[52] Yamamoto, H., "Investigation on Relationship Between Thermal Efficiency and NOx Formation in Ultra-Lean Combustion", SAE Technical Paper 1999-01-3328, 1999, doi:10.4271/1999-01-3328.

[53] Theis, J. R., Kim, J., and Cavataio, G., "Passive TWC+SCR Systems for Satisfying Tier 2, Bin 2 Emission Standards on Lean-Burn Gasoline Engines", *SAE Int. J. Fuels Lubr.* 8(2):460-473, 2015, doi:10.4271/2015-01-1004.

[54] Lavoie, G. A., Heywood, J. B., and Keck, J. C., "Experimental and Theoretical Study of Nitric Oxide Formation in Internal Combustion Engines", *Combustion Science and Technology* 1(4):313-326, 1970, doi:10.1080/00102206908952211.

[55] Amirante, R., Distaso, E., Tamburrano, P., and Reitz, R. D., "Laminar flame speed correlations for methane, ethane, propane and their mixtures, and natural gas and gasoline for spark-ignition engine simulations", *Int. J. Engine Research* 18(9):951-970, 2017, doi:10.1177/1468087417720018.

[56] Lavoie, G. A., Ortiz-Soto, E., Babajimopoulos, A., Martz, J. B., et al., "Thermodynamic sweet spot for high-efficiency, dilute, boosted gasoline engines", *Int. J. Engine Research* 14(3):260-278, 2012, doi:10.1177/1468087412455372.

[57] Shy, S. S., Liu, C. C., and Shih, W. T., "Ignition transition in turbulent premixed combustion", *Combustion and Flame* 157(2):341-350, 2010, doi:10.1016/j.combustflame.2009.08.005.

[58] Rowley, J. R., Rowley, R. L., and Wilding, W. V., "Estimation of the lower flammability limit of organic compounds as a function of temperature", *Journal of Hazardous Materials* 186:551-557, 2011, doi:10.1016/j.jhazmat.2010.11.039.

[59] Finney, C. E., Kaul, B. C., Daw, C. S., Wagner, R. M., et al., "A review of deterministic effects in cyclic variability of internal combustion engines", *Int. J. Engine Research* 16(3):366-378, 2015, doi:10.1177/1468087415572033.

[60] Matthias, N., Wallner, T., and Scarcelli, R., "Analysis of Cyclic Variability and the Effect of Dilute Combustion in a Gasoline Direct Injection Engine", *SAE Int. J. Engines* 7(2):633-641, 2014, doi:10.4271/2014-01-1238.

[61] Young, M. B., "Cyclic Dispersion in the Homogeneous-Charge Spark-Ignition Engine—A Literature Survey", SAE Technical Paper 810020, 1981, doi:10.4271/810020.

[62] Aleiferis, P. G., Taylor, A. M. K. P., Ishii, K., and Urata, Y., "The nature of early flame development in a lean-burn stratified-charge spark-ignition engine", *Combustion and Flame* 136(3):283-302, 2004, doi:10.1016/j.combustflame.2003.08.011.

[63] Metghalchi, M. and Keck, J. C., "Burning Velocities of Mixtures of Air with Methanol, Isooctane, and Indolene at High Pressure and Temperature", *Combustion and Flame* 48:191-210 1982, doi:10.1016/0010-2180(82)90127-4.

[64] Johansson, B., Neij, H., Aldén, M., and Juhlin, G., "Investigations of the Influence of Mixture Preparation on Cyclic Variations in a SI-Engine, Using Laser Induced Fluorescence", SAE Technical Paper 950108, 1995, doi:10.4271/950108.

[65] Hansel, J. G., "Lean Automotive Engine Operation - Hydrocarbon Exhaust Emissions and Combustion Characteristics", SAE Technical Paper 760760, 1971, doi:10.4271/760764.

[66] Berckmüller, M., Tait, N. P., and Greenhaigh, D. A., "The Influence of Local Fuel Concentration on Cyclic Variability of a Lean Burn Stratified-Charge Engine", SAE Technical Paper 970826, 1997, doi:10.4271/970826.

[67] Johansson, B., "Cycle to Cycle Variations in S.I. Engines - The Effects of Fluid Flow and Gas Composition in the Vicinity of the Spark Plug on Early Combustion", SAE Technical Paper 962084, 1996, doi:10.4271/962084.

[68] Miles, P. C. and Hinze, P. C., "Characterization of the Mixing of Fresh Charge with Combustion Residuals Using Laser Raman Scattering with Broadband Detection", SAE Technical Paper 981428, 1998, doi:10.4271/981428.

[69] Hinze, P. C. and Miles, P. C., "Quantitative Measurements of Residual and Fresh Charge Mixing in a Modern SI Engin Using Spontaneous Raman Scattering", SAE Technical Paper 1999-01-1106, 1999, doi:10.4271/1999-01-1106.

[70] Hanabusa, H., Kondo, T., Hashimoto, K., and Furutani, M., "Study on Cyclic Variations of Laminar Flame Speed in Homogeneous Lean charge Spark Ignition Combustion", SAE Technical Paper 2016-01-2173, 2016, doi:10.4271/2016-01-2173.

[71] Grünefeld, G., Beushausen, V., Andresen, P., and Hentschel, W., "A Major Origin of Cyclic Energy Conversion Variations in SI Engines: Cycle-by-Cycle Variations of the Equivalence Ratio and Residual Gas of the Initial Charge", SAE Technical Paper 941880, 1994, doi:10.4271/941880.

[72] Grünefeld, G., Beushausen, V., Andresen, P., and Hentschel, W., "Spatially resolved Raman scattering for multi-species and temperature analysis in technically

applied combustion systems: Spray flame and four-cylinder in-line engine", *Appl. Phys. B* 58:333–342, 1994, doi:10.1007/BF01082630.

[73] Aleiferis, P. G., Taylor, A. M. K. P., Whitelaw, J. H., Ishii, K., et al., "Cyclic Variations of Initial Flame Kernel Growth in a Honda VTEC-E Lean-Burn Spark-Ignition Engine", SAE Technical Paper 2000-01-1207, 2000, doi:10.4271/2000-01-1207.

[74] Patterson, D. J., "Cylinder Pressure Variations, A Fundamental Combustion Problem", *SAE Transactions* 75:621-632, 1967.

[75] Matekunas, F. A., "Modes and Measures of Cyclic Combustion Variability", SAE Technical Paper 830337, 1983, doi:10.4271/830337.

[76] Quader, A. A., "What Limits Lean Operation in Spark Ignition Engines-Flame Initiation or Propagation?", SAE Technical Paper 760760, 1976, doi:10.4271/760760.

[77] Quader, A. A., "Lean Combustion and the Misfire Limit in Spark Ignition Engines", SAE Technical Paper 741055, 1974, doi:10.4271/741055.

[78] Krüger, C., Schorr, J., Nicollet, F., Bode, J., et al., "Cause-and-effect chain from flow and spray to heat release during lean gasoline combustion operation using conditional statistics", *Int. J. Engine Research* 18(1-2):143–154, 2017, doi:10.1177/1468087416686721.

[79] Wang, Y., Zhang, J., Wang, X., Dice, P., et al., "Investigation of Impacts of Spark Plug Orientation on Early Flame Development and Combustion in a DI Optical Engine", *SAE Int. J. Engines* 10(3):995-1010, 2017, doi:10.4271/2017-01-0680.

[80] Wang, Y., Zhang, J., Yang, Z., Wang, X., et al., "Investigation of Flow Conditions and Tumble near the Spark Plug in a DI Optical Engine at Ignition", SAE Technical Paper 2018-01-0208, 2018, doi:10.4271/2018-01-0208.

[81] Teh, K.-Y., Ge, P., Wang, Y., and Hung, D., "Cycle-to-Cycle Variation of In-Cylinder Tumble Flow by Moment Normalization", SAE Technical Paper 2017-01-2214, 2017, doi:10.4271/2017-01-2214.

[82] Wagner, R. M., Drallmeier, J. A., and Daw, C. S., "Characterization of lean combustion instability in premixed charge spark ignition engines", *Int. J. Engine Research* 1(4):301-320, 2000, doi:10.1243/1468087001545209.

[83] Shen, X., Zhang, Y., and Shen, T., "Lower Bound of Variance Minimization in Lean Combustion Control", *IFAC-PapersOnLine* 51(31):303-307, 2018, doi:10.1016/j.ifacol.2018.10.064.

[84] Hanabusa, H., Kondo, T., Hashimoto, K., Sono, H., et al., "Study on Homogeneous Lean Charge Spark Ignition Combustion", SAE Technical Paper 2013-01-2562, 2013, doi:10.4271/2013-01-2562.

[85] Nakata, K., Nogawa, S., Takahashi, D., Yoshihara, Y., et al., "Engine Technologies for Achieving 45% Thermal Efficiency of S.I. Engine", *SAE Int. J. Engines* 9(1):179-192, 2016, doi:10.4271/2015-01-1896.

[86] Yu, X., Yang, Z., Yu, S., Huo, X., et al., "Boosted Current Spark Strategy for Lean Burn Spark Ignition Engines", SAE Technical Paper 2018-01-1133, 2018, doi:10.4271/2018-01-1133.

[87] Shiraishi, T., Teraji, A., and Moriyoshi, Y., "The Effects of Ignition Environment and Discharge Waveform Characteristics on Spark Channel Formation and Relationship between the Discharge Parameters and the EGR Combustion Limit", *SAE Int. J. Engines* 9(1):171-178, 2015, doi:10.4271/2015-01-1895.

[88] Lee, Y. G. and Boehler, J. T., "Flame Kernel Development and its Effects on Engine Performance with Various Spark Plug Electrode Configurations", SAE Technical Paper 2005-01-1133, 2005, doi:10.4271/2005-01-1133.

[89] Hayashi, N., Sugiura, A., Abe, Y., and Suzuki, K., "Development of Ignition Technology for Dilute Combustion Engines", *SAE Int. J. Engines* 10(3)SAE Technical Paper, 2017, doi:10.4271/2017-01-0676.

[90] Alger, T., Gingrich, J., Mangold, B., and Roberts, C., "A Continuous Discharge Ignition System for EGR Limit Extension in SI Engines", *SAE Int. J. Engines* 4(1):677-692, 2011, doi:10.4271/2011-01-0661.

[91] Doornbos, G., Hemdal, S., and Dahl, D., "Reduction of Fuel Consumption and Engine-Out NOx Emissions in a Lean Homogeneous GDI Combustion System, Utilizing Valve Timing and an Advanced Ignition System", SAE Technical Paper 2015-01-0776, 2015, doi:10.4271/2015-01-0776.

[92] Pineda, D. I., Wolk, B. B., Chen, J.-Y., and Dibble, R. W., "Application of Corona Discharge Ignition in a Boosted Direct-Injection Single Cylinder Gasoline Engine: Effects on Combustion Phasing, Fuel Consumption, and Emissions", *SAE Int. J. Engines* 9(3):1970-1988, 2016, doi:10.4271/2016-01-9045.

[93] Hampe, C., Kubach, H., Spicher, U., Rixecker, G., et al., "Investigations of Ignition Processes Using High Frequency Ignition", SAE Technical Paper 2013-01-1633, 2013, doi:10.4271/2013-01-1633.

[94] Yun, H., Idicheria, C., and Najt, P., "The effect of advanced ignition system on gasoline low temperature combustion", *Int. J. Engine Research* 22(2):417-429, 2019, doi:10.1177/1468087419867543.

[95] Doornbos, G., Hemdal, S., Denbratt, I., and Dahl, D., "Knock Phenomena under Very Lean Conditions in Gasoline Powered SI-Engines", *SAE Int. J. Engines* 11(1):1-16, 2018, doi:10.4271/03-11-01-0003.

[96] Suess, M., Guenthner, M., Schenk, M., and Rottengruber, H.-S., "Investigation of the potential of corona ignition to control gasoline homogeneous charge compression ignition combustion", *Proceedings of the Institution of Mechanical Engineers, Part D: Journal of Automobile Engineering* 226(2):275-286, 2012, doi:10.1177/0954407011416905.

[97] Bunce, M. and Blaxill, H., "Sub-200 g/kWh BSFC on a Light Duty Gasoline Engine", SAE Technical Paper 2016-01-0709, 2016, doi:10.4271/2016-01-0709.

[98] Bunce, M., Cairns, A., and Blaxill, H., "The use of active jet ignition to overcome traditional challenges of pre-chamber combustors under low load conditions", *Int. J. Engine Research*:1–15, 2020, doi:10.1177/1468087420972555.

[99] Bureshaid, K. I., Feng, D., Bunce, M., and Zhao, H., "Experimental Studies of Gasoline Auxiliary Fueled Turbulent Jet Igniter at Different Speeds in Single Cylinder Engine", SAE Technical Paper 2019-24-0105, 2019, doi:10.4271/2019-24-0105.

[100] Vedula, R. T., Song, R., Stuecken, T., Zhu, G. G., et al., "Thermal efficiency of a dual-mode turbulent jet ignition engine under lean and near-stoichiometric operation", *Int. J. Engine Research* 18(10):1055–1066, 2017, doi:10.1177/1468087417699979.

[101] Vera-Tudela, W., Barro, C., and Boulouchos, K., "Investigations on spark pre-chamber ignition and subsequent turbulent jet main chamber ignition in a novel optically accessible test rig", *Int. J. Engine Research*:1–13, 2021, doi:10.1177/14680874211019849.

[102] Glassman, I. and Yetter, R. A., "Combustion", 4 ed. Elsevier, 2008.

[103] Baum, E., Peterson, B., Böhm, B., and Dreizler, A., "On the Validation of Large Eddy Simulation Applied to Internal Combustion Engine Flows Part II: Numerical Analysis", *Flow Turbulence Combust* 92:269–297, 2014, doi:10.1007/s10494-013-9468-6.

[104] Baumann, M., Mare, F. d., and Janicka, J., "On the Validation of Large Eddy Simulation Applied to Internal Combustion Engine Flows Part II: Numerical Analysis", *Flow Turbulence Combust* 92:299–317, 2014, doi:10.1007/s10494-013-9472-x.

[105] Neußer, H.-J. and Geiger, J., "Continuous Variable Tumble - A New Concept for Future Lean Burn Engines", SAE Technical Paper 960607, 1996, doi:10.4271/960607.

[106] Larsson, T., Bergström, K. a., Hinderman, T., Hauptmann, L.-G., et al., "The Volvo 3-Litre 6-Cylinder Engine with 4-Valve Technology", SAE Technical Paper 901715, 1990, doi:10.4271/901715.

[107] Berntsson, A. W., Josefsson, G., Ekdahl, R., Ogink, R., et al., "The Effect of Tumble Flow on Efficiency for a Direct Injected Turbocharged Downsized Gasoline Engine", *SAE Int. J. Engines* 4(2):2298-2311, 2011, doi:10.4271/2011-24-0054.

[108] He, Y., Selamet, A., Reese, R. A., Vick, R. K., et al., "Effect of Intake Primary Runner Blockages on Combustion Characteristics and Emissions with Stoichiometric and EGR-Diluted Mixtures in SI Engines", SAE Technical Paper 2007-01-3992, 2007, doi:10.4271/2007-01-3992.

[109] Johansson, B. and Söderberg, F., "The Effect of Valve Strategy on In-Cylinder Flow and Combustion", SAE Technical Paper 960582, 1996, doi:10.4271/960582.

[110] Ogink, R. and Babajimopoulos, A., "Investigating the Limits of Charge Motion and Combustion Duration in a High-Tumble Spark-Ignited Direct-Injection Engine", *SAE Int. J. Engines* 9(4):2129-2141, 2016, doi:10.4271/2016-01-2245.

[111] Changming, H. and Sichuan, X., "The Investigation and Application of Variable Tumble Intake System on a GDI Engine", *SAE Int. J. Engines* 7(4):2022-2034, 2014, doi:10.4271/2014-01-2885.

[112] Malaquias, A. C. T., Netto, N. A. D., Costa, R. B. R. d., and Baêta, J. G. C., "Combined effects of internal exhaust gas recirculation and tumble motion generation in a flex-fuel direct injection engine", *Energy Conversion and Management* 217(15-16):2387-2404, 2020, doi:10.1016/j.enconman.2020.113007.

[113] Alger, T., Hall, M., and Matthews, R. D., "Effects of Swirl and Tumble on In-Cylinder Fuel Distribution in a Central Injected DISI Engine", SAE Technical Paper 2000-01-0533, 2000, doi:10.4271/2000-01-0533.

[114] Zhang, A., Cung, K., Lee, S.-Y., Naber, J., et al., "The Impact of Spark Discharge Pattern on Flame Initiation in a Turbulent Lean and Dilute Mixture in a Pressurized Combustion Vessel", *SAE Int. J. Engines* 6(1):435-446, 2013, doi:10.4271/2013-01-1627.

[115] Moriyoshi, Y., Kuboyama, T., Kaneko, M., Yamada, T., et al., "Fuel Stratification Using Twin-Tumble Intake Flows to Extend Lean Limit in Super-Lean Gasoline Combustion", SAE Technical Paper 2018-01-1664, 2018, doi:10.4271/2018-01-1664.

[116] Abdel-Gayed, R. G., Bradley, D., Hamid, M. N., and Lawes, M., "Lewis Number Effects on Turbulent Burning Velocity", *Symposium (International) on Combustion* 20(1):505-512, 1985, doi:10.1016/S0082-0784(85)80539-7.

[117] Sjöberg, M., Zeng, W., Singleton, D., Sanders, J. M., et al., "Combined Effects of Multi-Pulse Transient Plasma Ignition and Intake Heating on Lean Limits of Well-Mixed E85 DISI Engine Operation", *SAE Int. J. Engines* 7(4):1781-1801, 2014, doi:10.4271/2014-01-2615.

[118] Yamakawa, M., Youso, T., Fujikawa, T., Nishimoto, T., et al., "Combustion Technology Development for a High Compression Ratio SI Engine", *SAE Int. J. Fuels Lubr.* 5(1):98-105, 2012, doi:10.4271/2011-01-1871.

[119] Fujimoto, H., Yamamoto, H., Fujimoto, M., and Yamashita, H., "A Study on Improvement of Indicated Thermal Efficiency of ICE Using High Compression Ratio and Reduction of Cooling Loss", SAE Technical Paper 2011-01-1872, 2011, doi:10.4271/2011-01-1872.

[120] Serrano, D., Zaccardi, J.-M., Müller, C., Libert, C., et al., "Ultra-Lean Pre-Chamber Gasoline Engine for Future Hybrid Powertrains", *SAE Int. J. Advances & Curr. Prac. in Mobility* 2(2):607-6222019-24-0104, 2019, doi:10.4271/2019-24-0104.

[121] Osborne, R., Lane, A., Turner, N., Geddes, J., et al., "A New Generation Lean Gasoline Engine for Premium Vehicle CO2 Reduction", SAE Technical Paper 2021-01-0637, 2021, doi:10.4271/2021-01-0637.

[122] Grandin, B., Denbratt, I., Bood, J., Brackmann, C., et al., "The Effect of Knock on the Heat Transfer in an SI Engine: Thermal Boundary Layer Investigation using CARS Temperature Measurements and Heat Flux Measurements", SAE Technical Paper 2000-01-2831, 2000, doi:10.4271/2000-01-2831.

[123] Burgdorf, K. and Denbratt, I., "Comparison of Cylinder Pressure Based Knock Detection Methods", SAE Technical Paper 972932, 1997, doi:10.4271/972932.

[124] Grandin, B. and Ångström, H.-E., "Replacing Fuel Enrichment in a Turbo Charged SI Engine: Lean Burn or Cooled EGR", SAE Technical Paper 1999-01-3505, 1999, doi:10.4271/1999-01-3505.

[125] Grandin, B., Denbratt, I., Bood, J., Brackmann, C., et al., "Heat Release in the End-Gas Prior to Knock in Lean, Rich and Stoichiometric Mixtures With and Without EGR", SAE Technical Paper 2002-01-0239, 2002, doi:10.4271/2002-01-0239.

[126] Topinka, J. A., Gerty, M. D., Heywood, J. B., and Keck, J. C., "Knock Behavior of a Lean-Burn, H2 and CO Enhanced, SI Gasoline Engine Concept", SAE Technical Paper 2004-01-0975, 2004, doi:10.4271/2004-01-0975.

[127] Stokes, J., Lake, T. H., and Osborne, R. J., "A Gasoline Engine Concept for Improved Fuel Economy –The Lean Boost System", SAE Technical Paper 2000-01-2902, 2000, doi:10.4271/2000-01-2902.

[128] Ratnak, S., Kusaka, J., Daisho, Y., Yoshimura, K., et al., "Experiments and Simulations of a Lean-Boost Spark Ignition Engine for Thermal Efficiency Improvement", *SAE Int. J. Engines* 9(1):379-396, 2016, doi:10.4271/2015-32-0711.

[129] Melaika, M., Etikyala, S., and Dahlander, P., "Particulates from a CNG DI SI Engine during Warm-Up", SAE Technical Paper 2021-01-0630, 2021, doi:10.4271/2021-01-0630.

[130] Dahl, D., "Gasoline Engine HCCI Combustion," PhD, Applied Mechanics, Chalmers University of Technology, Göteborg, 2012.

[131] Tunestål, P., "Self-tuning gross heat release computation for internal combustion engines", *Control Engineering Practice* 17(4):518-524Journal, 2009, doi:10.1016/j.conengprac.2008.09.012.

[132] Ceviz, M. A. and Kaymaz, I., "Temperature and air–fuel ratio dependent specific heat ratio functions for lean burned and unburned mixture", *Energy Conversion and Management* 46(15-16): 2387-2404Journal, 2004, doi:10.1016/j.enconman.2004.12.009.

[133] Grandin, B., "Knock in Gasoline Engines," PhD, Department of Thermo and Fluid Dynamics, Chalmers University of Technology, Göteborg, 2001.

[134] Schwarz, F. and Spicher, U., "Determination of Residual Gas Fraction in IC Engines", SAE Technical Paper 2003-01-3148, 2003, doi:10.4271/2003-01-3148.

[135] Sandqvist, H., Wallensten, J., Enwald, K., and Strömberg, S., "Influence of Valve Overlap Strategies on Residual Gas Fraction and Combustion in a Spark-Ignition Engine at Idle", SAE Technical Paper 972936, 1997, doi:10.4271/972936.

[136] Burgdorf, K. and Denbratt, I., "A Contribution to Knock Statistics", SAE Technical Paper 982475, 1998, doi:10.4271/982475.

[137] Sjöberg, M. and Zeng, W., "Combined Effects of Fuel and Dilution Type on Efficiency Gains of Lean Well-Mixed DISI Engine Operation with Enhanced Ignition and Intake Heating for Enabling Mixed-Mode Combustion", *SAE Int. J. Engines* 9(2):750-767, 2016, doi:10.4271/2016-01-0689.

[138] Song, J., Choi, M., Kim, D., and Park, S., "Combustion Characteristics of Methane Direct Injection Engine Under Various Injection Timings and Injection Pressures", *Journal of Engineering for Gas Turbines and Power* 139(8), 2017, doi:10.1115/1.4035817].

[139] Song, J., Choi, M., and Park, S., "Comparisons of the volumetric efficiency and combustion characteristics between CNG-DI and CNG-PFI engines", *Applied Thermal Engineering* 121:595-603, 2017, doi:10.1016/j.applthermaleng.2017.04.110.

[140] Moon, S., "Comparisons of the volumetric efficiency and combustion characteristics between CNG-DI and CNG-PFI engines", *Applied Thermal Engineering* 136:41-48, 2018, doi:10.1016/j.applthermaleng.2018.01.068.

[141] Jiang, L. J., Shy, S., Nguyen, M. T., Huang, S. Y., et al., "Spark ignition probability and minimum ignition energy transition of the lean iso-octane/air mixture in premixed turbulent combustion", *Combustion and Flame* 187:87-95, 2018, doi:10.1016/j.combustflame.2017.09.006.

[142] Middleton, R. J., Martz, J. B., Lavoie, G. A., Babajimopoulos, A., et al., "A computational study and correlation of premixed isooctane air laminar reaction fronts diluted with EGR", *Combustion and Flame* 159:3146–3157, 2012, doi:10.1016/j.combustflame.2012.04.014.

[143] Stenlåås, O., Gogan, A., Egnell, R., Sundén, B., et al., "The Influence of Nitric Oxide on the Occurrence of Autoignition in the End Gas of Spark Ignition Engines", SAE Technical Paper 2002-01-2699, 2002, doi:10.4271/2002-01-2699.

[144] Roberts, P. J. and Sheppard, C. G. W., "The Influence of Residual Gas NO Content on Knock Onset of Iso-Octane, PRF, TRF and ULG Mixtures in SI Engines", *SAE Int. J. Engines* 6(4):2028-2043, 2013, doi:10.4271/2013-01-9046.

# Symbols and Acronyms

| | |
|---|---|
| $0$ | Denotes start or reference condition |
| $b$ | Burned |
| $C$ | Empirical constant |
| $c_p$ | Specific heat at constant pressure (J/kgK) |
| $c_v$ | Specific heat at constant pressure (J/kgK) |
| $H_c$ | Combustion enthalpy |
| $n$ | Empirical exponent |
| $P$ | Pressure |
| $Q_{ch}$ | Chemical heat, gross heat |
| $Q_{fuel}$ | Available heat of injected fuel |
| $Q_{ht}$ | Heat loss |
| $Q_{net}$ | Net heat |
| $r$ | Ratio |
| $S_L$ | Laminar flame speed |
| $S_T$ | Turbulent flame speed |
| $T$ | Temperature |
| $u$ | Unburned |
| $u'$ | Turbulence intensity |
| $V$ | Volume |
| $\gamma$ | Specific heat ratio, $c_p/c_v$ |
| $\eta_t$ | Ideal thermal efficiency |
| $\theta$ | Crank angle |
| $\kappa$ | Polytropic exponent |
| $\lambda$ | Relative air-fuel ratio, Relative air-dilution, Lambda |
| $\mu$ | Average |
| $\sigma$ | Standard deviation |
| $\tau$ | Auto ignition delay |
| $\varphi$ | Equivalence ratio, relative fuel-air ratio |
| $\delta$ | Relative total dilution |

| | |
|---|---|
| **ATC** | After top center |
| **BMEP** | Brake mean effective pressure |
| **BSFC** | Brake specific fuel consumption |
| **BTC** | Before top center |
| **CA** | Crank angle (degrees) |
| **CA00** | 0% mass fraction burned = spark timing |
| **CA10** | 10% mass fraction burned crank angle of- |
| **CA50** | 50% mass fraction burned, crank angle of- |
| **CA90** | 90% mass fraction burned crank angle of- |
| **CAaTDCf** | Crank angle (degrees) after top dead center firing |
| **CFD** | Computational fluid dynamics |
| **$CH_4$** | Methane |
| **CO** | Carbon monoxide |
| **$CO_2$** | Carbon dioxide |
| **CoV** | Coefficient of variation |
| **CR** | Compression ratio |
| **Cyl** | Cylinder |
| **DCI** | Dual coil ignition |
| **DI** | Direct injection |
| **DISI** | Direct injection spark ignition |
| **DOHC** | Double over-head camshafts |
| **E10** | 10% Ethanol |
| **EVC** | Exhaust valve closing |
| **EVO** | Exhaust valve opening |
| **$H_2O$** | Water |
| **HC** | Hydrocarbon |
| **HCCI** | Homogeneous charge compression ignition |
| **HFI** | High frequency ignition |
| **HLC** | Homogeneous lean combustion |
| **IC** | Internal combustion |
| **ICE** | Internal combustion engine |
| **IVC** | Inlet valve closing |
| **IVO** | Inlet valve opening |
| **KI** | Knock intensity |
| **KO** | Knock onset |

| | |
|---|---|
| **KT** | Knock tendency |
| **Lambda** | Relative air-fuel ratio |
| **LFL** | lower flammability limit |
| **LIF** | Laser induced fluorescence |
| **LNV** | Lowest normalized value |
| **MBT** | Maximum brake torque |
| **MFB** | Mass fraction burned |
| **MP** | Medium power |
| **$N_2$** | Nitrogen |
| **NMEP** | Net (indicated) mean effective pressure |
| **$NO_x$** | NO + NO2, nitrogen oxides |
| **RON** | Research octane number |
| **SCR** | Selective catalytic reduction |
| **SI** | Spark ignition |
| **Std** | Standard deviation |
| **TC** | Top center |
| **TDC** | Top dead center |
| **TF** | Tumble flap |
| **THC** | Total hydrocarbon |
| **TPA** | Three-pressure analysis |
| **TWC** | Three-way catalyst |
| **UHEGO** | Universal heated exhaust gas oxygen (sensor) |
| **WG** | Waste-gate |
| **WLTP** | Worldwide harmonized light vehicle test procedure |
| **VEP** | Volvo engine petrol |
| **VNT** | Variable nozzle turbine |
| **VTEC** | Variable valve timing & lift electronic control |